MODELLING AND QUALITY CONTROL FOR PRECISE GPS AND GLONASS SATELLITE POSITIONING

JINLING WANG

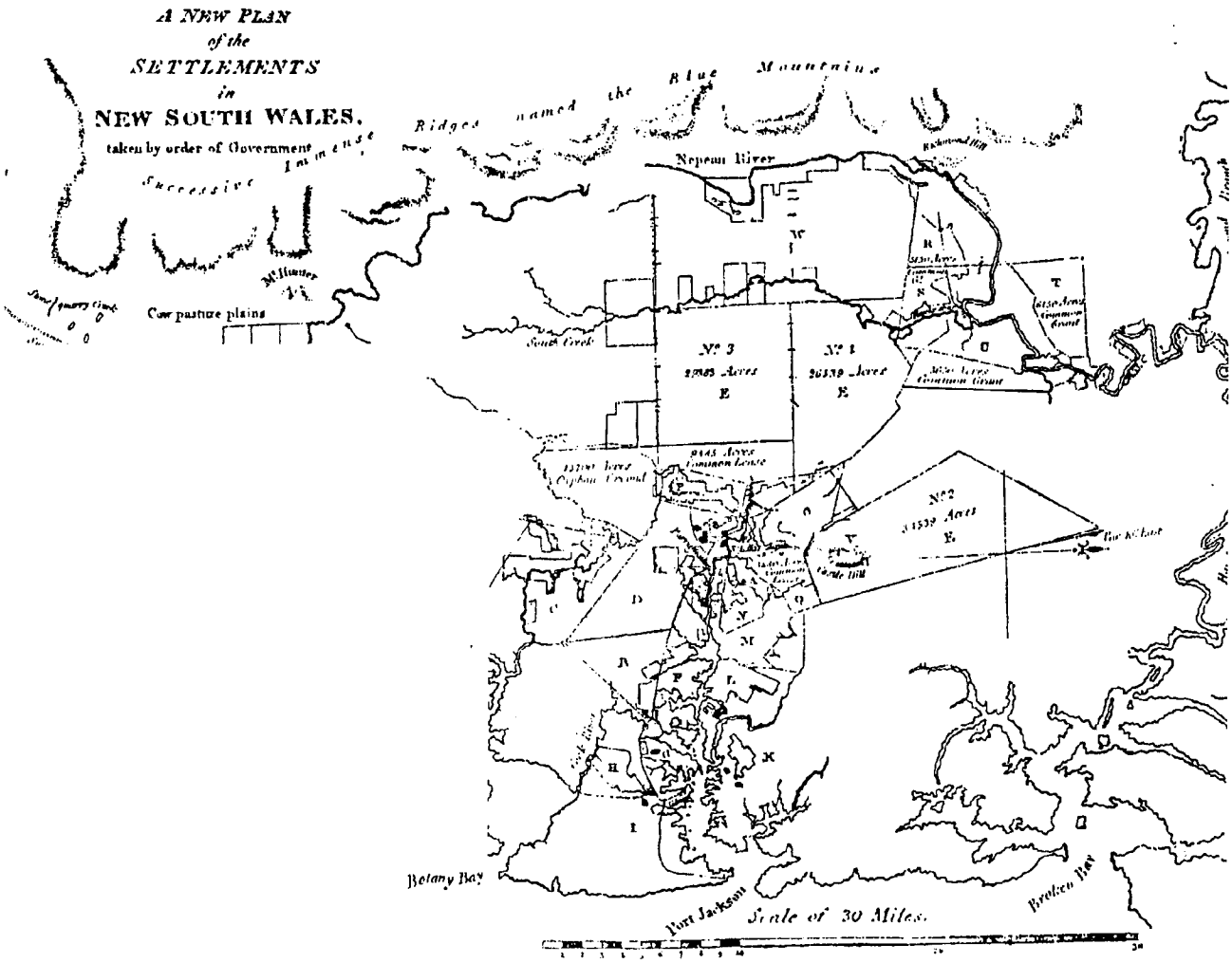

UNISURV S-61, 2001

Reports from

SCHOOL OF GEOMATIC ENGINEERING

THE UNIVERSITY OF NEW SOUTH WALES UNSW SYDNEY NSW 2052 AUSTRALIA

UNISURV REPORT S-61, 2001

MODELLING AND QUALITY CONTROL FOR PRECISE GPS AND GLONASS SATELLITE POSITIONING

JINLING WANG

Received: February 2001
Accepted: February 2001

SCHOOL OF GEOMATIC ENGINEERING
UNIVERSITY OF NEW SOUTH WALES
UNSW SYDNEY NSW 2052
AUSTRALIA

UNISURV REPORTS

Series Editor: Dr. J. M. Rüeger

National Library of Australia

Card No. and ISBN 0 - 7334 - 1766 - 3

EDITOR'S NOTE

The Unisurv-S series has been, since its beginnings in the mid-1960's, the vehicle for publishing research theses and major projects carried out within the School of Geomatic Engineering (and the former School of Surveying) at the University of New South Wales. Recently, this School has decided that research carried out at other Australasian Schools and Departments may be published within the Unisurv-S series, if of sufficient quality and relevance.

This report is based on the research carried out by Jinling Wang for his PhD at the School of Spatial Sciences of the Curtin University of Technology in Perth. Dr. Wang now undertakes postdoctoral studies at the School of Geomatic Engineering, University of New South Wales, funded under the Australian Research Council (ARC) Postdoctoral Fellowship Program for the period 2000 to 2002.

Jean M. Rüeger
Series Editor

February 2001

ABSTRACT

Satellite positioning technologies are increasingly becoming an indispensable part of the worldwide geo-spatial information infrastructure. The Global Positioning System (GPS) and the GLObal NAvigation Satellite System (GLONASS) are major satellite systems which are currently used in precise positioning. This study addresses the most challenging modelling and quality control issues in precise GPS and GLONASS positioning. Major contributions of this study are summarised below:

(a) Valid mathematical models for use in GLONASS and integrated GPS/GLONASS relative positioning have been analysed. Based on both theoretical derivation and empirical experiments, the optimal mathematical model that can deliver the best performance in both ambiguity resolution and precise positioning has been identified;

(b) A stochastic modelling procedure for use in static positioning has been proposed, directly estimating the elements of the measurement covariance matrix. With this new procedure, reliability and efficiency of the positioning results can be improved;

(c) A real-time stochastic modelling procedure for kinematic positioning has been developed, which uses the measurement filtering residuals to adaptively estimate the covariance matrix. The proposed procedure can significantly improve the reliability of ambiguity resolution in precise real-time positioning;

(d) A linear model discrimination test procedure has been developed to validate resolved integer ambiguities. The test statistic used in the ambiguity discrimination test is constructed by the difference between the minimum and second minimum quadratic form of the measurement residuals and its derivation. The distribution of the proposed statistic has been theoretically identified, and thus, the confidence levels for the ambiguity discrimination tests can be rigorously calculated;

(e) A novel approach to GLONASS ambiguity resolution has been developed. This new approach includes some critical strategies to cancel the receiver clock errors and combines both SD and DD ambiguity searches. Compared with existing approaches, the advantage of the new approach is that it is not sensitive to the biases in pseudoranges. Test results show this approach is feasible for GLONASS and integrated GPS/GLONASS positioning.

ACKNOWLEDGEMENTS

I would like to thank my supervisor, Dr. Mike Stewart, and co-supervisor, Dr. Maria Tsakiri for their guidance and support throughout the course of this study. Discussions with Associate Professor Will Featherstone and other members of the geodesy group at Curtin University have been very helpful. Special thanks go to the Head of the School of Spatial Sciences, Prof. Graham Lodwick, and other staff members for their encouragement and help during this study.

I would also thank Prof. P. J. G. Teunissen and his research group at Delft University of Technology for providing the elegant LAMBDA software; Dr. J. Beser (3S Navigation), Dr. F. V. Diggelen and Dr. M. Glutting (Ashtech), Dr. S. Han (University of the New South Wales, Sydney), Prof. G. W. Hein (University of FAF, Munich), Dr. H. Landau (TerraSat) and Dr. M. Pratt (Lincoln Laboratory, MIT) for sending me valuable reference papers.

I am grateful to Professor Yongqi Chen, Associate Professor Xiaoli Ding, Associate Professor H. B. Iz, Hong Kong Polytechnic University (HKPU); Professor Deren Li, Professor Jingnan Liu and Professor Zhenglu Zhang, Wuhan Technical University of Surveying and Mapping (WTUSM) for their encouragement, valuable advice and inspiration on a variety of research topics.

Sincere thanks are extended to my family, particularly my parents for their encouragement; my wife, Rong, and our daughter, Jieli, for their understanding and support during not only this study but also my academic career.

Finally, I would like to gratefully acknowledge Curtin University for awarding me both the Australian Overseas Postgraduate Research Scholarship (OPRS) and the Curtin University Postgraduate Research Scholarship (CUPRS), and also the U.S. Institute of Navigation (ION) for offering me a best student paper award and fully supporting me to attend the 11th International Technical Meeting of the ION Satellite Division ION GPS-98, held in Nashville, USA.

TABLE OF CONTENTS

APPENDICES

LIST OF FIGURES

Figures

LIST OF TABLES

Tables

Chapter 1

INTRODUCTION

1.1 Global Positioning System (GPS)

The Global Positioning System (GPS) is a passive, all-weather satellite-based radio navigation and time transfer system, which is deployed and operated by the U. S. Department of Defense. The development of the Global Positioning System began in the 1970s and obtained its full operational capability (FOC) in July, 1995. The system can continuously provide precise three-dimensional position and velocity in a common reference system, anywhere on or near the surface of the earth (e.g. Wooden, 1985; Lamons, 1990; Parkinson, 1979).

GPS comprises three segments, namely the control segment, the space segment (satellites) and the user segment (receivers). These components are briefly described in the following.

The GPS *control segment* consists of a master control station, five monitoring stations situated around the world and three ground control stations located in the United States. Since July 1998, the number of the monitoring stations has been increased to twelve to provide full-time coverage of the system (ION newsletter, Vol. 8, No. 2, p. 10). The main tasks of the control segment are tracking the satellites, predicting future satellite locations and future satellite clock time corrections, and uploading to the satellites their location and clock time correction information, which are then continuously transmitted by the satellites to the users as a part of the navigation message.

GPS employs the ECEF (earth-centred, earth-fixed) World Geodetic System 1984, known as WGS84 to compute its ephemerides. The U.S. National Imagery and Mapping Agency (NIMA) is responsible for the definition and maintenance of WGS84 (NIMA, 1997).

GPS time is referenced to the Universal Coordinated Time — UTC (U.S. Navy Observation, USNO) without any leap seconds. The major integer shift between the GPS time and UTC (USNO) is currently 13 seconds (as of January 1999).

The GPS *space segment* consists of a design constellation of 21 active satellites and three active spares. The satellites, also known as Space Vehicles (SVs), are deployed in six orbital planes with an inclination of 55 degrees and with four satellites in each plane. The satellite orbits are nearly circular, with an altitude of about 20,200km above the earth's surface and an orbital period of approximately 11 hours and 58 minutes. With this constellation, the space segment can provide global coverage with four to eight simultaneously observable satellites above 15 degree elevation at any time and anywhere on the earth (Hofmann-Wellenhof *et al.*, 1997).

Each GPS satellite continuously transmits ranging signals on two L-band frequencies, namely 1575.42 MHz (L1) and 1227.60 MHz (L2), which are generated by the use of onboard atomic oscillators (Spilker, 1978). The GPS ranging signal consists of a Pseudo-Random Noise (PRN) Coarse/Acquisition code known as C/A-code or a PRN Precise code known as P-code, together with navigation message including among other terms, satellite orbital information (ephemeris data), satellite clock time corrections, and almanac health status to support the position solution generation process. A PRN code consists of a series of binary digits generated by mathematical algorithms (Wells *et al.*, 1987). The PRN code for each satellite is unique and therefore allows the GPS receivers to differentiate between satellites. The C/A-code is a one-millisecond long PRN code broadcast at a bit rate of 1.023MHz, which is only modulated on the L1 carrier. The P-code comprises week-long segments of a 269-day PRN code broadcast at ten times the rate of the C/A-code, 10.23MHz, and is modulated on both the L1 and L2 carriers.

Compared with the C/A-code, the P-code has a higher modulation bandwidth and therefore is more precise. The P-code is primarily used by the Precise Position Service (PPS), while the C/A-code is mainly used by the Standard Position Service (SPS). The PPS ranging signal is intentionally encrypted by the system operators, under a policy known as *Anti-Spoofing*, and is only available to the military of the United States and its allies for users properly equipped with PPS receivers. The SPS

ranging signal is primarily designed to provide a less accurate positioning capability than the PPS ranging signal for civil and other users throughout the world. However, the GPS system operators have the capability to degrade the accuracy of the C/A code, which is known as *selective availability*. According to the SPS ranging signal specification (Parkinson, 1996), the SPS will provide horizontal positioning accuracies to within 100m (95 percent probability) and 300m (95 percent probability). In the past decade, some advanced techniques have been developed to overcome selective availability, allowing precise GPS positioning (Section 1.5).

The GPS *user segment* consists of the many types of GPS receivers collecting the satellite signals to satisfy a broad range of positioning and timing applications. A GPS receiver includes a number of components, namely an antenna and associated preamplifier, a radio frequency or RF front-end section, a signal tracker block, a micro-processor and installed firmware, memory unit, a command entry and display unit, and a power supply (Langley, 1996). Three-dimensional navigation is the primary function of the GPS system. For general navigation applications, GPS receivers may just decode the GPS SPS ranging signals to obtain unambiguous *pseudoranges*, which is the difference between the signal transmission time at the satellite (as defined by the satellite's clock) and the reception time at the receiver (as defined by the receiver's clock) multiplied by the speed of light. At least four satellites have to be tracked to calculate the coordinates and time at any specific point. For some precise GPS positioning, such as in geodetic surveying, GPS receivers are designed to observe the *carrier phase* measurement, which is the phase difference between the incoming carrier signal from the satellite and the signal generated in the receiver.

Although the PPS ranging signal is encrypted, it can still be accessed in some way with current receiver techniques, such as the *narrow-correlation*, *squaring*, *code-correlation squaring*, *cross-correlation*, *P-W tracking* techniques. For more detailed discussions see Hofmann-Wellenhof *et al.* (1997), Leick (1995), Ashjaee and Lorenz (1992), Hatch *et al.* (1992), Counselman (1987), Fenton *et al.* (1991) and Seeber (1993).

While the GPS system was mainly designed for military needs, it is being successfully used in an increasing number of civil applications, such as navigation, surveying, timing and communications. By the late 1990s, the GPS system has become an important part of the worldwide geospatial information infrastructure.

1.2 Global Navigation Satellite System (GLONASS)

Similar to GPS, the GLObal NAvigation Satellite System (GLONASS) provides precise three-dimensional position and velocity, as well as time information, continuously, in all-weather, and on a worldwide basis. GLONASS was conceived in the 1970s at the former Soviet Union's Scientific Production Association of Applied Mechanics (Kaplan, 1996), and is now developed and operated by the Russian Federation Space Forces.

GLONASS, like GPS, comprises three segments (Durnev and Silantiev, 1996), namely the control and monitoring segment, the space segment (satellites) and the user equipment segment.

The GLONASS *control and monitoring segment* consists of a system control centre scheduling and coordinating all system functions, a central synchroniser for disseminating GLONASS time, and a phase control system monitoring GLONASS time and phase offsets. In addition, this segment also includes three command and tracking stations measuring the satellite trajectories and uploading satellite ephemerides, two satellite laser ranging stations that track and periodically calibrate the radio ranging data, and navigation field control units that measure GLONASS navigation signals for system anomalies.

The GLONASS ephemerides are computed in the ECEF (earth-centred, earth-fixed) Parametry Zelmy (English translation "Parameters of the Earth") geodetic reference frame of 1990, which is known as PZ90. PZ90 is defined and maintained by the Russian Topographic Service of the Russian Federation Ministry of Defence.

Like GPS, the GLONASS system has its own time reference known as the GLONASS time, which is coordinated with UTC (Moscow, Commonwealth of Independent States, CIS). The shift between GLONASS system time and UTC(CIS)

is within one millisecond, whereas the accuracy of this shift is less than one microsecond (ICAO, 1995). GLONASS time is periodically corrected to include the UTC integer leap seconds (currently 13 seconds in January 1999), although there is a constant offset of three hours between GLONASS time and UTC(CIS).

The GLONASS *space segment* consists of a design constellation of 24 active satellites and one non-active spare. The GLONASS satellites are arranged in three orbital planes separated by 120 degrees, having an argument of latitude displacement of 45 degrees and an inclination of 64.8 degrees. The satellite orbits are nearly circular, with an altitude of about 19,100km and an orbital period of approximately 11 hours and 15 minutes. With a higher inclination angle, the GLONASS satellite constellation can provide better ground tracking coverage at the higher latitudes than the GPS satellite constellation.

Like GPS, GLONASS has two signal transmission bands, namely L1 band and L2 band. However, unlike GPS, each GLONASS satellite transmits its navigation signals at different frequencies. The original GLONASS frequency plan defines the centre frequencies of the channels as $1602 + 0.5625n$(MHz) in L1 band, and $1246 + 0.4375n$(MHz) in L2 band, where n =0, 1, 2, ..., 24 are channel numbers. However, to minimise interference in the radio astronomy band (1610.6-1613.8MHz), the GLONASS frequency channels 15 to 20 are currently not employed, and each of the frequency channels 21 to 24 is shared by a pair of satellites in antipodal positions. Recently, the frequency band between 1610-1626.5MHz, corresponding to GLONASS channels 15 to 24, has been allocated to a mobile satellite service (MSS). Therefore, the GLONASS frequencies are to be reallocated. According to the revised GLONASS Interface Control Document (ICAO, 1995), channels 0 to 12 will be temporally used for years 1998-2005 and channels -7 to 6 are designed as the final GLONASS frequency allocation.

Similar to the GPS system, the GLONASS ranging signal contains one or two PRN codes, system time reference and navigation data including the satellite ephemerides and almanac modulated on the two carriers. Again like the GPS system, the L1 carrier frequency of GLONASS satellites is modulated with both a PRN C/A-code available for civilian users, and a PRN P-code, which is reserved primarily for

authorised users. The L2 carrier is modulated with the P-code ranging signal only. In the GLONASS system, the C/A-code has a bit rate of 0.511MHz, whereas the P-code has a bit rate at 5.11MHz. These code modulation frequencies are approximately half that of the GPS system. Therefore, the GLONASS ranging signal is theoretically less precise than that of the GPS ranging signal (Walsh and Daly, 1998). However, unlike GPS, GLONASS has disavowed any plans to degrade the ranging signals available for civilian users. The GLONASS C/A-code ranging signal provides horizontal position accuracy of 60m (99.7 percent probability) and vertical position accuracy of 75m (99.7 percent probability), which are much better than those of GPS SPS (C/A-code) ranging signal (ICAO, 1995).

The GLONASS *user segment* consists of different GLONASS receivers which have a similar structure with the GPS receivers. In the global commercial market, there are many types of combined GPS/GLONASS receivers, for example, the Ashtech GG24 (L1) and Z-18 (L1/L2), 3S Navigation R100(L1/L2), JPS Legacy (L1/L2), and MAN NR124 (L1). These combined GPS/GLONASS receivers can collect both GPS and GLONASS satellite signals to satisfy a broader range of robust positioning and timing applications.

The GLONASS system reached its complete constellation in January 1996 when there were 24 operating satellites plus one spare. Since then, there have been a number of satellite failures as the satellites near the end of their projected lifespan. As of February 1999, there are 15 operating satellites and one spare. The Russian Space Forces plans to eventually replace the existing experimental satellites with the new GLONASS-M production satellites, which are expected to offer improved reliability and longer lifespan.

The satellite navigation and positioning community has been looking forward to the prospect of more satellites available for improved system integrity, greater redundancy and better accuracy, for example, in urban areas and mining sites. Accordingly, the integrated use of GPS and GLONASS is an important area of research.

1.3 Fundamental GPS and GLONASS Measurements

The positioning capability of both GPS and GLONASS systems is implemented by obtaining fundamental satellite signal measurements. These are the *pseudorange* and the *carrier phase*.

1.3.1 Code Pseudorange Measurement

A pseudorange is the measurement of the time shift required to align a replica of the satellite PRN code, generated by a receiver, with the code transmitted from a satellite. If the satellite and receiver clocks are fully synchronised with GPS or GLONASS time, the time delay between the transmission and the reception is exactly equal to the travel time of the satellite signal. This delay can be converted into the range between the satellite and the receiver. However, the satellite and receiver clocks have different accuracy levels and, normally, are not synchronised. Therefore, the range determined in this procedure inherently contains a clock error and is thus referred to as the *pseudorange*.

The pseudorange measurement is presented mathematically as:

$$R_k^p = \rho_k^p + c \cdot (dt^p - dt_k) + I_k^p + T_k^p + dr_k^p + dm_k^p + \varepsilon_k^p , \tag{1.1}$$

where

R_k^p pseudorange from receiver k to satellite p;

ρ_k^p topocentric distance between receiver k and satellite p;

c speed of light;

dt^p satellite clock error;

dt_k receiver clock error;

I_k^p ionospheric delay;

T_k^p tropospheric delay;

dr_k^p satellite orbital error;

dm_k^p multipath error;

ε_k^p pseudorange measurement error.

In applications where low accuracy but instantaneous positions are required, the pseudoranges are the preferred measurements.

1.3.2 Carrier Phase Measurement

The carrier phase is the measurement of the phase difference between the carrier signal generated by a receiver oscillator and the carrier signal from a satellite. The receiver can measure the fractional part of the phase, but cannot resolve the integer number of cycles between the receiver and the satellite. At the time of *lock-on*, the receiver selects an arbitrary integer number and is then able to track the changes to the phase. Consequently, the measured phase is ambiguous because an integer number of full cycles is undetermined, which is known as the *carrier phase ambiguity*.

The mathematical description for carrier phase measurement is given as:

$$\phi_k^p = \frac{1}{\lambda_p}\rho_k^p + \frac{c}{\lambda_p}\cdot(dt^p - dt_k) + N_k^p - \frac{1}{\lambda_p}I_k^p + \frac{1}{\lambda_p}T_k^p + \frac{1}{\lambda_p}dr_k^p + dm_k^p + e_k^p \tag{1.2}$$

where

ϕ_k^p carrier phase from receiver k to satellite p;

λ_p wavelength of the carrier frequency for satellite p;

N_k^p integer carrier phase ambiguity;

dm_k^p multipath error in the carrier phase;

ε_k^p carrier phase measurement error.

The definition of the other symbols are the same as in Equation 1.1. It is noted that Equation 1.2 is similar to Equation 1.1, with the major difference being the presence of the integer ambiguity term. Unlike the pseudorange Equation 1.1, the sign of

ionospheric delay in the carrier phase Equation 1.2 is negative. This is because the ionosphere, as a dispersive medium, actually increases the speed of the propagation of the carrier and slows down the modulation on the signal (e.g. Parkinson, 1996).

With modern receiver technology, the carrier phase can be measured with an accuracy of up to 1mm (JPS, 1998). Therefore, the carrier phases are the primary measurements in precise GPS and GLONASS positioning. To use carrier phase measurements, however, the carrier phase ambiguity must be resolved or accounted for in some way (e.g. Counselman and Shapiro, 1979; Wells *et al.*, 1987).

As shown in Equations 1.1 and 1.2, the fundamental GPS/GLONASS measurements are contaminated by many types of errors affecting position accuracy. The error sources in satellite positioning are to be discussed in the following.

1.4 Error Sources in GPS and GLONASS Positioning

The errors associated in GPS and GLONASS satellite positioning may be classified as: satellite related errors, signal-propagation errors, and receiver related errors. In addition, for combined GPS and GLONASS positioning, differences between the system time and datum frames may also deteriorate the positioning results.

1.4.1 Satellite Related Errors

The satellite related errors include satellite orbital errors, clock errors and selective availability.

Satellite orbital errors arise when the satellite navigation message does not transmit the correct satellite location. As a function of time, the satellite's location is predicted with previous satellite tracking measurements collected at the ground monitoring stations. Due to the limitations in the modelling of the measurements, in the hardware and software, satellite orbital errors are inevitable. GPS satellite orbital errors may be in the order of 10-40m when SA is active (e.g. Seeber, 1993), while GLONASS satellite orbital errors are defined as having mean square errors of 20m in the along track component, 10m in the across track component and 5m in the radial component (ICAO, 1995).

Starting on January 1, 1994, the International GPS Service (IGS) has been producing precise orbits for GPS satellites. These IGS orbits are computed with the GPS data collected from the IGS network of up to 78 stations around the world, with the accuracy reaching the (sub-) decimeter level (Beutler, 1996). Currently, the ongoing International GLONASS Experiment (IGEX-98) has also generated the precise orbits for the GLONASS satellites at a similar level accuracy (Rothacher, 1998). However, these precise satellite orbits are post-processed with a time delay between one day to 14 days and thus, cannot be used for real-time or near real-time satellite positioning. Recently, IGS centres also provide predict orbits to the users two hours before the valid period. The precision of these predict orbits is of the order of 1m.

The satellite clock shifts from the satellite system time frame are referred to as *satellite clock errors*. The predicted corrections to the individual satellite clock are transmitted as part of the navigation message to the users. The GPS satellites transmit the satellite clock corrections in the form of a second-order polynomial model, whilst the GLONASS satellites transmit the satellite clock corrections in the form of a first-order polynomial model (Kaplan, 1996). Even with the best efforts of the satellite system control centers in monitoring the behaviour of each satellite clock, the predicted clock corrections still contain errors. Any remaining satellite clock errors are typically in the order of a few nanoseconds, which cause a range error of about one metre (JPS, 1998). This residual clock error can be further eliminated by differencing the measurements from the same satellite tracked by two receivers (Section 1.5).

As discussed in Section 1.1, *Selective Availability* (SA) is the intentional degradation of the GPS satellite clock corrections and orbits available for the civilian users. This effect exists only in the GPS system. The SA bias on each satellite is different and varies with low frequency terms in excess of a few hours, with no obvious correlation between satellites (Georgiadou and Doucet, 1990). Therefore, it is difficult to model the effect of selective availability on the measurements (van Graas and Braasch, 1996). Since the GLONASS system does not utilise selective availability or anything similar to it, it is possible to calibrate GPS SA effects with the GLONASS only solution (Hein *et al.*, 1997). As with satellite clock error, the effect of SA can be eliminated by differencing the measurements from the same

satellite tracked by two receivers. Moreover, some IGS centers provide GPS satellite clock corrections at a high rate. Such products would be useful in some cases for post-processing data (Zumberge, *et al.*, 1998).

1.4.2 Signal-Propagation Errors

When propagating from satellite to receiver, the satellite ranging signals are contaminated by the ionospheric and tropospheric delays, and multipath effects.

The ionosphere is part of the atmosphere, extending from a height of about 50km to 1000km. Due to the free electrons in the ionosphere, the satellite ranging signals do not travel at the vacuum speed of light as they pass through this region. Whereas the propagation of the carrier phase is advanced, the propagation of the PRN modulation on the signal is delayed by the same amount (Parkinson, 1996). The *ionospheric delay* is proportional to the inverse of the carrier-frequency-squared and to the total electron content (TEC) along the path of the ranging signal. The TEC depends on time and geographic location, with major influencing factors being the solar activity and the geomagnetic field (Leick, 1995; Seeber, 1993; Rizos, 1996). Generally, ionospheric delays are in the order of 5 to 15m but can reach over 100m (Parkinson, 1996).

As the ionospheric delay is frequency-dependent, the higher the frequency, the less the delay. Therefore, by using two different carrier frequencies, the ionospheric delay can be effectively solved and thus, to a large extent (around 95 percent), removed from the measurements. For single-frequency GPS or GLONASS users, proper modelling of the ionospheric delays is required (Klobuchar, 1987; Qiu *et al.*, 1995). It is also noted that the ionospheric delays are highly correlated over distances of approximately 10km to 20km. This means that differencing the measurements between two receivers on short baselines can eliminate a large amount of the impact of the ionospheric delays.

The troposphere is the electronically neutral region of the atmosphere, which extends up to approximately 50km above the surface of the earth. As a nondispersive medium, the troposphere delays the codes and carrier phases by the same amount. The effects of the tropospheric delays are in the order of about 2m to 25m (Spilker,

1996, p. 517). These effects vary with satellite elevation angles and reach their minimum values at the zenith and maximum values near the horizon.

Unlike ionospheric delays, the effects of tropospheric delays cannot be removed using dual-frequency systems. One way to reduce tropospheric errors is by measuring its water vapor content, temperature and pressure, and applying a mathematical model that can estimate the tropospheric delays (Hopfield, 1969; Saastamoinen 1973). For some precise static applications, the residual tropospheric delays in the measurements may be considered as additional unknown parameters and estimated, together with other parameters using the least-squares method or Kalman filtering techniques (e.g. Dodson *et al.*, 1996; Rothacher *et al.*, 1990; Shardlow, 1994; Tralli and Lichten, 1990). However, this method is of limited use for kinematic applications. For short baselines of 10-15km, the tropospheric delays are nearly the same at both ends of the baseline, and therefore, differencing the measurements from the two receivers at the ends of the baseline can, to a large extent, cancel them out.

Multipath is a phenomenon whereby a ranging signal arrives at a receiver via more than one path due to reflection at the satellite itself (satellite multipath) and the surroundings of the receiver (receiver multipath). Multipath tends to be one of the major error sources in satellite positioning, although modern receiver technologies can significantly reduce the multipath effects in many situations. The mixed signals from different signal paths create an uncertainty about the true signal arrival time. Multipath signals are always delayed compared to the line-of-sight signals because of the travel paths of these reflected signals are longer. Theoretically, carrier phase multipath does not exceed a quarter of a cycle, whereas pseudorange multipath can take the value up to one chip length of the PRN code, for example, 293m for the GPS C/A code and 29.3m for GPS P code (Georgiadou and Kleusberg, 1989; Lachapelle, 1990; Wells *et al.*, 1987). Multipath is systematic in nature and can exhibit non-gaussian periodic trends. Moreover, multipath is difficult to model or eliminate using differencing procedures and can have an impact on ambiguity resolution which needs careful investigation. There have been an increasing number papers on GPS multipath effects, such as Brasssch and van Grass (1992), Georgiadou and Kleusberg

(1989), and van Nee (1993). Recently, Brodin (1996) has investigated multipath effects on combined GPS and GLONASS measurements.

1.4.3 Receiver Related Errors

The errors in the receiver's measurements of pseudorange and carrier phase are caused by the *receiver clock error*, *inter-channel biases*, *phase center variations*, and *receiver noise*.

The *receiver clock error* is the offset of the receiver clock time with regard to the system time frame, which may be chosen as the GPS system time or GLONASS system time in combined GPS and GLONASS receivers. Compared to the accurate atomic clocks onboard these satellites, the receiver clocks are much less accurate. A typical receiver clock has a drift of about 1000 nanoseconds every second (JPS, 1998). Some receivers, like NovAtel receivers, are designed to correct their clocks every second and keep the receiver clock time align to the satellite system time (Neumann *et al.*, 1997), which is the so-called *clock steering technique*. Most receivers, however, allow the receiver clock to drift naturally within a limited range, for example, one millisecond for Ashtech GG24 receivers. If the receiver clock differs by more than one millisecond, the receiver clock time will be corrected to maintain its alignment with the system time (Pratt *et al.*, 1997). In the case of single-point positioning (Section 1.5.1), the receiver clock error is estimated as an additional unknown parameter, whereas in the case of relative positioning (Section 1.5.3), the receiver clock error is typically eliminated by differencing the measurements from two satellites tracked by one receiver.

Modern GPS receivers are usually designed to record the measurements from each satellite at each frequency on dedicated channels. The length of ranging signal paths through different channels may vary slightly and therefore, inter-channel biases will exist in the measurements made on the signals in different channels. Seeber (1993) has recommended that parameters for these biases are included in the positioning solutions. In modern GPS receivers, these inter-channel biases can be calibrated out at the sub-millimetre level or better (Hofmann-Wellenhof *et al.*, 1997).

In GLONASS or combined GPS/GLONASS receivers, however, the inter-channel biases are significant, which is mainly due to the multiple frequencies of the GLONASS ranging signals (CAA-ISN, 1998; Hall *et al.*, 1997; Pratt *et al.*, 1997; Raby and Daly, 1993a, 1993b; Wang, 1998a, 1998c). These inter-channel biases depend on the frequencies and vary with temperature inside the receiver. The inter-channel biases may cause 4-6m errors in pseudoranges, although their effects on the carrier phase measurements are relatively insignificant for Ashtech GG24 receivers (Gourevitch *et al.*, 1996; Pratt *et al.*, 1997). However, there are reports of such biases existing in carrier phases collected using other receivers (Walsh and Daly, 1996). In this situation, the GLONASS inter-channel biases can be calibrated using GPS measurements (*ibid*).

The electronic position of the antenna for all the phase-derived distance measurements is referred to as the antenna phase centre. However, the phase centre for each ranging signal may vary with the azimuth of the satellite ranging signal received at the antenna (Schupler and Clark, 1991). In addition, the phase centre variations for the L1 and L2 frequencies may have different properties (Leick 1995; Rothacher *et al.*, 1990). Antennas of the same type tend to have similar behaviour in receiving the satellite signals and antenna phase variations can be eliminated in the differencing of the measurements collected with two same type antennas (Seeber, 1993). For carrier phase-based precise positioning, the offset of residual antenna phase centre variations may be estimated using empirical methods (Stewart, 1998).

The *receiver noise* consists mainly of the so-called thermal noise intercepted by the antenna or produced by the internal components of the receiver, which depend on the tracking bandwidth and the signal-to-noise ratio of the ranging signals. Modern GPS/GLONASS receiver technology is able to maintain a very low noise level, with the carrier phase noise being below one millimetre and the code noise a few centimetres (JPS, 1998). It must be added, however, that some dependence of the measurement precision on signal-to-noise ratio has been noted in literature (Langley, 1996).

1.4.4 Difference Between System Time Frames

As discussed in Sections 1.1 and 1.2, the system time frames used in GPS and GLONASS are different. Because combined GPS/GLONASS receivers can use only one of the two time frames to record the measurements, the difference between the two system time frames will lead to a systematic error in positioning solutions if this time difference is not properly accounted for.

GPS time and GLONASS time differ by the number of leap seconds (13 seconds in January, 1999) plus a small, slowly varying and time-dependent term in the order of 100 nanoseconds. For example, this term is 104 nanoseconds for August 30, 1998 (Bulletin E-09-98, 1998). Although the known integer number of leap seconds can be easily corrected, the small varying term is difficult to determine. The GLONASS operators are considering adding into the navigation message the system time difference between GPS and GLONASS (Misra and Slater, 1998). However, this broadcast time difference would only be a predicted value, and therefore, it is unclear whether it would be accurate enough for precise positioning.

In the case of single-point positioning (i.e. navigation) solutions, the time scale discrepancy between the two systems, as one of the unknown parameters, can be estimated using pseudoranges from both GPS and GLONASS systems (Kleusberg, 1990; Raby and Daly, 1993a; Riley *et al.*, 1995). In this situation, at least five satellites are required to estimate the three-dimensional coordinates and the two system time parameters.

On the other hand, the system time difference can be considered as part of the satellite clock error, because the measurements are aligned to the one system time. In the case of relative positioning (Section 1.5), the effects of the varying time difference term on positioning solutions can be largely eliminated. For the short baselines, the errors caused by the system time difference are thought to be insignificant (Landau and Vollath, 1996; Pratt *et al.*, 1997; Forward, 1998; Wang, 1998a).

1.4.5 Difference Between System Datum Frames

Both GPS and GLONASS are autonomous satellite navigation systems. They have different coordinate systems, namely WGS84 and PZ-90, respectively. For the combined use of GPS and GLONASS, the difference between the two geodetic datum frames must be defined. Some effort has been made to determine the transformation parameters for the two systems (Misra *et al.*, 1996; Rossbach *et al.*, 1996; Bazlov *et al.*, 1999), which show that the difference between the two geodetic frames is of the order of few metres. However, as these investigations are based on pseudorange solutions, the derived parameters may be not accurate enough for precise positioning. Actually, the coordinate difference manifests itself as satellite orbital errors. In the case of relative positioning (Section 1.5), small errors in the transformation parameters can be effectively eliminated for short baselines. For the longer baselines, and for the precise point positioning, a more definitive relationship between the two systems is required. This issue is expected to be resolved in the ongoing international GLONASS experiment (IGEX-98) (Slater *et al.*, 1998).

1.5 GPS and GLONASS Satellite Positioning Methods

As discussed above, satellite positioning may be viewed simply as a continuous series of ranging signals broadcast from orbiting satellites to a receiver on (or near) the surface of the earth. These ranging signals contain ephemeris information on the known locations of the satellites, as well as measurement data indicating the distance (code and phase ranges) to each satellite. By employing this fundamental information (measurements and satellite coordinates), different positioning methods, including *absolute*, *differential* and *relative* (interferometric) positioning, have been developed to satisfy various applications. These are discussed in the following.

1.5.1 Absolute Positioning

Absolute positioning, as an autonomous method, employs only one receiver. In fact, a satellite positioning solution can be reduced to a problem familiar in trigonometry, that is one of distance intersection or *trilateration* (Hurn, 1989). In theory, three measured distances from a receiver to three known points (satellites) are enough to determine the three-dimensional coordinates of the receiver. In satellite positioning, however, due to the receiver clock error (Section 1.4), the measured distance is, in fact, a pseudorange. Therefore, three measured pseudoranges are not sufficient for a

meaningful positioning solution. It is interesting to note that the receiver clock error will cause the same amount of distance error to all the ranges measured at the same time. Hence, it is possible to include the receiver clock error as an additional unknown parameter to be solved together with the coordinate parameters. In the case of integrated GPS/GLONASS positioning, the system time difference becomes an additional unknown parameter. Obviously, to obtain a point positioning solution, five or more satellites should be tracked simultaneously, which is ensured by the integrated GPS and GLONASS constellation.

The fundamental absolute positioning method is subject to all the errors discussed in Section 1.4. For GPS alone, the absolute positioning accuracy is only about 100m due to the SA effect (Parkinson, 1996; Section 1.4.1), whereas the accuracy of between 15 to 20m is routinely achievable for both the GLONASS system alone and the combined GPS/GLONASS system (Walsh and Daly, 1998). These accuracies represent 95 percent confidence limits and it should be noted that substantially wose solutions can be achieved in situation where bad geometry predominates (higher DOP). This is particularly relevant for the incomplete GLONASS constellation. For more accurate applications, the method of differential positioning is required.

1.5.2 Differential Positioning

In differential positioning, most of the natural and man-made errors that creep into normal satellite ranging signals are reduced to achieve an improved positioning accuracy. There are two types of differential positioning techniques, namely *local* and *wide* area differential positioning.

A local area differential positioning system usually employs only one reference station. Its receiver antenna is located in a known position relative to the desired geodetic frame. Assuming that the coordinates of the reference station and satellites are known, the correlated errors in ranging to the satellites (with the exception of multipath error which can actually increase in magnitude for a differential solution if it is not explicitly modelled at the reference station) can be calculated and then transmitted with the defined format known as RTCM SC-104 to the user receivers as range corrections (Hurn, 1993). With the corrected pseudoranges, the positioning accuracy can be improved, depending on the distance between the user receiver and

the reference station. Because only one reference station is used in local area differential positioning, the range corrections are valid only for a small area (up to 50 to 100km from the reference station).

Wide area differential positioning uses a network of reference stations to analyse the individual satellite positioning error sources (Delikaraoglou *et al.*, 1990; Brown, 1989; Kee *et al.*, 1991). Based on the analysis of all the data at the master control station, a vector correction for each satellite is formed, which includes individual corrections for the satellite clock, three components of the satellite position error and parameters of the ionospheric delay model. These corrections can be valid for a large area, for example, a continent or the whole territory of a country.

Differential GPS (DGPS) positioning has become one of standard surveying and navigation techniques. Many commercial companies around the world provide differential GPS services. Initial investigations on differential GLONASS (DGLONASS) and combined differential GPS/GLONASS (DGPS/DGLONASS) show encouraging results (Beser *et al.*, 1995; Diggelen, 1996; Ganin, 1995; Gourevitch *et al.*, 1996; Walsh *et al.*, 1995 and 1996).

The basic ideas of differential GPS positioning have been utilised in the Local Area Augmentation System (LAAS) and the Wide Area Augmentation System (WAAS). These are currently developed by the US Federal Aviation Administration (FAA) to ensure GPS as an efficient means of navigation for all the phases of the aircraft flight from *en route* through to precision approach. The LAAS is a ground-based augmentation system, which consists of ground reference station and airport-based pseudolites (APLs). The reference station calculates and broadcasts corrections to pseudoranges and integrity information to aircraft receivers, whereas airport pseudolites (APLs) transmit GPS-like ranging signals to improve the position determination geometry (Braff, 1997). The WAAS is a space-based augmentation system which employs geostationary satellites to transmit to users the vector corrections to each satellite, together with additional GPS-like ranging signals and an integrity monitoring message, improving availability and reliability (Enge and Van Dierendonck, 1996).

It has been shown that the performance of GPS/LAAS can be improved substantially by expanding the space segment with additional GLONASS ranging signals (Misra *et al.*, 1998; Walsh *et al.*, 1997). Similar to the WAAS, the European Geostationary Navigation Overlay Service (EGNOS) system is a regional augmentation service for GPS and GLONASS signals over Europe, which is called GNSS-1, setting up the first step for the future European global navigation satellite system (GNSS) (Romay *et al.*, 1998).

Generally, differential positioning techniques, which mainly utilise pseudorange measurements, can achieve an accuracy of between 0.5m and 5m, depending on the quality of the receivers used in positioning. For some applications with the very stringent accuracy requirements, relative positioning techniques have been developed. These will be discussed in the following.

1.5.3 Relative Positioning

Similar to differential positioning, relative positioning methods employ two or more receivers to simultaneously track the navigation satellites. The data processing principles behind these two positioning methods are quite different. Whilst differential positioning techniques are used to solve for the user's position, the relative positioning method is designed to determine the relative position or baseline components between the receiver antennae. In relative positioning, satellite measurements, in particular carrier phases, collected from all the receivers involved are processed together to achieve high precision (relative) positioning results.

The concept of satellite-based relative positioning has roots in very long baseline interferometry (VLBI) (Bossler *et al.*, 1980; Counselman and Shapiro, 1979; MacDoran, 1979; Preston *et al.*, 1972). The intrinsic principle inherited from VLBI is interferometry, the differencing of the phases of ranging signals received at the two ends of a baseline. In differencing measurements between receivers, the correlated atmospheric errors and satellite-related errors are greatly eliminated. Similarly, the differencing of the measurements between two satellites can reduce receiver clock errors. This data processing methodology is called *differential interferometry* in radio astronomy (Counselman *et al.*, 1972), and *double differencing* in GPS literature (Bossler *et al.*, 1980).

Commonly used relative positioning methods are mainly based on the use of the carrier phase measurements expressed by Equation 1.2. Although the pseudorange measurements are used to calculate an initial approximation position and improve the ambiguity resolution process. With the real-valued ambiguities, the geometry of baseline solutions (float solutions) is weak and thus degrades position accuracy. Resolving the carrier phase integer ambiguity transforms carrier phase data into precise pseudorange data and strengthen the geometry of baseline solutions (Bossler *et al.*, 1980). However, it should be noted that any significant systematic errors in carrier phases may lead to biased positioning results.

Various relative positioning techniques have been developed, which can be categorised as *static* and *kinematic* positioning modes.

In *static (relative) positioning*, receiver antennae are stationary during the period of data collection (*session*). The session length depends on the satellite constellation, baseline length, the quality of receivers and the accuracy requirement. A fixed network of receivers, called *multiple receiver antenna array*, is designed to continuously track the satellites for various applications, such as determining the precise satellite orbits (Yunck, 1996; Whalley, 1990), monitoring the earth orientation variation (Paquet and Louis, 1988; Freedman, 1991), crustal and local deformation (Bock, 1991; DeLoach, 1989). During the last decade, the *rapid static* relative positioning techniques have been introduced, with which the session length can be reduced to only a few minutes, even seconds, to obtain centimetre positioning accuracy over baselines up to 20km or so (Blewitt *et al.*, 1989; Euler *et al.*, 1990; Frei and Beutler, 1990).

The concept of *kinematic (relative) positioning* is first introduced in Remondi (1985). In kinematic positioning, one or more receiver antennae are in motion. In the case of *single baseline* positioning, one receiver antenna is stationary, called *reference station* or *base station*, while the other receiver antenna is in motion, called *rover station*. To improve the geometry of kinematic positioning, multiple reference stations may be employed (e.g. Abidin, 1993; Han and Rizos, 1997; Wanninger, 1995; Wübbena *et al.*, 1996).

In practice, a *multiple receiver antenna array* may be used to determine attitude parameters of a moving platform, called *attitude determination* (Cohen, 1996), or relative position between moving platforms, which is considered as a general case of kinematic positioning (Evans *et al.*, 1995; Hermann *et al.*, 1994; Lachapelle *et al.*, 1994). In these applications, all the receiver antennae are in motion.

Whilst some kinematic applications do not need real-time results and thus, collected data may be *post-processed*, many kinematic applications require real-time data processing, which is called *real-time kinematic* (RTK) positioning. In standard RTK satellite positioning, the reference station transmits carrier phase and pseudorange data over a radio link to a roving station, where the data are processed in real-time to obtain instantaneous positioning results (Langley, 1998; Talbot, 1993).

Generally, relative carrier phase based positioning techniques, which resolve carrier phase ambiguities, can achieve an accuracy of between 0.005m and 0.05m, depending on baseline length (Hatch, 1986; Goad, 1987).

1.6 Some Critical Issues in GPS and GLONASS Positioning

In GPS and GLONASS satellite positioning, unknown positioning parameters are commonly calculated using modern optimal estimation theory, such as *least-squares* or *Kalman filter*. The application of these estimation methods is based on the so-called *Gauss-Markov* models, which include a mathematical model and a stochastic model. Therefore, *mathematical and stochastic modelling* (Sections 1.6.1 and 1.6.2) are the first important steps in data processing. In the modelling of carrier phases, ambiguity parameters are initially treated as real values, which degrade the potential accuracy of the carrier phases. Hence, reliable *ambiguity resolution* (Section 1.6.3) is the key to high precision satellite positioning. To ensure that the quality of positioning results meet the designed requirements, it is important that *quality control* (Section 1.6.4) procedures must be employed in the whole process of positioning.

1.6.1 Mathematical Modelling

The mathematical model, also called the functional model, describes the mathematical relationships between measurements and unknown parameters,

(*measurement models*); or relationships between unknown parameters themselves (*dynamic models*). Whilst the dynamic models that are used in satellite-based kinematic positioning are well documented, much effort has been made to develop correct measurement models for new positioning systems, such as GLONASS.

Raw GPS and GLONASS observations are contaminated with many error sources, such as satellite clock errors and ionospheric and tropospheric delay errors. The mathematical representation of these raw observations, as shown in Equations 1.1 and 1.2, will involve some undesirable nuisance parameters. These nuisance parameters are dependent on each other and cannot be solved for individually. As a consequence of this, it is impossible to identify the integer ambiguity parameters from the raw (one-way) carrier phase measurements.

In GPS positioning, two different mathematical modelling strategies have been developed, namely, a) *double differencing* (Bossler *et al.*, 1980; Goad and Remondi, 1984; Bock *et al.*, 1986) and b) *generalised differencing* (Blewitt, 1989 and 1993; Goad, 1985; Hatch and Larson, 1985; Lindlohr and Wells, 1985). The double differencing procedure is designed to cancel or eliminate, to a large extent, the systematic errors existing in measurements and hence, the resulting mathematical models exclude some of these nuisance parameters. In the generalised differencing procedure, although the undifferenced measurements are directly processed, double-differenced ambiguity parameters are formed, which can be separated from the other reparametrised nuisance parameters. Obviously, the double differencing procedure will be computationally more efficient, because the nuisance parameters are removed from the measurement model (Blewitt, 1993).

Whilst the double differencing procedure has been widely used as a standard modelling method in GPS data processing, it does not work in the case of GLONASS or integrated GPS and GLONASS positioning. The reason for this is that GLONASS satellites transmit their ranging signals at different frequencies (Landau and Vollath, 1996; Leick *et al.*, 1995; Wang, 1998a and 1998b). Mathematical modelling in GLONASS or integrated GPS and GLONASS positioning therefore requires investigation, which is an aim of this study.

1.6.2 Stochastic Modelling

The stochastic model describes the statistical properties of the mathematical models, which are mainly given by the covariance matrices of the measurement errors associated with the measurement model, and process noises corresponding to the dynamic model. In high precision satellite-based positioning, the covariance matrix for dynamic model noise can be properly constructed to ensure positioning results independent of the dynamics of the roving stations (Lachapelle *et al.*, 1992; Wang, 1998b). In practice, however, stochastic modelling for the measurements is both a controversial topic and a difficult task to accomplish (Cross *et al.*, 1994; Wang and Stewart, 1996).

Whilst the mathematical models for GPS measurements have been very well established in the literature, the stochastic models of GPS measurements are mainly based on some simplified assumptions. In the currently used stochastic models, it is usually assumed that all the one-way carrier phases or pseudoranges have the same variance, and that they are statistically independent. Therefore, the time-invariant covariance matrix of the double-differenced (DD) measurements is constructed using the error propagation law. In this covariance matrix, the correlation coefficient between any two DD measurements is always $+0.5$. This so-called mathematical correlation is introduced by the double differencing process. To set up a simple stochastic model for DD measurements, it is further assumed that the time correlation is absent. Therefore, the covariance matrix of all the DD measurements in a session does have a simple block-diagonal matrix.

The above stochastic modelling method was proposed in some pioneer work (e.g. Bock *et al.*, 1986; Remondi, 1984) and has been widely used in both commercial and scientific software packages. Perhaps, the main reason for this is due to its simplicity. In practical applications, however, observing conditions vary from epoch to epoch. This simple universal weighting scheme may be not always realistic. Any mis-specifications existing in the stochastic models will lead to unreliable ambiguity resolution and biased positioning results. Hence, stochastic modelling for GPS and GLONASS measurements is still a challenging issue for precise positioning, which is addressed in this study.

1.6.3 Ambiguity Resolution

As stated earlier, ambiguity resolution refers to the determination of the unknown integer number of cycles associated with each set of carrier phase measurements. With fixed integer ambiguities, the carrier phases can be used as unambiguous precise range measurements. Consequently, the geometry of the mathematical models of the carrier phases is strengthened. Therefore, ambiguity resolution can be also considered as part of the mathematical modelling of the carrier phases.

The concept of ambiguity resolution has its origins in VLBI data processing (Rogers *et al.*, 1978). At the very beginning of GPS applications, the importance of ambiguity resolution for precise static relative positioning was emphasised (Counselman and Shapiro, 1979; Bossler *et al.*, 1980). For kinematic positioning, techniques for ambiguity resolution on-the-fly (AROF) were then introduced, with which the integer ambiguity can be resolved when receivers are in motion (Hatch, 1986, 1989,1990; Hwang, 1990; Loomis, 1989; Seeber and Wübbena, 1989).

An essential prerequisite for ambiguity resolution is that the ambiguity parameters to be identified are, in principle, distinguishable from other parameters. As discussed above, the ambiguity parameter in the raw GPS measurement (Equation 1.2) cannot be separated from the satellite and receiver clock errors. In some specific applications, such as attitude determination, dedicated GPS receivers can be connected to the same clock. Then, differencing the carrier phase measurements from a pair of receivers to a common satellite, called single-differencing procedure, can efficiently cancel out both satellite and receiver clock errors. In this case, therefore, the single-differenced (SD) integer ambiguities can be resolved.

Normally, every receiver has a built-in clock and thus, the single differencing procedure cannot cancel receiver clock errors. Consequently, in GPS data processing, the double-differencing procedure is commonly utilised to cancel the clock errors. Thus, ambiguity resolution actually is to determine the double-differenced (DD) integer ambiguity parameters. In GLONASS and integrated GPS and GLONASS positioning, however, a differencing procedure cancelling satellite and receiver clock errors results in the presence of both SD and DD ambiguities (Leick, 1998; Habrich, 1998; Rossbach and Hein, 1996). The problem here is that

the SD and DD ambiguities are theoretically inseparable (Section 6.3.1; Wang, 1998a and 1999). To deal with this problem, a feasible approach to GLONASS ambiguity resolution is required, which is an aim of this study.

1.6.4 Quality Control

The performance and quality of satellite positioning mainly refers to the *availability*, *precision, reliability,* and *integrity* of the positioning results. Availability refers to the percentage of time that the system is available for use in positioning, which is a major concern in real-time applications such as aircraft navigation. Availability, mainly maintained by the constellations of satellite systems and/or some augmented elements, will not be further discussed here. Precision, reliability and integrity are dependent on many aspects of the positioning process, such as the quality of receivers and ranging signals, positioning procedures, satellite constellation, environment conditions, modelling methods and much more. In quality control, the geometry of positioning solution and the quality of mathematical and stochastic models used in positioning are emphasised. The assessment of the model quality is often based on statistical theory. This type of assessment is known as *statistical quality control.*

Quality measures for the *precision* of positioning solutions have been very well documented. Commonly used terms are the DOPs (dilution of precision indicators) for point positioning (Wells, 1987), BDOPs for baseline relative positioning (Goad, 1987; Wang, 1994b), ADOPs specifically for ambiguity resolution (Teunissen, 1997). More rigorous definition of precision measures can be found in Cross *et al.* (1994) and Teunissen (1998).

It is known that the reliability of positioning results estimated with least-squares or Kalman filtering procedures is highly dependent on the correct definition of both the mathematical and stochastic models. Possible deficiencies in the stochastic model can be remedied using efficient stochastic modelling methods, such as the *Minimum Norm Quadratic Unbiased Estimation* (MINQUE) developed by Rao (1970, 1971, 1979). Common abnormal errors relating to mathematical models are outliers, cycle-slips and wrong ambiguities fixed in the final solution. These errors are not

taken into account in the models, called *mathematical model errors*, and thus, will bias final positioning results if they are included in the measurements.

A cycle-slip refers to a sudden jump of an integer number of cycles in the instantaneous accumulated carrier phase. Cycle-slips could be caused by many factors, such as obstructions of the ranging signals, malfunctioning receiver signal processing or atmospheric scintillation. Based on the fact that carrier phases vary smoothly, different empirical test quantities have been proposed to detect and repair possible cycle-slips (Bastos and Landau, 1988; Blewitt, 1990; Cross and Ahmad, 1988; Goad, 1985; Hilla, 1986; Lichtenegger and Hofmann-Wellenhof, 1989; Remondi, 1984; Westrop *et al.*, 1989). Detailed reviews of the cycle slip detection and repair methods can be found in Hofmann-Wellenhof *et al.* (1997) and Seeber (1993). Some modern receivers have built-in algorithms that eliminate the possibility of cycle slips (JPS, 1998). Actually, small cycle slips and outliers can be more rigorously treated using classic outlier detection methods such as *data-snooping* (Baarda, 1968; Wang and Chen, 1994a and 1994b) or a recently developed DIA (detection, identification and adaptation) procedure for kinematic positioning (Teunissen and Salzmann, 1989; Lu and Lachapelle, 1992). The testing statistics used in both the data snooping and DIA procedure are derived using the mean-shift principle (Wang *et al.*, 1997b).

For some specific real-time applications, such as aircraft navigation, the integrity of positioning systems is extremely important. Integrity refers to the ability of a system to provide timely warnings to users when the system should not be used for navigation. One of the integrity checking approaches is the so-called Receiver Autonomous Integrity Monitoring (RAIM), which is implemented by some designed failure (model error) detection and isolation (FDI) procedures (Brown, 1996). It is noted that both the FDI and DIA procedures are based on statistical testing (Salzmann, 1993; Gao, 1993; Sang and Kubik, 1997).

Since statistical testing is the tool used for the detection and identification (isolation) of the model errors or failures in the system, the key to the quality control is the performance of statistical testing, which is described by the internal and external *reliability* measures (Baarda, 1968, Cross *et al.*, 1994; Teunissen, 1998; Tiberius,

1998; Wang, 1994a). The *internal reliability* is defined by the Marginally Detectable (model) Errors (MDE). The *external reliability* is described by the largest positional MDE, which is the assessment of the effect of the undetected (mathematical) model errors on the final positioning results. Both the internal and external reliability measures are highly dependent on the accuracy of the measurements, the redundancy and geometry of the positioning systems. The mathematical description of these reliability measures can be found in Baarda (1968), Teunissen (1998) and Wang (1994a).

In precise relative positioning, the reliability of the positioning results also depends on the correct resolution of the carrier phase ambiguities. Ambiguity resolution consists of two steps, namely, ambiguity search and ambiguity validation. As part of the quality control procedure used in satellite positioning, ambiguity validation is critical for reliable positioning. Currently, in the field of ambiguity validation, although well documented ambiguity acceptance test procedures are available, a rigorous ambiguity discrimination test procedure is still lacking (Teunissen, 1996; Wang *et al.*, 1997a and 1998a), which is investigated in this thesis.

Given the data collected with available hardware, the accuracy and reliability of the final positioning results rely on the way how the data are processed. Therefore, modelling, ambiguity resolution, and statistical quality control are critical issues for robust GPS and GLONASS satellite positioning.

1.7 Contributions of This Study

In this study, the critical issues discussed in the last section have been investigated, with the focus being on the GPS, GLONASS and integrated GPS/GLONASS relative static and kinematic positioning modes. The major contributions of this study are briefly summarised as follows:

(a) Feasible mathematical models for use in GLONASS and integrated GPS/GLONASS relative positioning have been analysed. Based on both theoretical derivation and empirical experiments, an optimal mathematical model has been identified;

(b) A stochastic modelling procedure for static positioning has been proposed, which is based on a rigorous statistical method. With this new procedure, three different stochastic models have been tested and analysed;

(c) A real-time stochastic modelling method for kinematic positioning has been developed, in which the measurement filtering residuals are used to adaptively estimate the measurement covariance matrix. This proposed method can be implemented along with the standard Kalman filtering process, with no significant time delay in data processing;

(d) A linear model discrimination test procedure has been developed to validate resolved integer ambiguities. The test statistic used in the ambiguity discrimination test is constructed by the difference between the minimum and second minimum quadratic form of the measurement residuals and its derivation. The distribution of the proposed statistic has been theoretically identified, and thus, the confidence level for the ambiguity discrimination tests can be rigorously calculated;

(e) An approach to GLONASS ambiguity resolution, which is not sensitive to the biases in pseudoranges, has been developed. This new approach includes some critical strategies to cancel the receiver clock errors and search for the most likely single-differenced (SD) ambiguity.

1.8 Thesis Outline

This thesis consists of seven chapters. The contents of the following chapters are outlined as follows.

In Chapter 2, existing mathematical modelling methods for integrated GPS/GLONASS positioning are reviewed. The single-differencing (SD) and double-differencing (DD) procedures are theoretically analysed. Possible mathematical models and their relative redundancy in integrating GPS and GLONASS observations are presented. Based on the analysis of the ambiguity success rate and model sensitivity, the optimal model is identified.

Chapter 3 presents a stochastic modelling procedure for static GPS positioning. Following the introduction of the computational framework of the MINQUE method,

three different stochastic models for satellite measurements are analysed using a real static baseline data set.

Chapter 4 presents a real-time stochastic modelling method for kinematic positioning. This method is formulated within the framework of Kalman filtering. The test results with both GPS dual frequency and GPS/GLONASS single frequency data sets are described.

Chapter 5 presents a framework for ambiguity validation tests, including the acceptance test and discrimination test. Whilst the ambiguity acceptance test is constructed using classic statistical testing theory, the ambiguity discrimination test is treated as a comparison between non-nested linear models. A testing procedure is derived using the likelihood method and the artificial nesting method. The performance of the new ambiguity discrimination test procedure in ambiguity resolution is examined.

Chapter 6 emphasises an approach to GLONASS ambiguity resolution. A mathematical description of this approach and practical strategies for data processing are presented, and tested using GLONASS and integrated GPS/GLONASS data sets.

Finally, Chapter 7 presents conclusions and suggestions for future development of this research.

Chapter 2

MATHEMATICAL MODELS FOR INTEGRATED GPS AND GLONASS POSITIONING

2.1 Introduction

The main GPS relative positioning techniques are well established, having been successfully used for surveying and navigation applications for over a decade. The most attractive recent development is kinematic GPS positioning, which uses pseudorange and carrier phase measurements to resolve the carrier phase ambiguities almost instantaneously. Kinematic techniques improve productivity in surveying applications and also apply well to navigation. Reliable kinematic positioning results depend on the availability of a large number of GPS satellites. GPS kinematic positioning techniques, therefore, may not be feasible for some situations, such as positioning in built-up areas, where the number of visible satellites is limited (Stewart and Tsakiri, 1997). One possible scheme to increase the availability of satellites is to combine the GPS and GLONASS satellite systems.

The combination of the two systems offers the increases in accuracy and integrity gained by the doubling of visible satellites. Of the total of 48 satellites available from both systems, the number of satellites in view can reach 12 to 20 under good observing conditions (Kleusberg, 1990). The increase in satellite availability will also make fast static and kinematic positioning much more feasible than with each system alone (e.g. Ashkenazi *et al.*, 1995; Langely, 1997).

The combination of GPS and GLONASS measurements inevitably faces some incompatibility problems. Mainly these include differences in the coordinate datum, the time frame, the carrier phase frequencies, and the Selective Availability (S/A) in GPS measurements (e.g. Hein *et al.*, 1997; Leick, 1995; Mirsa *et al.*, 1996; Rossbach *et al.*, 1996). For short baselines, as discussed in Sections 1.4.4 and 1.4.5, the effects of the differences between GPS and GLONASS in the coordinate datum and the time frame are thought to be insignificant (e.g. Pratt *et al.*, 1997). A detailed discussion about the effects of the time frames is given in Landau and Vollath (1996). The

differencing procedure applied to the measurements from two receivers can effectively cancel out S/A effects in GPS measurements (e.g. Leick, 1995). Due to the multiple frequencies of the GLONASS carrier phases, however, the relative receiver clock errors cannot be cancelled in the double-differenced (DD) carrier phase measurements. In integrated GPS and GLONASS positioning, therefore, the standard DD procedure results in rank deficiency of the design matrix. Thus, the normal matrix becomes singular, indicating that meaningful positioning results cannot be achieved (see Appendix A). Therefore, a feasible modelling method must be developed, which is one aim of this study.

In this chapter, following a review of the existing modelling methods, the single- and double-differencing procedures are theoretically analysed. The mathematical models for integrating all the pseudorange and carrier phase measurements are presented. The performance of the different models is investigated using test data sets. The concept of the model sensitivity to the receiver clock parameters is introduced and employed to analyse the intrinsic structure of the models. Based on this model sensitivity analysis, the comparison of different models is made and the optimal model is then identified.

2.2 A Review of Existing Modelling Methods

To remove the singularity in the normal matrix caused by the standard double difference procedure in GLONASS carrier phase modelling, a number of methods have been proposed in the literature. These methods can be generally classified into two different groups: a) *eliminating* the receiver clock errors; and, b) *estimating* the receiver clock errors.

2.2.1 Eliminating Receiver Clock Errors

Three specific modelling methods have been proposed to remove the receiver clock error parameters in DD GLONASS carrier phase measurement equations.

The *first method* is to estimate the receiver clock errors from the single-difference (SD) pseudoranges and correct the DD carrier phase measurements accordingly (e.g. Raby and Daly, 1994; Pratt *et al.*, 1997). This method actually divides the parameter estimation into two stages. The estimated receiver clock parameters in the first stage

may be contaminated by large pseudorange errors. This will inevitably increase the uncertainty of the estimated coordinates and ambiguities in the second stage, because the clock parameters are treated as having known (true) values.

The s*econd method* is to scale carrier phases into distances or a chosen frequency (e.g. Leick *et al.*, 1995; Leick, 1998; Landau and Vollath, 1996). If this frequency is chosen as f_0 and its wavelength is λ_0, from Equation 1.2, double differenced carrier phase measurement equation is obtained as (e.g. Leick, 1998; Wang, 1998a):

$$\varphi_{km,\lambda_0}^{pq} \equiv \frac{\lambda_p}{\lambda_0}\varphi_{km}^{p} - \frac{\lambda_q}{\lambda_0}\varphi_{km}^{q} = \frac{1}{\lambda_0}\rho_{km}^{pq} + \frac{\lambda_p}{\lambda_0}N_{km}^{p} - \frac{\lambda_q}{\lambda_0}N_{km}^{q} \tag{2.1}$$

where φ_{km}^{p} and φ_{km}^{q} are respectively the single-differenced (SD) carrier phases (between stations k and m) for satellite p and q, with N_{km}^{p} and N_{km}^{q} being their (SD) ambiguities; ρ_{km}^{pq} is the double-differenced topocentric distances between the receivers (k, m) and the satellites (p, q). It is easy to see from Equation 2.1 that the choice of λ_0 is arbitrary. Scaling carrier phases to the specified frequency with the wavelength of λ_0=1m is equivalent to scaling carrier phases to distances. Although this method does cancel out the clock errors completely from DD measurement equations, the resulting DD ambiguities are unfortunately non-integers. One possible remedy for this deficiency is to estimate one of the SD ambiguity terms from pseudoranges and then correct the associated carrier phases (e.g. Leick *et al.*, 1995; Leick, 1998). However, correct estimate of the SD ambiguities relies on high quality pseudoranges. A more efficient approach is developed in Chapter 6, which is not sensitive to pseudorange errors.

The *third method* is designed to cancel out the clock errors and at the same time, to preserve the integer nature of the DD ambiguity parameters. This can be achieved when the following condition is met:

$$\lambda_0 = \frac{\lambda_p}{k_p} = \frac{\lambda_q}{k_q} \tag{2.2}$$

where k_p and k_q are integers (Rossbach and Hein, 1996). The disadvantage of this method is that magnitude of the resulting wavelengths is in the order of micrometers, and thus the associated integer ambiguities cannot be resolved. Leick (1998) recommends finding suitable factors k_p and k_q that can result in larger wavelengths. However, this remedy is unfeasible. As shown in Appendix B, for the GLONASS-GLONASS satellite pair, the largest possible value of λ_0 is 0.00126m for the current frequency allocation and 0.000593m for the final frequency plan. With such small wavelengths, it is still extremely difficult (if not impossible) to fix the associated ambiguities.

Therefore, the above mathematical modelling methods are either not rigorous or unfeasible for use in GLONASS or integrated GPS and GLONASS positioning.

2.2.2 Estimating Receiver Clock Errors

It has been noted that the rank deficiency existing in the DD carrier phase measurement equations can be removed by adding in the SD pseudorange measurements. This approach can produce an estimation of the (relative) receiver clock parameter, together with other parameters (Rapoport, 1997). Actually, if the SD pseudorange measurements are included in the mathematical models, it is also possible to combine DD and SD carrier phase measurements, in which the SD ambiguities are transformed into DD ambiguity parameters. This was first suggested by Walsh and Daly (1996), but explicitly derived by Kozlov and Tkachenko (1997) and see also Wang (1998a).

As commented by Kozlov and Tkachenko (1997), however, the above methods cannot guarantee reliable positioning results if the GPS-GLONASS DD carrier phase measurements are employed in the models. The reason is that the error sources of the GPS and GLONASS measurements are different. For example, inter-channel hardware biases in GLONASS measurements may have different size, but such biases in GPS measurements are all the same. Therefore, the difference between the error features of the GPS and GLONASS measurements should be considered as another critical incompatibility problem. To reduce the effects of this incompatibility in positioning, suitable SD and/or DD carrier phase and pseudorange

measurement combinations should be employed in data processing. The optimal combination should be less sensitive to this kind of incompatibility.

It has been found that the GPS-GPS and GLONASS-GLONASS DD carrier phase measurement combination, called *the separated DD carrier phase formulation,* is more reliable than the GPS-GLONASS DD carrier phase measurement combination, the so-called *the mixed DD carrier phase formulation* (e.g. Pratt *et al.*, 1997; Kozlov and Tkachenko, 1997). Similar to the DD carrier phase formulations, the pseudorange measurements from GPS and GLONASS can also be 'separated' in such a way to form the SD GPS and DD GLONASS or DD GPS and SD GLONASS pseudorange measurements (the clock parameters are excluded from the DD pseudorange measurement equations). It can be expected that each of these different pseudorange measurement formulations will have a different impact on the positioning solution.

In the mathematical models including receiver clock parameters, all the GPS and GLONASS measurements are processed together. Theoretically speaking, all the mathematical model formulations including the SD GPS (or GLONASS) pseudorange measurements are valid. These possible mathematical models may produce different solutions, however. The investigation of the performance of the different mathematical model formulations in positioning, in particular, in ambiguity resolution, and the identification of the optimal model are of great importance for integrated GPS and GLONASS positioning.

2.3 Mathematical Model Formulations

For high precision GPS relative positioning, single- and double-differencing strategies are favoured because the integer nature of the carrier phase ambiguities still remains (e.g. Bock *et al.*, 1986; Bossler *et al.*, 1980, Goad and Remondi, 1984; Remondi, 1985a and 1985b). These measurement formulations are also useful in integrated GPS and GLONASS data processing.

2.3.1 Single Differencing

To simplify the following discussion, the linear(ised) sets of m SD carrier phases and m SD pseudoranges measured between two receivers are expressed as

$$\phi_i = A_{\phi_i} x_{c_i} + B_{\phi_i} x_{t_i} + E_m x_k \tag{2.3}$$

$$r_i = A_{r_i} x_{c_i} + B_{r_i} x_{t_i} \tag{2.4}$$

where

ϕ_i and r_i are the $m \times 1$ vectors of the observed minus computed SD carrier phases and pseudoranges, respectively, at epoch i ;

x_{c_i} is the 3×1 vector containing baseline component unknowns at epoch i ;

x_{t_i} is the between receivers clock error parameter at epoch i ;

x_k is the $m \times 1$ vector of SD ambiguities;

A_{ϕ_i} and A_{r_i} are the $m \times 3$ SD design matrices relating to three baseline component unknowns for carrier phase and pseudorange measurements, respectively;

B_{ϕ_i} and B_{r_i} are the $1 \times m$ vectors containing the partials relating to the relative receiver clock parameter, for carrier phase and pseudorange measurements, respectively, i.e., $B_{\phi_i} = (\lambda_1^{-1}, \lambda_2^{-1}, \ldots, \lambda_m^{-1})^T$, where λ_j is the wavelength of the frequency utilised by satellite j, and $B_{r_i} = (1,1,\ldots,1)^T = l_m$;

E_m is an $m \times m$ unit matrix.

It is known that if only the SD carrier phase measurements, expressed by Equation 2.3, are used to form the normal matrix, it will be singular, which means that the SD ambiguity parameters theoretically cannot be separated from the clock error parameters (Teunissen and Kleusberg, 1996). The singularity can be removed by adding in the SD pseudorange measurements expressed by Equation 2.4 (Goad, 1996). In this situation, if four or more satellites are simultaneously tracked, single epoch data is enough to solve for all the unknown parameters. Theoretically speaking, if high precision pseudoranges are available and unmodelled systematic errors in the SD measurements are negligible, the SD ambiguities can be easily fixed to their correct integer values with currently available ambiguity resolution

techniques. In practice, however, the estimated SD ambiguities may be contaminated by initial phases (*ibid.*), destroying the integer nature of the SD ambiguities. Moreover, the accuracy of pseudorange measurements is much lower than carrier phase measurements. This results in a very high correlation between the relative receiver clock parameters and the SD ambiguities. Therefore, it is very difficult to separate the SD ambiguities from the relative receiver clock parameters. It is noted that the DD ambiguities can be more easily fixed to their integer values. This is because the DD ambiguities are integers by definition, and the correlation between the clock parameters and the DD ambiguity parameters are much lower.

Similar to the DD carrier phase measurement formulations, there are two possible options to form the DD ambiguities in the SD carrier phase measurement equations: a) the *mixed DD ambiguity formulation*, i.e., selecting only one GPS or GLONASS satellite as reference satellite; b) the *separated DD ambiguity formulation*, i.e., only GPS-GPS and GLONASS-GLONASS DD ambiguities are constructed (Kozlov and Tkachenko, 1997).

For instance, in the case of the mixed formulation, if satellite j is used as the reference satellite, the SD ambiguities are reparametrized as

$$x_k = \overline{E}_m x'_k \tag{2.5}$$

with

$$\overline{E}_m = \begin{bmatrix} 1 & 0 \\ l_{m-1} & E_{m-1} \end{bmatrix}, \tag{2.6}$$

$$x'_k = \begin{bmatrix} x_{k(j)} \\ \bar{x}_k \end{bmatrix}, \tag{2.7}$$

in which $x_{k(j)}$ is the SD ambiguity, and

$$\bar{x}_k = [x_{k(1)} - x_{k(j)}, \ldots, x_{k(m)} - x_{k(j)}]^T \tag{2.8}$$

is an $(m-1)\times 1$ DD vector of ambiguity parameters.

Whilst the DD ambiguity parameters are to be fixed to their integer values, the SD ambiguity parameter is still treated as a real-valued parameter. Inserting Equation 2.5 into Equation 2.3, the reparametrised SD carrier phase measurement equation is obtained as

$$\phi_i = A_{\phi_i} x_{c_i} + B_{\phi_i} x_{t_i} + \overline{E}_m x'_k \tag{2.9}$$

Another approach to convert the SD ambiguities into the DD ambiguities is differencing the estimated SD ambiguities, which may have some flexibility in its implementation (Kozlov and Tkachenko, 1997). It can be theoretically proved, however, that this approach is identical to the above SD ambiguity reparametrisation approach. From Equation 2.5, one can obtain

$$x'_k = \overline{E}_m^{-1} x_k \tag{2.10}$$

where

$$\overline{E}_m^{-1} = \begin{bmatrix} 1 & 0 \\ -l_{m-1} & E_{m-1} \end{bmatrix} = \begin{bmatrix} e_1 \\ D \end{bmatrix}, \tag{2.11}$$

where $e_1 = (1, 0, \ldots, 0)$ is a unit vector with one as its first element and D is the standard $(m-1)\times m$ double differencing operator matrix (Teunissen, 1997). Substitution of Equation 2.11 into Equation 2.10 gives

$$x'_k = \begin{bmatrix} x_{k(j)} \\ \bar{x}_k \end{bmatrix} = \begin{bmatrix} e_1 \\ D \end{bmatrix} x_k \tag{2.12}$$

thus,

$$\bar{x}_k = D x_k, \tag{2.13}$$

$$Q_{\bar{x}_k} = DQ_{x_k}D^T . \tag{2.14}$$

Equations 2.8, 2.13 and 2.14 show that the DD ambiguities obtained by differencing the estimated SD ambiguities are identical to the directly estimated DD ambiguities from the reparametrised SD measurement equations.

An advantage of using single differences is that all measurements have diagonal covariance matrices. The slight disadvantage is that the nuisance parameters, ie. x_{t_i} and $x_{k(j)}$, still remain in the models.

2.3.2 Double Differencing

The advantage of the double differencing procedure is that it can further remove the nuisance parameters in the SD measurement equations. The linearised sets of double-differenced carrier phase and pseudorange measurements reads

$$D\phi_i = DA_{\phi_i}x_{c_i} + DB_{\phi_i}x_{t_i} + E_{m-1}\bar{x}_k \tag{2.15}$$

$$Dr_i = DA_{r_i}x_{c_i} \tag{2.16}$$

In the case of the separated DD carrier phase measurement formulation, D is an $(m-2)\times m$ double differencing matrix with a special structure (see Equation 2.22).

It is noted that, unlike the situation of processing GPS data only, in combined GPS and GLONASS data processing, the relative receiver clock parameter cannot be removed from measurement Equation 2.15. This is because the GLONASS satellites transmit their signals using different frequencies. Therefore, there is a rank deficiency of one in the DD measurement equations expressed by Equations 2.15 and 2.16. The linear dependent combination of the column vectors of the design matrix is given by $(0, 1, -DB_{\phi_i})^T$, ie.

$$\begin{bmatrix} DA_{\phi_i} & DB_{\phi_i} & E_{m-1} \\ DA_{\dot{r}_i} & 0 & 0 \end{bmatrix} \begin{bmatrix} 0 \\ 1 \\ -DB_{\phi_i} \end{bmatrix} = \begin{bmatrix} 0 \\ 0 \end{bmatrix}. \tag{2.17}$$

That means that the DD ambiguities theoretically cannot be separated from the relative receiver clock parameters (Teunissen and Kleusberg, 1996). The rank deficiency in Equations 2.15 and 2.16 can be removed by using the SD GPS and GLONASS pseudoranges, or the DD GPS and SD GLONASS pseudoranges (e.g. Rapoport, 1997).

Actually, if the SD pseudoranges are included in the models, it is possible to integrate the DD and SD carrier phase measurements, in which the SD ambiguities should be reparametrized. Therefore, there are many mathematical models that can be used in combined GPS and GLONASS positioning.

2.3.3 Mathematical Models

To simplify the discussion, the following notation is employed to represent the different models :

$$[a][b]\_[c][d]\_[e] \tag{2.18}$$

where

- $[a]$ is the GPS pseudorange mode;
- $[b]$ is the GLONASS pseudorange mode;
- $[c]$ is the GPS carrier phase mode;
- $[d]$ is the GLONASS carrier phase mode;
- $[e]$ is the DD carrier phase or DD ambiguity formulation approach (reference) mode.

The measurement modes for $[a]$, $[b]$, $[c]$ and $[d]$ can be *S*, standing for the single-differencing mode or, *D*, standing for the double-differencing mode. $[e]$ can be *M*, standing for the mixed formulation approach or, *S*, representing the separated

formulation approach. For example, the notation *DS_DD_S* represents the model which uses the double-differenced GPS pseudorange, the single-differenced GLONASS pseudorange, GPS-GPS and GLONASS-GLONASS double-differenced carrier phase measurements and thus, the DD GPS and GLONASS ambiguities are formed separately.

With the above model formulation procedure, a total of 18 different models can be formed. It is noted in all experiments that the results of models *SS_SD_S*, *SD_SD_S* and *DS_SD_S* are identical to those of models *SS_DS_S*, *SD_DS_S*, and *DS_DS_S*. The possible reason for this is that these two groups of the models have a similar geometric structure. Therefore, only 15 models, listed in Table 2.1, need be analysed further.

Model Number	Model Name	Relative Redundancy
1	*SS_SS_S*	$3n_e$ - 2
2	*SS_SD_S*	$2n_e$ - 1
3	*SS_DD_S*	n_e
4	*SD_SS_S*	$2n_e$ - 2
5	*SD_SD_S*	n_e - 1
6	*SD_DD_S*	0
7	*DS_SS_S*	$2n_e$ - 2
8	*DS_SD_S*	n_e - 1
9	*DS_DD_S*	0
10	*SS_SS_M*	$3n_e$ - 2
11	*SS_DD_M*	$2n_e$ - 1
12	*SD_SS_M*	$2n_e$ - 2
13	*SD_DD_M*	n_e - 1
14	*DS_SS_M*	$2n_e$ - 2
15	*DS_DD_M*	n_e - 1

Table 2.1 Mathematical models for integrated GPS and GLONASS positioning

The relative redundancy for each model in kinematic mode is also presented in Table 2.1, in which n_e is the number of epochs in a solution. For example, if the number of the satellites is n_S, in the case of model 1, the number of the measurements is $n_e(2n_S - 1)$ and the number of the unknown parameters is $4n_e + n_S - 1$. Therefore,

the redundancy for model 1 is $n_e(2n_s-5)-n_s+1$. Similarly, in the case of model 9, the number of the measurements is $n_e(2n_s-3)$ and the number of the unknown parameters is $4n_e+n_s-2$, and thus, the redundancy for model 9 is $n_e(2n_s-7)-n_s+2$. Based on these derivations, the relative redundancy between models 1 and 9 is calculated as $2n_e-1$.

Among all the mathematical models listed in Table 2.1, models *SS_SS_S* and *SS_SS_M* have the highest redundancy, whereas models *SD_DD_S* and *DS_DD_S* have the lowest redundancy. It is noted that, although some models happen to have the same redundancy, such as models *DS_SD_S* and *DS_DD_M*, the internal structures of these models are different. Therefore, their performance in ambiguity resolution may be different. This will be discussed in the following section.

2.4 Model Performance in Ambiguity Resolution

As reliable ambiguity resolution is one of the critical steps in integrated GPS and GLONASS relative positioning, the performance of the different mathematical models in ambiguity resolution is of great interest. To compare the reliability of different models in ambiguity resolution, five test data sets, collected on different baselines with various satellite constellations, were processed. These data were collected by the author, in Perth, Western Australia, using two Ashtech GG24 GPS/GLONASS receivers. In this study, whilst GPS satellites are numbered in the range from one to 32, GLONASS satellites are numbered in the range from 33 to 56. In all the data sets, the cut-off elevation angle was set to ten degrees. The details of the test data sets are presented in Table 2.2.

Baseline Names	Baseline Length (meters)	GPS/ GLONASS Satellites	Data Span (minutes)	Data Interval (seconds)	Segments (seconds)	Survey Date
B-1	zero	5/5	10	1	1	22.7.97
B-2	223	7/3	20	1	5	11.12.97
B-3	285	6/4	20	1	5	09.02.98
B-4	425	7/3	25	1	10	15.02.98
B-5	1216	7/5	30	1	10	16.02.98

Table 2.2 Details of the five test data sets

In data processing, the true ambiguities for all measurement formulations were recovered from the whole data set, which was then divided into short segments with data spans ranging from one to ten seconds depending on the baseline length (see Table 2.2). All segments were further processed in the kinematic mode, which assumes an antenna is in motion (Section 1.5.3). In all the solutions, the standard deviations for one-way carrier phase and pseudorange measurements were set to 0.05 cycles and 1.0m (based on Seeber, 1993, p.290) , respectively. Based on the statistics obtained from the float solution, the best ambiguity set was identified using the LAMBDA ambiguity search method (Teunissen, 1993).

The best ambiguity sets were compared with the corresponding ambiguity values recovered from the whole data set. The correct rates of the best ambiguity sets were then calculated and are listed in Table 2.3. It should be noted that these numbers just vary with different data sets. Unlike the success rate of the ambiguity resolution, which may vary with different validation procedures, the correct ambiguity rates are not affected by mistakes in the ambiguity validation step, which is based on statistical testing procedures (Sections 5.3 and 5.4).

Model Number	Model Name	Correct rates of the best ambiguity sets (%)					Averaged Correct Rates (%)
		B-1	B-2	B-3	B-4	B-5	
1	*SS_SS_S*	100	88.3	72.1	90.6	97.8	89.8
2	*SS_SD_S*	100	88.3	72.1	90.6	97.8	89.8
3	*SS_DD_S*	100	88.3	72.1	90.6	97.8	89.8
4	*SD_SS_S*	100	94.2	96.3	96.6	98.9	97.2
5	*SD_SD_S*	100	94.2	96.3	96.6	98.9	97.2
6	*SD_DD_S*	100	94.2	96.3	96.6	98.9	97.2
7	*DS_SS_S*	100	96.7	96.3	96.6	97.8	97.5
8	*DS_SD_S*	100	96.7	96.3	96.6	97.8	97.5
9	*DS_DD_S*	100	96.7	96.3	96.6	97.8	97.5
10	*SS_SS_M*	98.5	91.2	86.3	94.6	28.3	79.8
11	*SS_DD_M*	98.5	91.2	86.3	94.6	28.3	79.8
12	*SD_SS_M*	100	82.1	84.2	95.3	90.6	90.4
13	*SD_DD_M*	100	82.1	84.2	95.3	90.6	90.4
14	*DS_SS_M*	99.2	86.3	99.6	100	9.4	78.9
15	*DS_DD_M*	99.2	86.3	99.6	100	9.4	78.9

Table 2.3 Correct rates of the best ambiguity sets

2.4.1 Comparison between Separated and Mixed DD Ambiguity or DD Carrier Phase Formulations

It can be seen from Table 2.3 that the performance of the models using the separated DD ambiguity or DD carrier phase formulations (models 1-9) is generally better than that of the models using the mixed DD ambiguity or DD carrier phase formulations (models 10-15). In the cases of the mixed formulations, the correct ambiguity rates vary largely from 9.4 percent to 100 percent. The reason is that the differences between the GPS and GLONASS frequencies are much larger that the differences between the GLONASS frequencies themselves. If any systematic errors in GLONASS measurements are significant, the separated formulations may eliminate these errors more effectively than the mixed formulations (e.g. Pratt *et al.*, 1997). However, it must be noted that Table 2.3 represents only a limited number of data sets. A geometric analysis of the 15 models is given in Section 2.5.

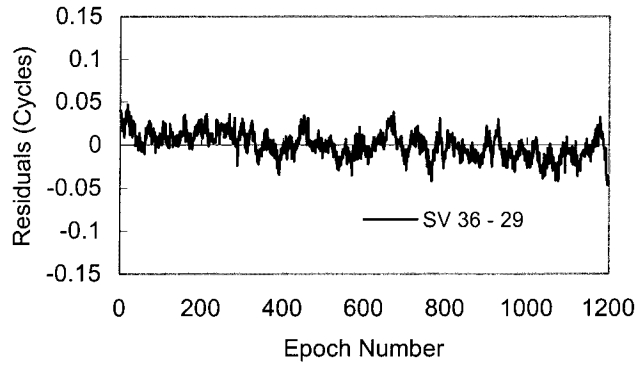

Figure 2.1 DD phase residuals from the B-3 data set

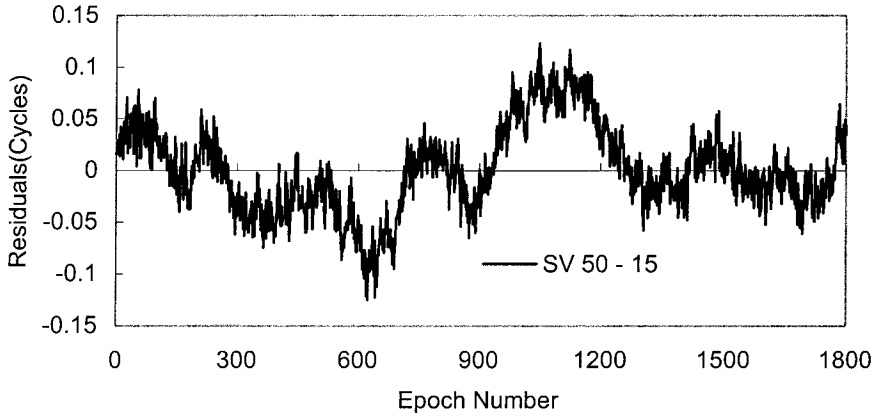

Figure 2.2 DD phase residuals from the B-5 data set

The remaining errors in GLONASS-GPS DD carrier phase measurements mainly come from the effects of inter-channel hardware delays and multipath. However, the inter-channel hardware delays are unpredictable, varying with the temperature of the receiver (e.g. Raby and Daly, 1993a and 1993b). For example, it can be seen from Figure 2.1 that the effects of the inter-channel hardware delays in the B-3 data set vary randomly with a slightly systematic trend. In the case of the B-5 data set, however, the DD phase residuals shown in Figure 2.2 indicate that these effects are significant, particularly during the period between epoch one and 600. Most likely, Figure 2.2 shows a combination of the inter-channel hardware delays and multipath. This can explain the fact that the models utilising the mixed DD ambiguity or DD carrier phase formulation can produce better results in the case of the B-3 data set, compared to the case of the B-5 data set.

2.4.2 Comparison Between Pseudorange Formulations

Similar to the models using the mixed DD carrier phase measurement formulation, models 1-3 and 10-11 using GPS and GLONASS SD pseudorange measurements only are generally worse than the models 4-9 and 12-15 (with ambiguity success rates 90 percent versus 97 percent and 80 percent versus 85 percent) due to the effects of the remaining systematic errors in the GLONASS pseudorange measurements. The models 4-9 and 12-15 employ either GPS or GLONASS SD pseudorange measurements, in conjunction with GPS and GLONASS carrier phase measurements.

As commented in the literature (e.g. Pratt *et al.*, 1997; Hall *et al.*, 1997), the effects of inter-channel hardware delays in the pseudorange measurements are significant, which can be seen in the test data sets. Although DD GPS and GLONASS pseudorange measurements are not used in all the models, they can be employed to indicate the large size of the effects of the inter-channel hardware delays. For example, for the same satellite pair SV 36-29 in the B-3 data shown in Figure 2.1, in Figure 2.3 there is approximately a one-metre shift in the DD pseudorange residuals, which may be caused by the inter-channel hardware delays. To compensate their effects in positioning with models 1-3 or 10-11, GLONASS pseudorange measurements should be properly down-weighted (e.g. Hall *et al.*, 1997; Kozlov and Tkachenko, 1997).

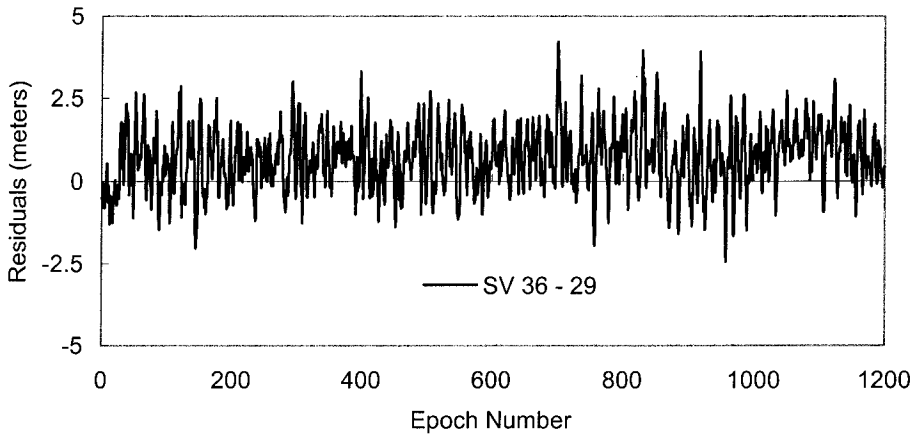

Figure 2.3 DD pseudorange residuals from the B-3 data set

2.4.3 Comparison Between the SD and DD Carrier Phase Formulations

For the models using the same pseudorange formulation, but using the *SS, SD* or *DD* carrier phase formulations defined by Equation 2.18, i.e., models grouped as 1-3, 4-6, 7-9, 10-11, 12-13 or 14-15, the correct ambiguity rates are the same. However, differences in the ambiguity discrimination test statistics (for a detailed discussion of ambiguity resolution quality control procedures, see Chapter 5, Sections 5.1 and 5.2) still exist between them, because they do have different levels of redundancy (see Table 2.1).

In ambiguity resolution, the F-ratio is commonly used as a discrimination test statistic (e.g. Pratt *et al.*, 1997; Walsh and Daly, 1997). The larger the F ratio, the more reliable the ambiguity resolution. Thus, the F-ratio differences between the models are of interest. For example, when models 14 and 15 are applied to the B-4 data set, both of them have a 100 percent ambiguity correct rate. However, the F-ratio values of model 15, shown in Figure 2.4 (represented by F15), are larger than the F-ratio values of model 14, with the differences between them ranging from 0.01 to 0.56.

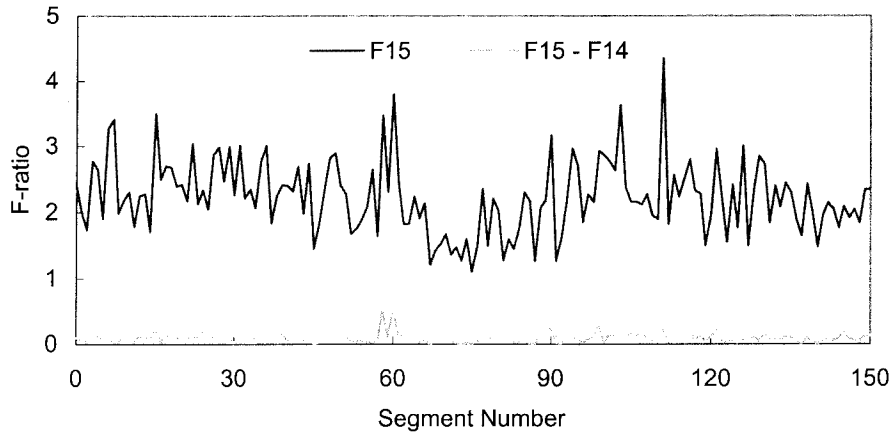

Figure 2.4 F-ratio values from the B-4 data set

Similar results were observed when a new ambiguity discrimination test statistic *Ws* called W-ratio (see, Section 5.4), was used in ambiguity resolution. Again, the larger the W-ratio, the more reliable the ambiguity resolution. The W-ratio values for models 14 and 15 are shown in Figure 2.5 (represented by W14, W15), indicating that, in most cases (81 percent), the models using the DD carrier phase formulation have bigger W-ratio values than the models using the SD carrier phase formulation.

Thus, the models with the higher redundancy may not always have a strong internal structure. In order to look into the intrinsic structures of the different models, the model sensitivity will be further investigated in the following section.

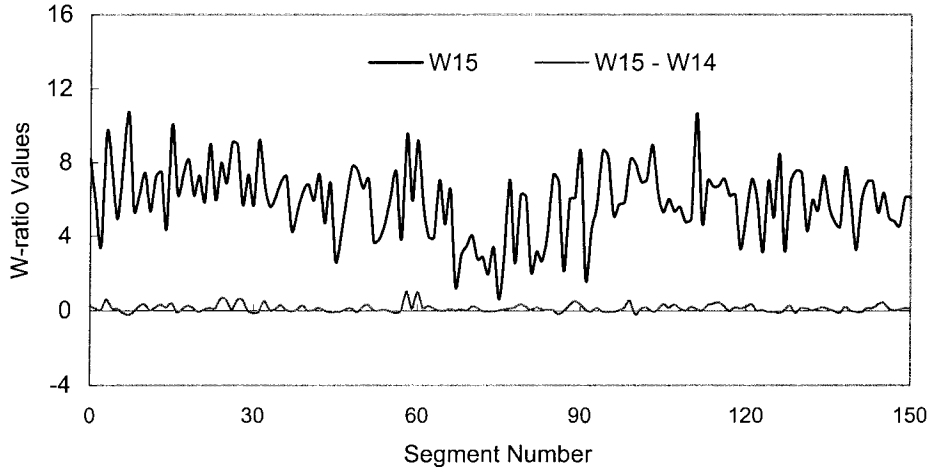

Figure 2.5 W-ratio values from the B-4 data set

2.5 Model Sensitivity with Respect to Receiver Clock Errors

2.5.1 Definition of the Model Sensitivity

When considering integrated GPS and GLONASS relative positioning, the control of the relative receiver clock errors is one of the critical issues. Because the receiver clock errors are unstable, it is difficult to model them properly. Instead, it is common to estimate them every epoch. It has been noted that the clock behaviour in the pseudorange and carrier phase measurements may be different (Langely, 1996), and hardware delays between the carrier phase and pseudorange channels may also exist (Goad, 1996). Due to these and other remaining errors in the SD or DD measurements, the estimated clock parameters may be biased (Leick, 1995). What one hopes is that the model parameters of interest, ie., the baseline components and the DD ambiguities, are not sensitive to the biased receiver clock parameters.

Generally speaking, the higher the correlation between the parameters in a model, the higher the sensitivity of the model to the parameters. Therefore, the model sensitivity can be measured by the correlation coefficients between the parameters. For the models used in integrated GPS and GLONASS positioning, the correlation between the receiver clock parameter, and the baseline components and the DD ambiguities is of direct interest.

Suppose the covariance matrix of the parameters x_{t_i}, x_{c_i} and $\bar{x}_k$ at epoch i is expressed as

$$Q_i = \begin{bmatrix} q_t & Q_{tck} \\ Q_{tck}^T & Q_{ck} \end{bmatrix}, \tag{2.19}$$

where q_t is the variance of x_{t_i}; Q_{ck} is the covariance matrix of x_{c_i} and $\bar{x}_k$; Q_{tck} is the vector of the covariances between x_{t_i} and x_{c_i} and $\bar{x}_k$. The (multiple) correlation coefficient between the receiver clock parameter and, the baseline component and the DD ambiguity parameters ($\rho_{t,ck}$), is defined as

$$\rho_{t,ck} = \sqrt{\frac{Q_{tck} Q_{ck}^{-1} Q_{tck}^{T}}{q_t}} \tag{2.20}$$

It is expected that each of the models listed in Table 2.1 may have a different model sensitivity, which can be used as an efficient tool for model evaluation.

2.5.2 Model Sensitivity Analysis for Test Data Sets

To compare the sensitivity of the different models with respect to receiver clock parameters, the correlation coefficients for the same test data sets discussed in Table 2.2 were calculated at every epoch. The averaged correlation coefficients are listed in Table 2.4.

Model Number	Model Name	Correlation Coefficients (averaged in a data set)					Averaged Correlation Coefficients
		B-1	B-2	B-3	B-4	B-5	
1	*SS_SS_S*	0.969	0.957	0.966	0.955	0.940	0.957
2	*SS_SD_S*	0.969	0.957	0.966	0.955	0.940	0.957
3	*SS_DD_S*	0.969	0.899	0.909	0.884	0.801	0.892
4	*SD_SS_S*	0.944	0.939	0.956	0.940	0.918	0.939
5	*SD_SD_S*	0.944	0.939	0.956	0.940	0.918	0.939
6	*SD_DD_S*	0.944	0.864	0.889	0.853	0.751	0.860
7	*DS_SS_S*	0.942	0.890	0.918	0.874	0.865	0.898
8	*DS_SD_S*	0.942	0.890	0.918	0.874	0.865	0.898
9	***DS_DD_S***	**0.942**	**0.782**	**0.815**	**0.750**	**0.675**	**0.793**
10	*SS_SS_M*	0.986	0.976	0.983	0.973	0.975	0.979
11	*SS_DD_M*	0.986	0.942	0.953	0.931	0.898	0.942
12	*SD_SS_M*	0.985	0.972	0.984	0.970	0.975	0.977
13	*SD_DD_M*	0.985	0.932	0.955	0.924	0.896	0.938
14	*DS_SS_M*	0.984	0.971	0.979	0.965	0.968	0.973
15	*DS_DD_M*	0.984	0.930	0.938	0.920	0.883	0.931

Table 2.4 Correlation coefficients $\rho_{t,ck}$ for the test data sets

Based on the correlation coefficients listed in Table 2.4, it can be concluded that:

(a) With the same pseudorange formulation, the models using the *mixed DD ambiguity and DD carrier phase formulations* are always more sensitive to receiver clock parameters than the models using *the separated DD ambiguity and DD carrier phase formulations*. For example, models 14 and 15 have an

averaged correlation coefficient 0.952, but for models 7, 8 and 9, the averaged correlation coefficient is only 0.863. This is consistent with the correct ambiguity rates shown in Table 2.3;

(b) With the same DD ambiguity or DD carrier phase formulation, the models using *DS* pseudorange formulation defined by Equation 2.18, have lower correlation than the models using the *SS* or *SD* formulation defined by Equation 2.18. For example, the average correlation coefficient for model 9 (*DS_DD_S*) is 0.793, but for model 3 (*SS_DD_S*), the averaged correlation coefficient reaches 0.893;

(c) With the same pseudorange formulation, the models using the *DD* carrier phase formulation have lower correlation coefficients than the models using the *SS or SD* carrier phase formulations defined by Equation 2.18. To show this more clearly, a segment of 180 epoch data in the B-4 data set was processed in kinematic mode using models 8, 9, 14, 15, respectively. The correlation coefficients were calculated at each epoch, which are shown in Figures 2.6 and 2.7, indicating that models 8 and 14 are more sensitive to the receiver clock errors than models 9 and 15, respectively. This can explain the fact that in the B-4 data set, the F-ratio values for model 15 are larger than those for model 14.

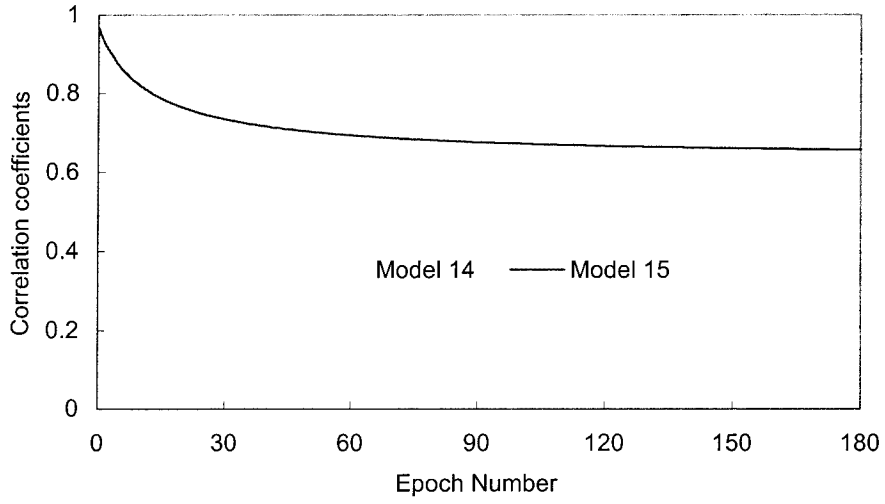

Figure 2.6 Correlation coefficients for models 14 and 15 (B-4 data set)

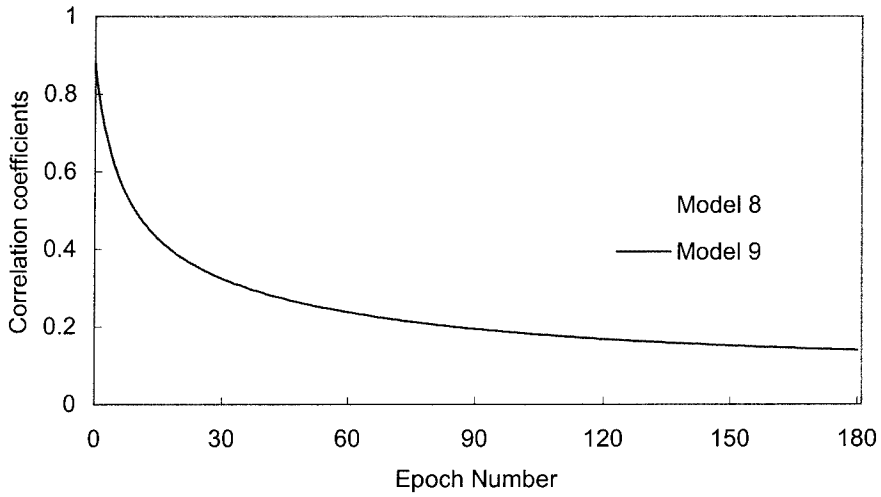

Figure 2.7 Correlation coefficients for models 8 and 9 (B-4 data set)

It is noted that, with the same pseudorange formulation, the models using the *SD* or *SS* carrier phase formulation, such as models 1 and 2, 7 and 8, have almost the same model sensitivity within the employed computing accuracy (these numbers should theoretically be different, for example, in the case of the B-4 data set, after 180 epochs, the difference is just 0.003). This is expected because, for the models using the SD and SS carrier phase formulation, the only difference between them is that the former includes one SD ambiguity nuisance parameter and the latter includes two SD ambiguity parameters. In addition, the correlation between the SD ambiguity parameters and other parameters is very high.

Similar to the case of GPS data processing, it is noted from Table 2.4 that the DD carrier phases are still the desirable quantities for integrated GPS and GLONASS data processing because they are less sensitive to clock errors than the SD carrier phases. This result is consistent with the comments by Leick (1995, p. 537). According to the sensitivity analysis results from the test data sets, model 9 (*DS_DD_S*) is the optimal model, which is highlighted in Table 2.4. It is this model that has been employed in commercial software for integrated GPS and GLONASS data processing (Rapoport, 1997).

2.5.3 Theoretical Results on the Model Sensitivity

The above model sensitivity analysis is based on the numerical results for specific data sets. One may ask how valid are the above conclusions and how much may these conclusions be geometry-dependent? The correct answer for this question requires much theoretical work to be conducted. The initial results in this direction have shown that the above conclusion (a) can be theoretically proved in the case of single epoch solutions, which is summarised as follows.

With the same pseudorange formulation defined by Equation 2.18, the models using the *SS*, *SD* or *DD* carrier phase formulation defined by Equation 2.18 are identical in the case of single epoch solutions. This can be easily proved using the Schaffrin-Grafarend theorem (Schaffrin and Grafarend, 1986). Therefore, in the case of single epoch solutions, only the models using the DD carrier phase formulation need to be further discussed here.

Suppose m_1 GPS satellites and m_2 GLONASS satellites are tracked and the one-way carrier phase measurements are independent and have the same variance α.
Define $\overline{D}_r$ as the pseudorange differencing operator matrix. For integrated GPS and GLONASS data processing, $\overline{D}_r$ has a special structure. For example, in the case of combining the DD GPS and SD GLONASS pseudoranges,

$$\overline{D}_r = \begin{bmatrix} D_1 & 0 \\ 0 & E_{m_2} \end{bmatrix}, \tag{2.21}$$

where D_1 is an $(m_1 - 1) \times m_1$ standard DD operator matrix and E_{m_2} is an $m_2 \times m_2$ unit matrix. The weight matrix for the differenced pseudoranges and carrier phase are P_r and P_ϕ, respectively.

Define $\overline{D}_\phi$ as the carrier phase differencing operator matrix, which can be the mixed or separated DD operator. In the case of the mixed DD carrier phase formulation, $\overline{D}_{\phi\_M}$ is a standard $(m-1) \times m$ DD operator matrix, where $m = m_1 + m_2$; in the case of the separated DD carrier phase formulation,

$$D_{\phi\_S} = \begin{bmatrix} D_1 & 0 \\ 0 & D_2 \end{bmatrix}, \tag{2.22}$$

where D_1 and D_2 are the $(m_1 - 1) \times m_1$ and $(m_2 - 1) \times m_2$ standard DD operator matrices, respectively. The weight matrices for the mixed and separated DD carrier phase formulations are

$$P_{\phi\_M} = \frac{1}{\alpha}(\overline{D}_{\phi\_M}\overline{D}_{\phi\_M}^T)^{-1}; \tag{2.23}$$

$$P_{\phi\_S} = \frac{1}{\alpha}(\overline{D}_{\phi\_S}\overline{D}_{\phi\_S}^T)^{-1}. \tag{2.24}$$

For a single epoch solution, the corresponding normal matrix is formed as

$$N = \begin{bmatrix} N_{cc} & N_{ct} & N_{ck} \\ N_{ct}^T & N_{tt} & N_{tk} \\ N_{ck}^T & N_{tk}^T & N_{kk} \end{bmatrix}, \tag{2.25}$$

with

$$N_{cc} = A_{\phi_i}^T \overline{D}_\phi^T P_\phi \overline{D}_\phi A_{\phi_i} + A_{r_i}^T \overline{D}_r^T P_r \overline{D}_r A_{r_i};$$

$$N_{tt} = B_{\phi_i}^T \overline{D}_\phi^T P_\phi \overline{D}_\phi B_{\phi_i} + B_{r_i}^T \overline{D}_r^T P_r \overline{D}_r B_{r_i};$$

$$N_{kk} = P_\phi;$$

$$N_{ct} = A_{\phi_i}^T \overline{D}_\phi^T P_\phi \overline{D}_\phi B_{\phi_i} + A_{r_i}^T \overline{D}_r^T P_r \overline{D}_r B_{r_i};$$

$$N_{ck} = A_{\phi_i}^T \overline{D}_\phi^T P_\phi;$$

$$N_{tk} = B_{\phi_i}^T \overline{D}_\phi^T P_\phi.$$

It can be proved that the multiple correlation coefficients are independent of the inverse of the covariance matrix. Using the normal matrix instead of the covariance matrix to derive the correlation coefficient is more convenient. The multiple correlation coefficient between x_{t_i} and x_{c_i}, x_k is calculated by

$$\rho_{t,ck}^2 = \frac{\overline{N}_{tck}\overline{N}_{ck}^{-1}\overline{N}_{tck}^T}{N_{tt}} = \frac{\gamma_1 + \gamma_2}{\gamma_3 + \gamma_2}, \tag{2.26}$$

with

$$\overline{N}_{tck} = \begin{bmatrix} N_{tc} & N_{tk} \end{bmatrix};$$

$$\overline{N}_{ck} = \begin{bmatrix} N_{cc} & N_{ck} \\ N_{ck}^T & N_{kk} \end{bmatrix};$$

$$\gamma_1 = B_r^T \overline{D}_r^T P_r \overline{D}_r A_r Q_{cc} A_r^T \overline{D}_r^T P_r \overline{D}_r B_r;$$

$$\gamma_2 = B_\phi^T \overline{D}_\phi^T P_\phi \overline{D}_\phi B_\phi;$$

$$\gamma_3 = B_r^T \overline{D}_r^T P_r \overline{D}_r B_r;$$

$$Q_{cc} = (A_r^T \overline{D}_r^T P_r \overline{D}_r \overline{A}_r)^{-1}.$$

For the mixed and separated DD carrier phase formulations, the corresponding (multiple) correlation coefficients are denoted as ρ_{t,ck_M} and ρ_{t,ck_S}, respectively. Therefore, initial theoretical results are given in theorem (2.1) below:

Theorem (2.1) (model sensitivity)
In the case of single epoch solutions, *for the same pseudorange formulation,*

$$\rho_{t,ck\_M} > \rho_{t,ck\_S} \tag{2.27}$$

Proof: see Appendix C.

Much theoretical work is needed to verify whether or not the above conclusions (a), (b) and (c) are geometry-dependent, which is beyond the scope of this study. Further research in this direction is discussed in Section 7.2.1.

2.6 Summary

The existing mathematical modelling methods for integrated GPS and GLONASS positioning have been reviewed. Based on the theoretical analysis of the single- and

double-differencing procedures, the possible mathematical models for integrated GPS and GLONASS pseudorange and carrier phase measurements and their relative redundancy have been presented. The performance of these mathematical models in terms of ambiguity resolution is different. For specific test data sets, the correct ambiguity rates of these models range from 78.9 percent to 97.5 percent. In addition, it has been theoretically proved that differencing the estimated SD ambiguities is equivalent to reparametrising the SD ambiguities as DD ambiguities in the models.

The concept of model sensitivity to the receiver clock parameters has been introduced. This has been used to evaluate the different mathematical models for integrated GPS and GLONASS positioning. As with the commonly used DOPs in GPS positioning, the measure of model sensitivity is independent of the real measurements and can be calculated before positioning is conducted. It has been shown that, similar to the case of GPS data processing, the DD carrier phases are still the desirable quantities for integrated GPS and GLONASS data processing because they are less sensitive to the clock errors than the SD carrier phases.

In the case of single epoch solutions, it has been theoretically proved that, the models using the mixed DD carrier phase or DD ambiguity formulation have a higher sensitivity to clock parameters than the models using the separated DD carrier phase or DD ambiguity formulation.

Based on the investigation into the model performance in ambiguity resolution and model sensitivity to the receiver clock errors, the optimal mathematical model has been identified. This model uses DD GPS and SD GLONASS pseudorange measurements and the GPS-GPS and GLONASS-GLONASS DD carrier phase measurements. This optimal mathematical model can deliver the best performance in ambiguity resolution.

Chapter 3

STOCHASTIC MODELLING FOR STATIC GPS POSITIONING

3.1 Introduction

In GPS relative positioning, double differenced GPS measurements are favoured because they can, to a large extent, cancel out many systematic errors and have a simplified functional model. In practice, however, stochastic modelling for double differenced GPS measurements is not trivial. Although major parts of the systematic errors can be modelled or cancelled out by differencing the GPS measurements between the satellites and receivers, residual (or unmodelled) systematic errors may be present (e.g. Bock *et al.*, 1986; Goad, 1987; Leick, 1995). In these cases, not only measurement random errors but also residual systematic errors, considered as randomised errors, may influence the stochastic models of GPS double differenced measurements.

As pointed out in Chapter 1, the widely used approach to construct the covariance matrices of GPS double differenced measurements is based on the variance-covariance propagation law. It is usually assumed that all the raw measurements are independent and have the same accuracy. Unfortunately, these assumptions are not realistic. The raw measurements are correlated and it is exactly on this fact that the double difference method is based (Gianniou, 1995; Roberts *et al.,* 1997; Miller *et al.*, 1997; Wang and Stewart, 1996). On the other hand, the accuracy of GPS measurements may change with different measuring conditions, such as the elevation angle of tracked satellites. Adopting incorrect stochastic models for double differenced measurements in GPS data processing will inevitably result in unreliable statistics for ambiguity resolutions and thus, biased positioning solutions (Cannon and Lachapelle, 1995). Therefore, it is appropriate to investigate the construction of appropriate covariance matrices for double differenced GPS measurements.

Recently, some effort has been made to improve the stochastic models used in GPS relative positioning. Euler and Goad (1991), Gerdan (1995), Jin (1996) and Han

(1997) have used an exponential formula to approximate the standard deviations of GPS measurements, which are considered to be dependent on the elevation angles of the tracked satellites. Based on the use of the signal-to-noise ratio, some similar exponential formulae have also been proposed to describe the error features of the satellite measurements (eg. Gianniou and Groten, 1996; Harting and Bruner, 1998; Barnes *et al.*, 1998; Talbot, 1988). In these exponential formulae, the coefficients are determined using empirical methods with experimental data. In Gianniou (1995), Newton's divided-difference method is used to evaluate the noise levels of GPS measurements, which in turn are used to directly construct the covariance matrix of the GPS double differenced measurements. With these methods, however, the statistical properties of the estimations are unclear.

Fortunately, in static or, even fast-static GPS relative positioning, redundant measurements are available, from which realistic covariance matrices can be estimated by using modern statistical methods. Geodesists have used some statistical methods to evaluate the accuracy of conventional angle, levelling, EDM measurements and GPS-derived baseline components; see, for example, Grafarend *et al.* (1980); Welsch (1981); Schaffrin (1983); Koch (1988); Chen *et al.* (1990); Sahin *et al.* (1992); Kuang (1993); Ananga *et al.* (1994). In this chapter, the most commonly used method for estimating variance-covariance components, MINQUE, will be employed to construct the covariance matrices of double differenced GPS measurements. Three different stochastic models for GPS measurements are to be tested and analysed with a static GPS baseline data set.

3.2 Computational Procedure of MINQUE

In the following Gauss-Markov model with n measurements and t unknowns:

$$l = Ax + v, \tag{3.1}$$

$$C = \sum_{i=1}^{k} \theta_i T_i, \tag{3.2}$$

l and v are $n \times 1$ vectors of the measurements and residuals, respectively; A is the $n \times t$ design matrix with $Rank(A) = t$; x is $t \times 1$ vector of the unknown parameters; $\theta_1, \theta_2, \ldots, \theta_k$ are the variance-covariance components of the measurements to be

estimated; k is the number of variance covariance components; and $T_1, T_2, \ldots, T_k$ are the so-called *accompanying matrices*, which will be discussed further in the next section. According to Rao (1970 and 1971), a minimum norm quadratic unbiased estimation of the linear function of $\theta_i\,(i = 1,2,\ldots\ldots,k)$, i.e., $g_1\theta_1 + g_2\theta_2 + \ldots + g_k\theta_k$, is the quadratic function $l^T Ml$ if the matrix M is determined by solving the following matrix trace minimum problem (Rao, 1971 and 1979)

$$Tr\{MCMC\} = \min, \tag{3.3}$$

Subject to

$$MA = 0, \tag{3.4}$$

$$Tr\{MT_i\} = g_i \quad (i = 1,2,\ldots,k) \tag{3.5}$$

where $Tr(\circ)$ is the trace operator of a matrix. Based on Equations 3.3, 3.4 and 3.5, the variance-covariance components can be estimated as (Rao, 1979):

$$\hat{\theta} = (\hat{\theta}_1, \hat{\theta}_2, \ldots, \hat{\theta}_k)^T = S^{-1}q, \tag{3.6}$$

where the matrix $S = \{s_{ij}\}$ with

$$s_{ij} = Tr\{RT_iRT_j\}, \tag{3.7}$$

and the vector $q = \{q_i\}$ with

$$q_i = l^T RT_i Rl, \tag{3.8}$$

and

$$R = C^{-1}[E - A(A^T C^{-1} A)^{-1} A^T C^{-1}], \tag{3.9}$$

where E is an $n \times n$ identity matrix. It is noted from Equations 3.6, 3.7, 3.8 and 3.9 that the estimated variance-covariance components depend on matrix C, which includes the variance-covariance components themselves. Therefore, an iterative process must be performed. Initially, an *a priori* value of θ_i is given by θ_i^0. With Equation 3.6, the initial estimate $\hat{\theta}^1$ is then obtained. In the $(j+1)th$ iteration, using the previous estimate $\hat{\theta}^j$ as the *a priori* values, the new estimate is:

$$\hat{\theta}^{j+1} = S^{-1}(\hat{\theta}^j)q(\hat{\theta}^j) \qquad (j = 0,1,2,.....), \tag{3.10}$$

which is called the iterated MINQUE. If $\hat{\theta}$ converges, the limiting value of $\hat{\theta}$ will satisfy the following equation:

$$S(\hat{\theta})\hat{\theta} = q(\hat{\theta}), \tag{3.11}$$

which can be further expressed as (Rao, 1979):

$$Tr\{R(\hat{\theta})T_i\} = l^T R(\hat{\theta})T_i R(\hat{\theta})l, \qquad (i = 1,2,...,k). \tag{3.12}$$

If all the matrices $T_1, T_2, \ldots, T_k$ are non-negative definite, a modified iterative procedure can be defined as (Rao and Kleffe, 1988):

$$\hat{\theta}_i^{j+1} = \hat{\theta}_i^j \frac{Tr\{R(\hat{\theta}^j)T_i\}}{l^T R(\hat{\theta}^j)T_i R(\hat{\theta}^j)l}, \qquad (i = 1, 2,..., k). \tag{3.13}$$

The advantage of the above modified procedure is that it can guarantee that the estimated variances are always positive. With given convergence tolerance δ_0, when the following inequalities hold:

$$\left|\hat{\theta}_i^{j+1} - \hat{\theta}_i^j\right| < \delta_0, \qquad (i = 1,2,\ldots,k), \tag{3.14}$$

the iteration process stops. From the above, it can be seen that one of the critical steps in using the MINQUE method is to construct the appropriate stochastic models as presented by Equation 3.2.

3.3 Stochastic Models of GPS Measurements

In this section, three different stochastic models, called *Models A*, *B* and *C*, respectively, will be discussed. *Model A* is a homoscedastic and uncorrelated error model, in which all the raw GPS measurements are assumed to be statistically independent and have the same variance. This is the most commonly used stochastic model in GPS data processing. *Model B* is a heteroscedastic and uncorrelated error model, in which the raw GPS measurements obtained from different satellites will be assigned with various variances, although they are still considered to be statistically independent. In *Models A* or *B*, with the estimated variances, the covariance matrices of the double differenced measurements are constructed by using variance-covariance propagation law. In *Model C*, the two assumptions involved in *Model A* do not hold and the variance-covariance components for the double differenced measurements are directly estimated. Therefore, *Model C* may considered as a heteroscedastic and correlated error model. For each model, formulae will be derived in the following.

3.3.1 Homoscedastic and Uncorrelated Error Model

Suppose m satellites are tracked at epoch i by two receivers. The raw GPS measurements collected from receivers 1 and 2 at epoch i are $\Phi_r = (\phi_r^1, \phi_r^2, \ldots, \phi_r^m)^T$, $r = 1, 2$, respectively. The double differenced measurements l for epoch i are, then, formed as

$$l(i) = D\Phi(i), \tag{3.15}$$

where $i = 1, 2, \ldots, s$ and s is the number of epochs in the processed session; $\Phi(i) = [\Phi_1^T(1), \Phi_2^T(i)]$; and the matrix D is the so-called *double-difference operator* (Bock *et al.*, 1986; Leick, 1995). If all the raw GPS measurements are assumed to be uncorrelated and have the same variance σ^2, the covariance matrix for the raw GPS

measurements at epoch i is $C_{Ai} = \sigma^2 E$, where E is a $(m-1)\times(m-1)$ identity matrix. The covariance matrix of the double differenced measurements is constructed with the variance-covariance propagation law as follows:

$$C_{l(i)} = DC_{Ai}D^T = \sigma^2 DD^T = \sigma^2 T_{li}, \tag{3.16}$$

$$\text{where } T_{li} = DD^T = \begin{bmatrix} 4 & 2 & . & 2 \\ 2 & 4 & . & 2 \\ . & . & . & . \\ 2 & 2 & . & 4 \end{bmatrix}. \tag{3.17}$$

For a session solution with s epochs of data, the covariance matrix of all the double differenced measurements is $C = \theta_1 T_1$, where

$$T_1 = diag(T_{li}), \quad (i = 1,2,\ldots,s). \tag{3.18}$$

Obviously, $\theta_1 (= \sigma^2)$ is a unique unknown in *Model A*. With Equation 3.6, the MINQUE estimator of the variance σ^2, denoted as $\hat{\sigma}^2$, is represented as:

$$\theta_1 = \hat{\sigma}^2 = \frac{l^T R T_1 R l}{Tr\{R T_1 R T_1\}} = \frac{v^T T_1^{-1} v}{n-t}, \tag{3.19}$$

which has been proved in Koch (1988, p. 276). If σ^2 is considered as an *a priori* variance factor in *Model A*, $T_1^{-1} = P$ is the corresponding weight matrix. Therefore, Equation 3.19 is identical with the formula for computing the estimate of the variance factor in the least-squares solutions. Moreover, it is noted from Equation 3.19 that the estimate of σ^2 is independent of its initial value and, hence, no iteration is needed in *Model A*.

3.3.2 Heteroscedastic and Uncorrelated Error Model

In *Model B*, the raw GPS measurements are assigned with different variances. These variances are defined as a function of specific factors that may impact the

measurement accuracy, such as satellite elevation angles, signal-to-noise ratios and multipath. Unknown parameters in the function are estimated using the MINQUE method. Theoretically, this type of function is very difficult to construct due to incomplete knowledge of the error sources. In practice, the variances of raw GPS measurements could be approximated as a function of the satellite elevation angles as:

$$\sigma^2_{\phi^s_r(i)} = a^2 + b^2 \cdot f(h^j_r(i)), \tag{3.20}$$

where, a^2 and b^2 are the unknown constant terms; $h^j_r(i)$ is the elevation angle under which satellite j is tracked from receiver r at epoch i; and $f(h^j_r(i))$ is the *accuracy diluting function* (ADF). Assuming there are no spatial correlations existing in the GPS measurements, the covariance matrix of the double differenced measurements at epoch i is constructed by using variance propagation law as:

$$C_{l(i)} = a^2 \cdot T_{1i} + b^2 \cdot T_{2i}, \tag{3.21}$$

where $T_{1i} = DD^T$ as presented by Equation 3.17; and

$$T_{2i} = \begin{bmatrix} f_{1i} + f_{2i} & f_{1i} & f_{1i} & \cdot & f_{1i} \\ f_{1i} & f_{1i} + f_{3i} & f_{1i} & \cdot & f_{1i} \\ \cdot & \cdot & \cdot & \cdot & \cdot \\ f_{1i} & f_{1i} & f_{1i} & \cdot & f_{1i} + f_{mi} \end{bmatrix}, \tag{3.22}$$

and $f_{ji} = f(h^j_1(i)) + f(h^j_2(i))$, $j = 1,2,\ldots, m$. Letting $\theta_1 = a^2$ and $\theta_2 = b^2$, the covariance matrix of all the double differenced measurements for a session solution with s epochs of data is $C = \sum_{i=1}^{2} \theta_j T_j$, where $T_j = diag(T_{ji})$, $j = 1,2$; $i = 1,2,\ldots,s$. In *Model B*, therefore, there are two unknown variance components that need to be estimated. Since both accompanying matrices T_1 and T_2 are non-negative definite, Equation 3.13 can be used.

3.3.3 Heteroscedastic and Correlated Error Model

The philosophy behind *Model C* is to directly estimate every element of the covariance matrix for the DD measurements without making the unrealistic assumptions used in *Models A* and *B*. Therefore, *Model C* can be expected to be more reliable than *Models A* and *B*.

Define $r = m - 1$ as the number of double differenced measurements at epoch i. The covariance matrix of the double differenced measurements at epoch i is represented by:

$$C_{l(i)} = \begin{bmatrix} \sigma_{11}^2 & \sigma_{12} & . & \sigma_{1r} \\ \sigma_{21} & \sigma_{22}^2 & . & \sigma_{2r} \\ . & . & . & . \\ \sigma_{r1} & \sigma_{r2} & . & \sigma_{rr}^2 \end{bmatrix} = \sum_{j=1}^{k} \theta_j T_{ji}, \tag{3.23}$$

where

$$\begin{aligned} \theta &= (\theta_1, \theta_2, \ldots, \theta_k)^T \\ &= (\sigma_{11}^2, \sigma_{22}^2, \ldots, \sigma_{rr}^2, \sigma_{12}, \sigma_{13}, \ldots, \sigma_{1r}, \sigma_{23}, \ldots \sigma_{2r}, \ldots\ldots, \sigma_{(r-1)r})^T, \end{aligned} \tag{3.24}$$

is the vector of the unknown variance and covariance components; and

$$T_{1i} = \begin{bmatrix} 1 & 0 & . & 0 \\ 0 & 0 & . & 0 \\ . & . & . & . \\ 0 & 0 & . & 0 \end{bmatrix}, \; T_{2i} = \begin{bmatrix} 0 & 0 & . & 0 \\ 0 & 1 & . & 0 \\ . & . & . & . \\ 0 & 0 & . & 0 \end{bmatrix}, \; \ldots\ldots, \; T_{ri} = \begin{bmatrix} 0 & 0 & . & 0 \\ 0 & 0 & . & 0 \\ . & . & . & . \\ 0 & 0 & . & 1 \end{bmatrix}, \tag{3.25a}$$

$$T_{(r+1)i} = \begin{bmatrix} 0 & 1 & 0 & . & 0 & 0 \\ 1 & 0 & 0 & . & 0 & 0 \\ 0 & 0 & 0 & . & 0 & 0 \\ . & . & . & . & . & . \\ 0 & 0 & 0 & . & 0 & 0 \\ 0 & 0 & 0 & . & 0 & 0 \end{bmatrix}, \; T_{(r+2)i} = \begin{bmatrix} 0 & 0 & 1 & . & 0 & 0 \\ 0 & 0 & 0 & . & 0 & 0 \\ 1 & 0 & 0 & . & 0 & 0 \\ . & . & . & . & . & . \\ 0 & 0 & 0 & . & 0 & 0 \\ 0 & 0 & 0 & . & 0 & 0 \end{bmatrix}, \ldots, \tag{3.25b}$$

$$T_{ki} = \begin{bmatrix} 0 & 0 & 0 & . & 0 & 0 \\ 0 & 0 & 0 & . & 0 & 0 \\ 0 & 0 & 0 & . & 0 & 0 \\ . & . & . & . & . & . \\ 0 & 0 & 0 & . & 0 & 1 \\ 0 & 0 & 0 & . & 1 & 0 \end{bmatrix}, \tag{3.25c}$$

are the so-called *accompanying matrices*. $k = r(r+1)/2$ is the number of the unknown variance and covariance components in *Model C*. For a session solution with s epochs of data, the covariance matrix of all the double differenced measurements is $C = \sum_{j=1}^{k} \theta_j T_j$, where $T_j = diag(T_{ji})$, $i = 1,2,\ldots,s$ and $j = 1,2,\ldots,k$. It is evident that *Model C* will be computationally intensive as the number of GPS measurements increase.

3.4 Test Results and Analysis

A GPS static baseline data set was used to test the performance of the various stochastic models in GPS static data processing. The data were collected on November 18 1996, in Perth, Australia, using two Leica System 300 dual frequency GPS receivers. The baseline length was about 1km and the data sampling rate was 15 seconds. The cut-off elevation angle was set to 15 degrees. During the session of 35 minutes, the same six satellites were tracked. This data set was first processed using dual frequency data to recover the true ambiguity values, which were then used to check the correctness of the resolved ambiguities from the tests.

3.4.1 Residual Analysis

The least-squares residuals (from ambiguity-float solution) of the L1 double differenced (DD) phase measurements, from two satellite pairs (SV 19-18, 19-29), are displayed in Figure 3.1, which demonstrates that GPS measurements observed from different satellites do have different noise levels. Using *model C*, the whole covariance matrix for all the L1 DD carrier phase measurements is estimated and listed in Table 3.1, which clearly shows that the DD carrier phase measurements do have different variances. For example, the standard deviations for the satellite pairs SV 19-18 and 19-29 have been estimated as 0.002m and 0.005m, respectively. Using *Model A*, however, the standard deviation for all the DD measurements was

estimated as 0.005m. Furthermore, it is noteworthy that the correlations in the estimated covariance matrix range from 0.02 to 0.39, while in *Model A*, the correlations are always equal to 0.50. Therefore, simply assigning the same variance to all the measurements and assuming that they are statistically dependent cannot truly reflect reality.

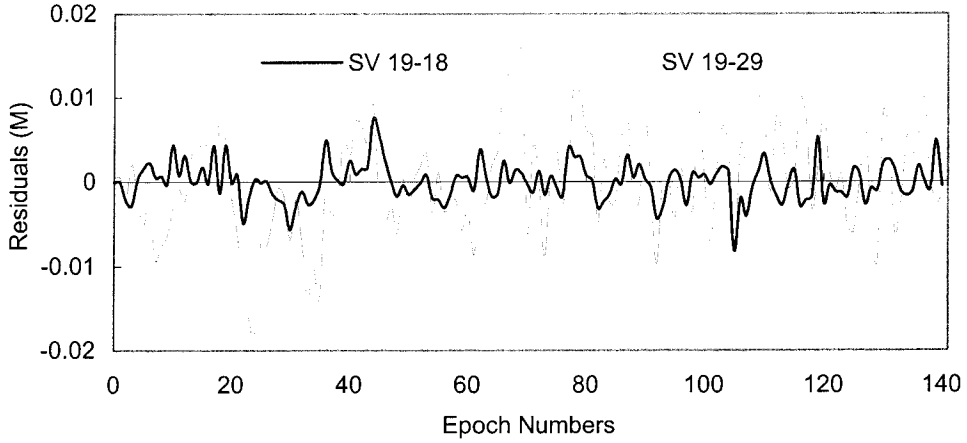

Figure 3.1 Comparison of L1 DD phase residuals from two satellite pairs

Satellite Pairs	SV 19-04	SV 19-18	SV 19-24	SV 19-25	SV 19-29
SV 19-04	0.1065	0.0279	0.0084	0.0210	0.0178
SV 19-18	0.0279	0.0472	0.0256	0.0247	0.0307
SV 19-24	0.0084	0.0256	0.2169	0.0308	0.0712
SV 19-25	0.0210	0.0247	0.0308	0.0983	0.0657
SV 19-29	0.0178	0.0307	0.0712	0.0657	0.2803

Table 3.1 Estimated variance and covariance components for GPS L1 DD carrier phase measurements ($\times 10^{-4}$ m^2)

3.4.2 Relation Between Accuracy and Elevation

The estimated standard deviations for L1 and L2 DD phase measurements with *Model C* and the corresponding satellite elevation angles are listed in Table 3.2. It is noted from this data set that the accuracy of the GPS measurements is closely related to the satellite elevation angle. Because the wavelength of L2 signal is longer than that of L1 signal, as indicated in Table 3.2, the L1 phase measurements are generally more precise than the L2 phase measurements.

The relationship between the true variances of the GPS measurements and the satellite elevation angles cannot be exactly formulated due to other unknown factors, such as multipath. Generally, the lower the satellite elevation, the bigger the variance of the measurements. For simplicity, the following accuracy diluting functions were used in *Model B,*

$$f_1(h) = h^{-2}, \tag{3.26a}$$

$$f_2(h) = \exp(-h), \tag{3.26b}$$

$$f_3(h) = [\sin(h)]^{-1}. \tag{3.26c}$$

In functions (3.26a) and (3.26b) the elevation angle h is scaled by ten (degrees), while in function (3.26c) the elevation angle h must be converted into radian values.

Satellite Pairs	L1 Phase Std Deviations (m)	L2 Phase Std Deviations (m)	Averaged Satellite Elevation (Degrees)
SV 19-04	0.003	0.004	41.4
SV 19-18	0.002	0.003	61.6
SV 19-24	0.005	0.005	26.0
SV 19-25	0.003	0.004	34.9
SV 19-29	0.005	0.007	31.4

Table 3.2 Relation between GPS measurement accuracy and satellite elevation angle (model C)

In data processing, besides the whole session solution, the data set was also divided into seven batches of five minutes. Therefore, the total of eight solutions were computed for L1 and L2 frequency data, respectively. In each solution, the stochastic models *A*, *B* and *C* were tested. Since the results of L1 and L2 phase measurements are very similar, the results related only to L1 data are shown below.

Table 3.3 demonstrates the estimated coefficients for *Model B.* As expected, the coefficients vary for different accuracy diluting functions because the functions expressed by Equations 3.26a, 3.26b, 3.26c have different curvatures. For all these accuracy diluting functions, however, the coefficient b is always much larger than

the coefficient a. This means that for the tested data set, the accuracy of the measurements strongly depends on the satellite elevation angles.

Solution Numbers	Length of data (Min.)	$f_1(h)$		$f_2(h)$		$f_3(h)$	
		a	b	a	b	a	b
1	5	0.02	0.74	0.09	1.11	0.03	0.16
2	5	0.02	0.86	0.10	1.13	0.04	0.18
3	5	0.05	0.61	0.10	0.83	0.03	0.13
4	5	0.04	0.60	0.09	0.84	0.03	0.13
5	5	0.02	0.74	0.10	1.09	0.03	0.15
6	5	0.07	0.70	0.12	0.97	0.03	0.15
7	5	0.01	0.66	0.08	0.99	0.02	0.14
8	35	0.02	0.82	0.11	1.03	0.03	0.17

Table 3.3 Estimated coefficients for *model B* ($\times 10^{-2}$ m)

3.4.3 Accuracy of Float Ambiguities

Table 3.4 shows the determinants (times 10^8) of the ambiguity covariance matrix estimated with the three stochastic models *A*, *B* and *C*. According to Teunissen (1997, p. 520), the volume of ambiguity search space depends on these determinants. The smaller the determinant, the smaller the search space and the faster the ambiguity search process.

Solution Numbers	Length of data (Min.)	Model A	Model B			Model C
			$f_1(h)$	$f_2(h)$	$f_3(h)$	
1	5	64.91	26.45	24.07	41.47	16.87
2	5	110.90	48.47	26.75	74.35	6.55
3	5	21.75	10.46	10.06	14.38	4.41
4	5	36.02	7.34	6.99	12.66	4.36
5	5	39.37	16.22	14.30	25.62	9.24
6	5	39.62	16.83	15.24	24.70	6.82
7	5	25.23	7.25	5.66	14.19	1.56
8	35	0.0018	0.0007	0.0005	0.0011	0.0004

Table 3.4 Determinant of ambiguity covariance matrix ($\times 10^8$)

From Table 3.2, it is clearly indicated that *Models B* and *C* produce much smaller ambiguity search spaces than the commonly used *Model A*. Compared with *Model A*, for example, the use of *Model C* has reduced the determinant of the ambiguity

covariance matrix by 84 percent. More accurate estimation of the floated ambiguity will be of importance for reliably resolving carrier phase integer ambiguities.

3.4.4 Reliability of Resolved Ambiguities

In ambiguity resolution, a significant difference between the best and second best ambiguity combination is critical for assuming the reliability of the resolved ambiguities. The *F*-ratio is commonly used as an ambiguity discrimination statistic (see more discussions in Section 5.1). Calculated *F*-ratio values are listed in Table 3.5. The larger the *F*-ratio value, the more reliable the ambiguity resolution. The critical value of the *F*-ratio is commonly chosen to be 2.0 (e.g. Landau and Euler, 1992). If *Model A* is used, one solution will be rejected at this critical value. However, if *Models B* or *C* are used, all the solutions are accepted. Compared with the averaged *F*-ratio value for the ambiguity resolution using *Model A*, the averaged *F*-ratio value for the ambiguity resolution using *Model C* is increased by 62 percent, and thus, the reliability of the resolved ambiguity is improved. Overall, the computed *F*-ratio value is higher for *Model C*.

Solution Numbers	Length of data (Min.)	Model A	Model B			Model C
			$f_1(h)$	$f_2(h)$	$f_3(h)$	
1	5	2.92	3.40	3.15	3.20	4.07
2	5	2.09	2.13	2.61	2.10	3.35
3	5	2.43	2.79	2.92	2.58	2.68
4	5	3.83	5.86	5.86	4.61	7.86
5	5	2.87	2.88	2.97	2.90	3.17
6	5	2.71	3.73	3.80	3.19	4.27
7	5	1.95	2.45	2.62	2.16	3.80
8	35	23.76	36.55	36.64	29.93	39.97

Table 3.5 *F*-ratio values in ambiguity validation tests

The ambiguity validation tests can be also based on the newly developed statistic *W*-ratio (W_λ) presented in Chapter 5. The *W*-ratio values are listed in Table 3.6. Similar to the *F*-ratio statistic, the larger the *W*-ratio value, the more reliable the ambiguity resolution. Overall, the computed *W*-ratio value is higher for *Model C*.

Solution Numbers	Length of data (Min.)	Model A	Model B			Model C
			$f_1(h)$	$f_2(h)$	$f_3(h)$	
1	5	6.81	6.44	6.00	7.26	7.54
2	5	4.66	4.31	5.06	4.26	6.64
3	5	4.79	5.46	5.71	5.05	5.16
4	5	8.07	10.48	10.56	8.92	12.27
5	5	6.62	6.59	6.79	6.65	6.78
6	5	5.42	7.55	7.63	6.31	7.87
7	5	3.51	4.66	5.05	4.00	7.18
8	35	62.75	77.84	77.86	69.89	82.01

Table 3.6 *W*-ratio values in ambiguity validation tests

3.4.5 Relative Efficiency of Baseline Estimation

It should be noted that the covariance matrix of GPS measurements estimated from the ambiguity-float solution may not fit the associated ambiguity-fixed solution particularly well, because in ambiguity-float solutions unknown ambiguity parameters may absorb some residual systematic errors in GPS measurements. It will be wise to reconstruct the covariance matrix using *Models B or C* for ambiguity-fixed solutions.

Solution Numbers	Length of data (Min.)	Model A	Model B			Model C
			$f_1(h)$	$f_2(h)$	$f_3(h)$	
1	5	1.00	1.18	1.27	1.06	3.35
2	5	1.00	1.16	1.31	1.03	3.73
3	5	1.00	1.15	1.60	1.05	1.90
4	5	1.00	1.07	1.05	1.02	1.86
5	5	1.00	1.15	1.19	1.06	1.56
6	5	1.00	1.17	1.15	1.09	2.35
7	5	1.00	1.31	1.38	1.13	1.77
8	35	1.00	1.17	1.28	1.11	1.32

Table 3.7 Relative efficiency of baseline component estimations

In the ambiguity-fixed solutions, the performance (goodness) of *Models B or C* relative to *Model A* can be measured by a ratio. This ratio is of the determinants of the covariance matrices of the baseline components estimated with *Model A* and *Model B* (or *C*), the so-called *relative efficiency* (e.g. Bloomfield and Watson, 1975). The relative efficiency values, listed in Table 3.7, indicate that *Models B* or *C*, are

better than *Model A*. Furthermore, the realistic covariance matrix of the baseline components obtained using *Models B* or *C* is of great help in any consequent network adjustment. It is also noted that in this data set, the largest difference between the baseline components estimated using *Model A* and *Model C* reaches 0.004m.

The results listed in Tables 3.4, 3.5, 3.6 and 3.7 have also demonstrated that, among three different *accuracy diluting functions* used in *Model B*, the decaying exponential function can be generally identified as the best one, based on the results from this data set. It is evident that, overall, *Model C* is better than *Models B* and *A*. This is as expected, because *Model C* is theoretically more rigorous than *Models B* and *A*.

3. 5 Summary

In GPS data processing, the common practice of assigning the same variance to all the raw measurements and assuming they are statistically independent is not realistic. Unrealistic stochastic models will inevitably lead to biased statistics for ambiguity resolution and positioning results.

In this chapter, three different stochastic models, namely *Models A, B* and *C*, have been tested and analysed. The unknown parameters in these stochastic models are estimated using the MINQUE method. Therefore, the estimated stochastic parameters have well defined statistical properties. Test results indicate that using *Models B* or *C*, the volume of ambiguity search space is reduced and the reliability of the ambiguity resolution is improved. For the tested data set, *Model C* reduces the determinant of the ambiguity covariance matrix by 84 percent and increases the *F*-ratio value by 62 percent, compared with *Model A*. In ambiguity-fixed solutions, *Models B* or *C* can produce more efficient baseline component estimations than *Model A*. Among the three different stochastic models, *Model C* is generally identified as the best one. It should be pointed out that the stochastic modelling method discussed above is designed for static post-processing applications. The MINQUE method is computationally intensive. With current computer technology, the proposed modelling algorithms might be not feasible for real-time applications. This issue will be further discussed in the next chapter.

Chapter 4

STOCHASTIC MODELLING FOR KINEMATIC POSITIONING

4.1 Introduction

In kinematic positioning, state parameters may include the position of a moving platform and other parameters of interest, such as unknown carrier phase ambiguities. The determination of these parameters is achieved by continuously tracking GPS/GLONASS satellites in view and taking a series of measurements (code pseudoranges and carrier phases) to the satellites at constant intervals or epochs. The real-time estimates of the state parameters can be performed using the *Kalman filtering* technique (e.g. Chen, 1994; Gao *et al.*, 1996; Landau and Euler, 1992; Qin *et al.*, 1992).

With the Kalman filtering technique, the state parameters can be not only estimated recursively in real-time mode, but also have statistically defined optimal properties. It is well known, however, that the optimum filtering results are highly dependent on the correctness of the adopted stochastic models. In practice, stochastic modelling for code and carrier phase measurements is not trivial, in particular for real-time applications.

In Chapter 3, the modern statistical method MINQUE has been applied to estimate the covariance matrix for the double differenced GPS measurements. Although the MINQUE method has some very well defined properties, it requires an iterative procedure and the number of required iterations depends on the properties of the data and the models themselves. Thus, this method is unsuitable for real-time kinematic positioning.

Some empirical stochastic modelling methods do meet the requirements of real-time calculation. For example, based on the assumption that the accuracy of one-way measurements is dependent on the signal-to-noise ratio (e.g. Gianniou and Groten, 1997; Talbot, 1988) or satellite elevation angle (e.g. Euler and Goad, 1991; Gerdan,

1995; Han, 1997; Jin, 1996; Rizos *et al.*, 1997), some approximate formulae have been proposed to calculate the standard deviations of one-way GPS and GLONASS measurements. The covariance matrix of the differenced measurements is then formed using the covariance propagation law, in which the one-way measurements, however, are still considered to be statistically independent. On the other hand, constant coefficients in these formulae, empirically estimated using some data sets under specific observing conditions, may not always fit other data sets very well. Therefore, a suitable method should be one utilising current data for real-time stochastic modelling.

In this chapter, the commonly used Kalman filtering technique and the existing methods for measurement covariance matrix estimation will be briefly reviewed. Based on the measurement filtering residuals, a real-time (adaptive filtering) algorithm for estimating measurement covariance matrix will be presented. The applications of the proposed algorithm will be demonstrated with examples from real GPS and combined GPS/GLONASS data sets.

4.2 Parameter Estimation in Kinematic Positioning

4.2.1 Standard Kalman Filtering Scheme

Similar to static positioning, mathematical models and stochastic models are required to estimate the unknown state parameters in kinematic positioning. The mathematical models include:

the measurement model:

$$z_k = H_k x_k + \varepsilon_k , \tag{4.1}$$

and the dynamic (state) model:

$$x_k = \Phi_{k,k-1} x_{k-1} + \tau_k , \tag{4.2}$$

The corresponding stochastic models are further assumed as:

$$E(\varepsilon_k \varepsilon_i^T) = \begin{cases} R_k & i = k \\ 0 & i \neq k \end{cases}, \tag{4.3a}$$

$$E(\tau_k \tau_i^T) = \begin{cases} Q_k & i = k \\ 0 & i \neq k \end{cases}; \tag{4.3b}$$

$$E(\varepsilon_k \tau_i^T) = 0, \tag{4.3c}$$

where

z_k	is an $n \times 1$ vector of measurements and n is the number of measurements;
H_k	is an $n \times t$ design matrix and t is the number of state parameters;
$\Phi_{k,k-1}$	is a $t \times t$ state transition matrix;
x_k	is a $t \times 1$ state parameter vector;
ε_k	is an $n \times 1$ measurement noise vector;
τ_k	is a $t \times 1$ random error vector;
R_k	is an $n \times n$ measurement noise covariance matrix;
Q_k	is a $t \times t$ process noise covariance matrix;
i, k	are the time indices.

In kinematic GPS/GLONASS positioning, in order to shorten the time period of ambiguity recovery, all the available code and carrier phase measurements should be used. In the case of processing GPS data only, the double differenced (DD) pseudorange and carrier phase measurements are commonly formed to simplify the measurement equations. In the case of processing GLONASS data only or integrated GPS/GLONASS data, as discussed in Chapter 2, an optimal option is to utilise the DD GPS and single differenced (SD) GLONASS pseudorange measurements together with the GPS-GPS and GLONASS-GLONASS DD carrier phase measurements. Because the receiver clock errors are unstable, it is common to estimate them every epoch (Leick, 1995; Pratt *et al.*, 1997). In these situations, the state parameter vector contains the time-dependent parameters (i.e. three components of position and receiver clock bias) and the time-independent carrier phase ambiguity parameters if they have not been resolved.

Based on the mathematical models presented by Equations 4.1-4.3, Kalman filtering techniques can be used to estimate the unknown state parameters. The basic Kalman filtering computation procedure may be described by the standard prediction, filtering and smoothing equations (e.g. Krakiwsky, 1975; Cross, 1994). For real-time kinematic positioning applications, only the prediction and filtering equations are required. The predicted state values $\bar{x}_k$ and their associated covariance matrix are presented as:

$$\bar{x}_k = \Phi_{k,k-1}\hat{x}_{k-1}, \tag{4.4}$$

$$Q_{\bar{x}_k} = \Phi_{k,k-1}Q_{\hat{x}_{k-1}}\Phi_{k,k-1}^T + Q_k, \tag{4.5}$$

where $\hat{x}_{k-1}$ is an optimal estimator of the state parameters at the previous epoch $(k-1)$. Real-time estimates of the state parameters are computed using the following filtering equations:

$$\hat{x}_k = \bar{x}_k + G_k d_k, \tag{4.6}$$

$$Q_{\hat{x}_k} = Q_{\bar{x}_k} - G_k Q_{d_k} G_k^T, \tag{4.7}$$

with

$$G_k = Q_{\bar{x}_k} H_k^T Q_{d_k}^{-1}, \tag{4.8}$$

$$d_k = z_k - H_k \bar{x}_k, \tag{4.9}$$

$$Q_{d_k} = R_k + H_k Q_{\bar{x}_k} H_k^T, \tag{4.10}$$

being the *gain matrix,* the *innovation vector* and its covariance matrix, respectively.

4.2.2 Special Filtering Settings

It should be noted that in GPS/GLONASS kinematic positioning, the precise carrier phase measurements with code pseudoranges can generate accurate positioning results (Wang and Iz, 1998). In the cases of good satellite constellation, with dual frequency GPS or single frequency GPS/GLONASS receivers, the positioning

accuracy may reach the meter or sub-meter level without fixing integer carrier phase ambiguities (which, sometimes, can be recovered with single epoch data, see Section 4.4). In many physical situations, therefore, it is very difficult to model the dynamic behaviour of a moving platform with the accuracy that GPS/GLONASS measurements can give.

In order to avoid the effect of errors in the process noise covariance matrix on the state estimation, the filter can be set up to operate only on the measurement noise. The basic concept regarding this filter operating mode has been discussed extensively in the literature (e.g. Hwang and Brown, 1990; Lachapelle *et al.*, 1992). It has been theoretically proven that a filter operating only on the measurement noise has a good performance of convergence (e.g. Sangsuk-Iam and Bullock, 1990). In that case, the process noise covariance matrix must be properly constructed, i.e. assigning the very large variance (say, 10^6) to the time-dependent state parameters and zero variance to the time-independent carrier phase ambiguity parameters. With these specific filter settings, the filtering results will not be affected by the dynamics of the moving platform and thus will be identical to sequential least-squares adjustment results. Similar filtering settings can be found in other applications (e.g. Euler and Goad, 1991; Goad, 1990).

Whilst the impact of the process noise covariance matrix is eliminated, the measurement covariance matrix should be realistically estimated in real-time to obtain reliable parameter estimates.

4.3 Real-time Stochastic Modelling

4.3.1 Existing Methods

In the field of automatic control, the procedures for the real-time (on-line) estimation of measurement (and process) noise matrices are termed *adaptive filtering techniques* (e.g. Chin, 1979; Mehra, 1972). Adaptive filtering techniques are divided into four categories: *Bayesian*, *maximum likelihood* (ML), *correlation* and *covariance-matching* methods. Whilst the *correlation* method is mainly applicable to constant coefficient systems (i.e. the elements in the design matrix are time-invariant), the *Bayesian* and *ML* methods are computationally intensive and cannot

be realistically used for real-time data processing (Chin, 1979). Compared to these methods, the *covariance-matching* method is computationally more efficient.

The basic concept of the *covariance-matching* method is to make the elements of the actual innovation covariance matrix consistent with their theoretical values. The actual covariance matrix of the innovations sequence d_k is calculated approximately by its sample covariance. By matching this estimated sample covariance matrix with its theoretical form presented by Equation 4.10, the measurement noise covariance matrix is calculated as (Mehra, 1972):

$$\hat{R}_k = \hat{Q}_{d_k} - H_k Q_{\bar{x}_k} H_k^T = \frac{1}{m} \sum_{i=1}^{m} d_{k-i} d_{k-i}^T - H_k Q_{\bar{x}_k} H_k^T \tag{4.11}$$

where m is chosen empirically to provide some statistical smoothing. Many numerical tests indicate, however, that the innovations sequences are very sensitive to the approximate values used in the linearization of the GPS measurements equations (Wang *et al.*, 1997a). More importantly, as Equation 4.11 is the difference between two positive definite matrices, it cannot be guaranteed that the resulting matrix $\hat{R}_k$ is positive definite. Therefore, Equation 4.11 is inadequate as an estimator of the stochastic model (covariance matrix).

4.3.2 Proposed Method

In order to obtain a realistic estimator of the measurement noise covariance matrix instead of the innovation sequence, a more precise estimator of the measurement noise level should be used. To this end, the Kalman filtering estimation formulae are derived using the least-squares method.

By integrating the measurements z_k and the predicted values of state parameters $\bar{x}_k$, the optimal estimators of the state parameters x_k can be obtained using the least-squares technique (e.g. Cross, 1994; Krakiwsky, 1975; Pelzer, 1985). The Gauss-Markov models are :

$$E(l_k) = A_k x_k \quad \text{or} \quad l_k = A_k x_k + v_k, \tag{4.12}$$

$$C_{l_k} = P^{-1} = \begin{bmatrix} R_k & 0 \\ 0 & Q_{\bar{x}_k} \end{bmatrix}, \tag{4.13}$$

with $l_k = \begin{bmatrix} z_k \\ \bar{x}_k \end{bmatrix}$, $v_k = \begin{bmatrix} v_{z_k} \\ v_{\bar{x}_k} \end{bmatrix}$, $A_k = \begin{bmatrix} H_k \\ E \end{bmatrix}$, and

v_{z_k} is an $n \times 1$ residual vector of measurements (Z_k);

$v_{\bar{x}_k}$ is a $t \times 1$ residual vector of the pseudo-measurements ($\bar{x}_k$);

E is a $t \times t$ identity matrix;

C_{l_k} is an $(n+t) \times (n+t)$ covariance matrix of measurement vector l_k;

P is an $(n+t) \times (n+t)$ weight matrix.

With the least-squares principle, the optimal estimators of the state parameters and their covariance matrix are formulated as Equations 4.6 and 4.7. For a detailed derivation of these equations, see Cross (1994) and Pelzer (1985). The advantage of this derivation is that it generates the most desirable least-squares residuals (i.e., the measurement filtering residuals):

$$v_{z_k} = z_k - H\hat{x}_k, \tag{4.14}$$

which is the optimal estimator of the measurement noise level because the estimated values $\hat{x}_k$ (not the predicted values $\bar{x}_k$) of the state parameters are used in their computations. In order to obtain the covariance matrix of the measurement filtering residuals, Equation 4.14 is further derived as:

$$v_{z_k} = z_k - H_k(\bar{x}_k + G_k d_k) = (E - H_k G_k) d_k \tag{4.15}$$

By applying the error propagation law to Equation 4.15, one obtains:

$$Q_{v_{z_k}} = R_k - H_k Q_{\hat{x}_k} H_k^T \tag{4.16}$$

It is interesting to note that Equations 4.10 and 4.16 are similar. Based on the same philosophy as that used in the *covariance-matching* method, a new method for estimating the covariance matrix of measurements can be constructed with Equation 4.16. In Equation 4.16, if the covariance matrix $Q_{v_{z_k}}$ is computed using the measurement filtering residuals from the previous m epochs, the covariance matrix R_k can be estimated as:

$$\hat{R}_k = \hat{Q}_{v_{z_k}} + H_k Q_{\hat{x}_k} H_k^T = \frac{1}{m} \sum_{i=0}^{m-1} v_{z_{k-i}} v_{z_{k-i}}^T + H_k Q_{\hat{x}_k} H_k^T \tag{4.17}$$

which can be used in the computation of epoch $k+1$. In Equation 4.17, m is called *width of moving windows*. Unlike Equation 4.11 which is constructed with the predicted quantities, Equation 4.17 is based on the estimated parameters and thus is more robust. The covariance matrix $\hat{R}_k$ estimated with Equation 4.17 is always positive definite because it is the sum of the two positive definite matrices. Compared to Equation 4.11, a slight disadvantage of Equation 4.17 is that it requires some extra computations for both v_{z_k} and $H_k Q_{\hat{x}_k} H_k^T$, which are not generated by the standard Kalman filtering process. Fortunately, the amount of these additional computations is small and leads to no significant time delay in the data processing.

4.4 Test Results and Analysis

Both GPS dual frequency and integrated GPS/GLONASS single frequency data sets have been employed to test the performance of the above proposed stochastic modelling method.

4.4.1 Description of the Tests

The first data set was collected in a marine kinematic GPS positioning test. The test was carried out on July 18, 1997, at the Fremantle port in Perth, Australia, using two Trimble 4000SSE dual frequency receivers. The rover receiver antenna was mounted on a boat, and was moved around the offshore test area (about 7.3km away from the reference station). The trajectory of the roving antenna for this test is shown in Figure 4.1. The cut-off elevation angle was set to 15 degrees. During the ten minutes of the test, seven satellites were tracked. The data interval is one second.

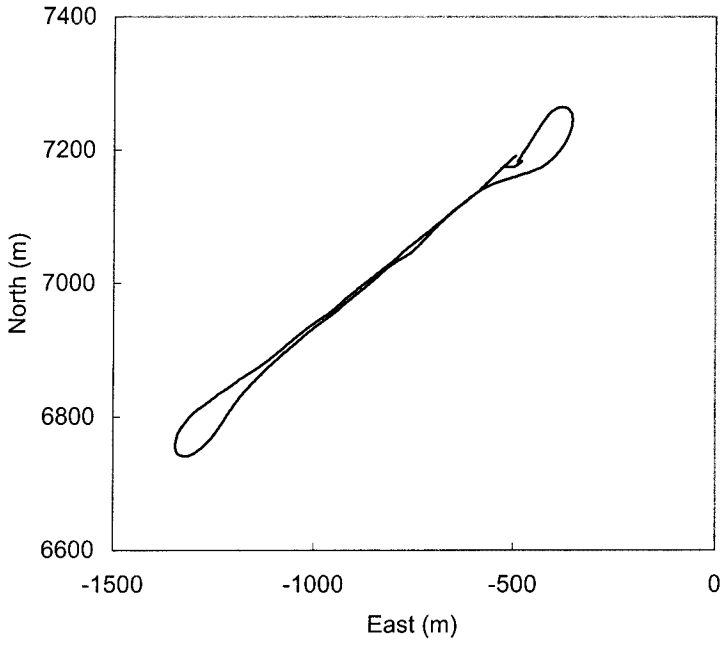

Figure 4.1 Boat trajectory for the marine GPS kinematic positioning test

Another data set was collected on a 1.2km (static) baseline, on February 16, 1998, in Perth, Australia, using two Ashtech GG24 GPS/GLONASS receivers. The data span of this single frequency data set is ten minutes with the data interval of one second. The cut-off elevation angle was set to ten degrees. During the whole session of observation, seven GPS and five GLONASS satellites were tracked.

The true carrier phase ambiguities for this data set were firstly recovered from the whole session. Then, ambiguity resolutions were performed on-the-fly for each segment of one epoch. In the data processing, the initial standard deviations for the one-way pseudorange and carrier phase measurements were defined as 1.0m and 0.05 cycles, respectively. The width of the moving windows for estimating the measurement covariance matrix was set to eight epochs and the initial estimate was calculated using measurement filtering residuals from the first eight epochs with ambiguities being fixed (discussion about the width of the moving window is given in Section 4.4.5). In theory, the covariance between different groups of measurements, such as carrier phase and code, or L1 and L2 code, may exist. In this study, the value of this covariance is assumed to be zero, which can significantly speed up the filtering process. Investigation into cases where such covariance is non zero is given in Teunissen, *et al.* (1998).

4.4.2 Comparison of Various Modelling Methods

It has been found that the existing covariance matching method expressed by Equation 4.11 does not always generate a positive definite covariance matrix for these data sets. For the purpose of comparison, the stochastic model based on the satellite elevation was also tested for the GPS data set (in the literature, no such kind of empirical formula is available for the Ashtech GG24 receivers). According to Euler and Goad (1990) and Jin (1996), the standard deviation of the one-way code measurements can be approximated by an exponential function of satellite elevation h as:

$$\sigma(h) = a_0 + a_1 \cdot \exp(-\frac{h}{h_0}) \tag{4.18}$$

where the constant terms a_0, a_1 and h_0 are empirically derived. For example, for the Trimble 4000SSE receivers, these terms are 0.12m, 1.1m, 14 degrees for L1 code measurements, and 0.14m, 3.0m, 11 degrees for L2 code measurements, respectively (Jin, 1996). The standard deviations for the L1 and L2 carrier phase measurements are determined as 1/100 of the pseudorange standard deviations (Kee *et al.*, 1997). The covariance matrices for the double differenced measurements are constructed using the error propagation law.

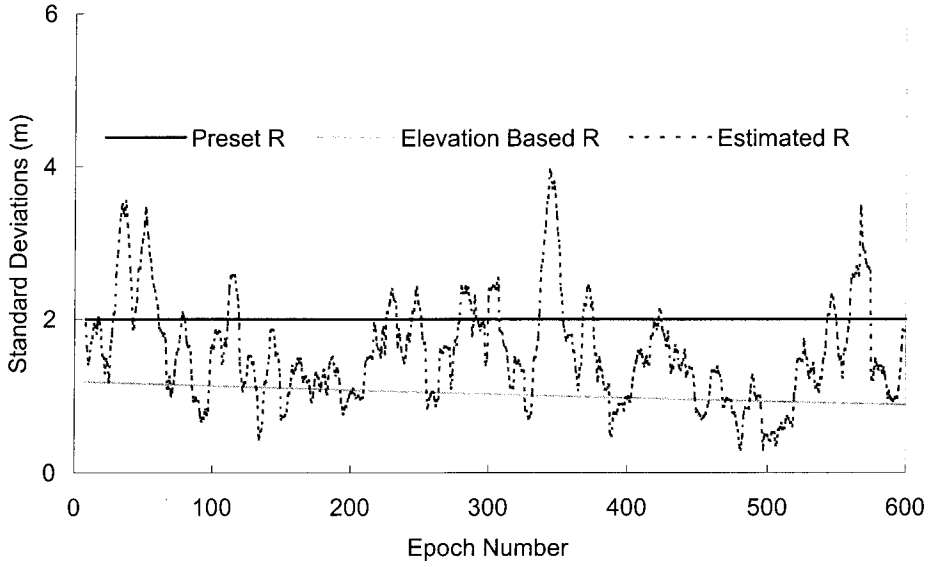

Figure 4.2 Standard deviations of DD L2 code measurements for SV 15-7 in the GPS dual frequency data

Figure 4.2 illustrates the standard deviations for the DD L2 code measurements of the satellite pair SV 15-7, which were preset, calculated using the satellite elevation and estimated using Equation 4.17. It is evident that big differences exist between these three stochastic models. Actually, the accuracy of the measurements may be influenced by many factors. The stochastic model based on satellite elevation cannot properly reflect the reality in some practical situations (e.g. Roberts *et al.*, 1997).

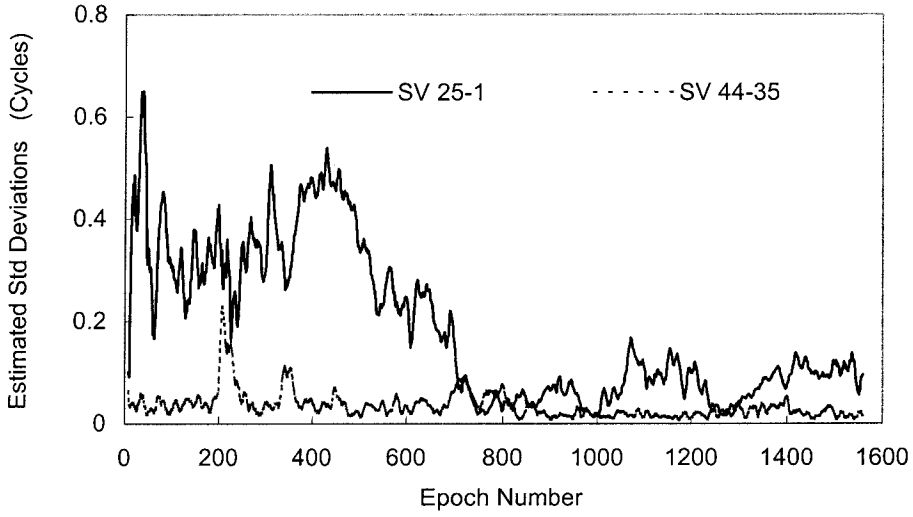

Figure 4.3 Estimated standard deviations of the DD carrier phases for GPS/GLONASS single frequency data

Similar to the situation of static GPS baseline data processing discussed in Chapter 3, estimated measurement covariances in the case of kinematic positioning may be negative. For instance, in the case of GPS/GLONASS single frequency data, the estimated covariance matrix for SD GLONASS code measurements (at epoch 100) is

$$\begin{bmatrix} 1.805 & 0.033 & -0.263 & 0.983 & -0.405 \\ & 1.368 & 0.736 & 0.435 & -0.233 \\ & & 6.408 & 0.855 & -1.230 \\ & & & 1.515 & -0.631 \\ & & & & 0.479 \end{bmatrix} (\mathrm{m}^2)$$

in which the correlation coefficients range from -0.74 to 0.59. In the commonly used or elevation dependent stochastic models, however, these correlation coefficients are always equal to zero. Therefore, it is not realistic to assume that all the one-way

measurements are independent. It is further noted that, as shown in Figure 4.3, the measurements do have different accuracy, and that some GLONASS measurements may be more accurate than GPS measurements. (For example, if GLONASS satellites have higher elevations than GPS satellites). Thus, in combined GPS/GLONASS data processing, the method of down-weighting the GLONASS measurements may lead to unreliable results. It is also noted that in Figure 4.3, the estimated standard deviation is as large as 0.6 cycle. This may be caused by using a short window (8 epochs), which provides a limited amount of information. If the window size is large, the estimated standard deviations are smaller and change smoothly but might not produce better results in ambiguity resolution (Section 4.4.5).

4.4.3 Critical Statistics in Ambiguity Resolution

A realistic estimation of measurement covariance matrices provides reliable statistics for ambiguity resolution. To demonstrate this more clearly, both the solutions with the preset and estimated covariance matrices were generated. The ADOP (*ambiguity dilution of precision*) measure defined by Teunissen and Odijk (1997) is designed to describe the impact of the receiver-satellite geometry on the precision of ambiguity parameters. The calculated values for the(ADOP), which is are illustrated in Figures 4.4 and 4.5.

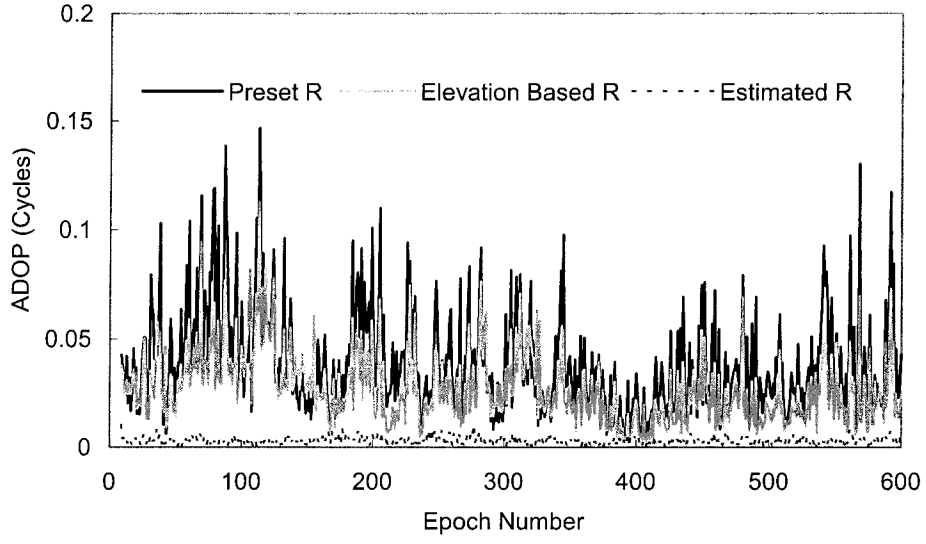

Figure 4.4 Ambiguity dilution of precision (ADOP) for

the GPS dual frequency data

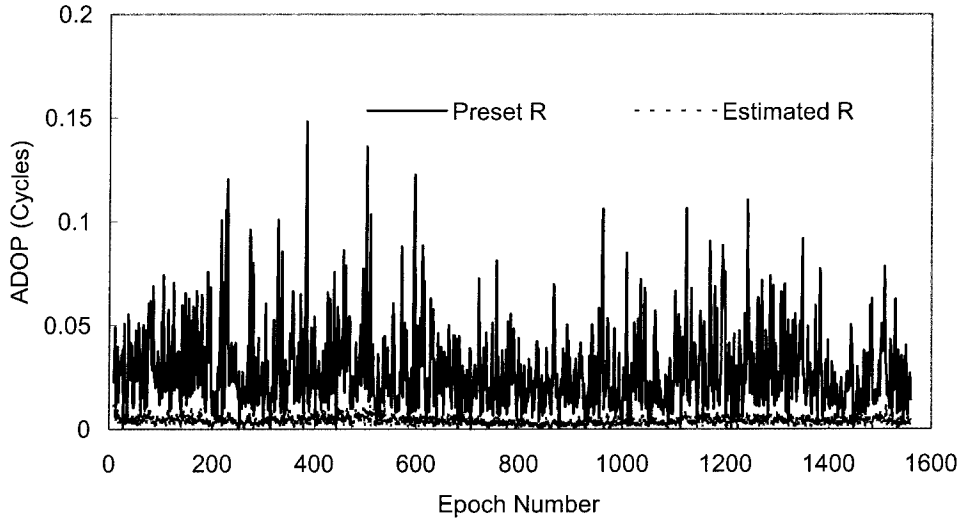

Figure 4.5 Ambiguity dilution of precision (ADOP)

for the GPS/GLONASS single frequency data

Figures 4.4 and 4.5 indicate that the precision of the estimated ambiguities is greatly improved with the estimated covariance matrix. As a consequence of this, the ambiguity search volumes are significantly reduced and a faster search process can be expected (Laudau and Euler, 1992; Teunissen and Odijk, 1997).

The improved float ambiguity estimates are of great importance for the ambiguity validation test, which is a critical step in ambiguity resolution (see Section 5.1). The results regarding the commonly used ambiguity validation test statistic *F-ratio* (*ibid.*) are graphed in Figures 4.6 and 4.7. In all the cases, the ambiguity validation test statistics with the estimated measurement covariance matrices are much larger than those with the preset measurement covariance matrices. If the critical value of the F-ratio is chosen to be 2.0, as commonly accepted (e.g. Landau and Euler, 1992), the success rates of the ambiguity resolutions using the preset covariance matrices are only 49 percent and 21 percent for GPS and GPS/GLONASS data sets, respectively, whereas the success rates of the ambiguity resolution using the estimated covariance matrices reach 100 percent. However, for the GPS data set, if the measurement covariance matrix is constructed using satellite elevation, the success rate of the ambiguity resolution is as low as 68 percent, which is slightly increased compared to using the preset measurement covariance matrix.

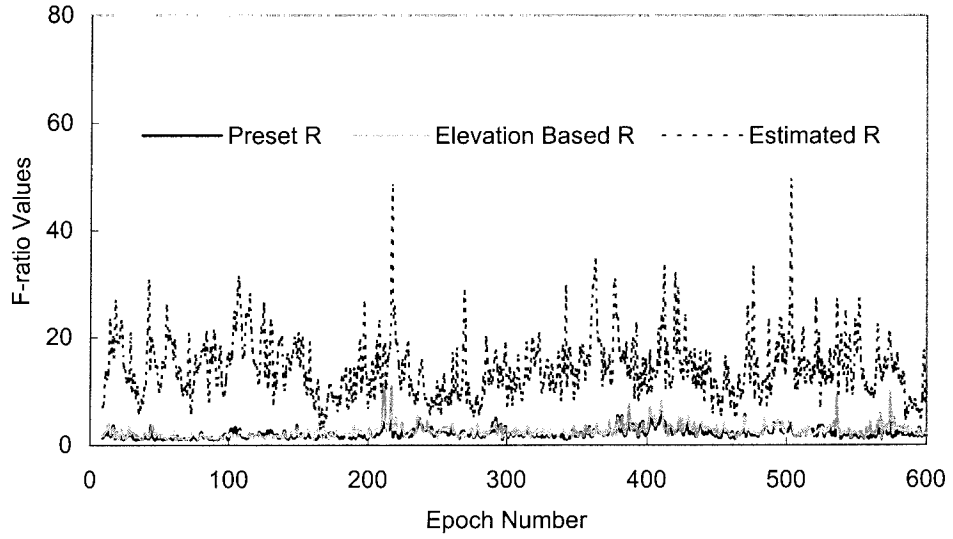

Figure 4.6 F-ratio values for the GPS dual frequency data

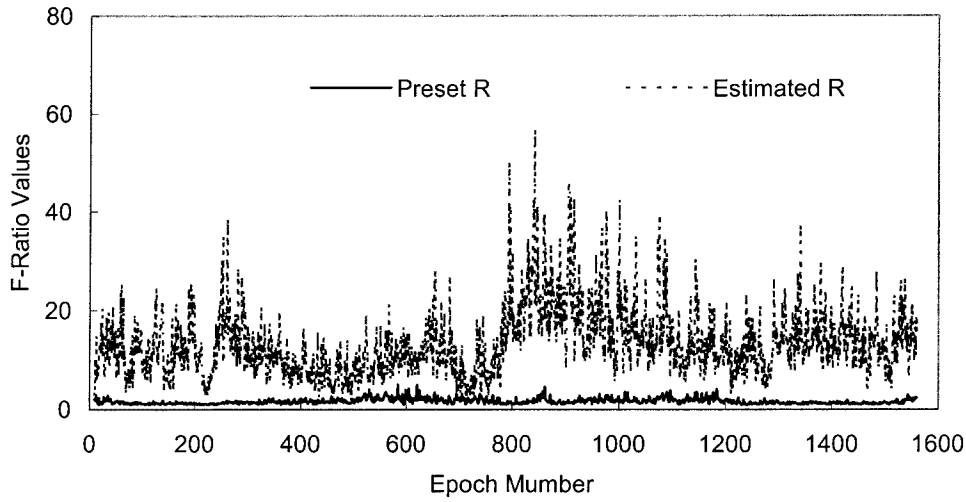

Figure 4.7 F-ratio values for the GPS/GLONASS single frequency data

As shown in Figures 4.8 and 4.9, similar results are also observed using a newly developed ambiguity validation test statistic *Ws* (see Chapter 5). The advantage of this new statistic is that the confidence level of the ambiguity resolution can be rigorously evaluated. For instance, in the case of the GPS data set, the averaged confidence levels of the ambiguity resolution for the three different stochastic models (i.e., preset, elevation based and estimated R) are 87 percent, 92 percent and 100 percent, respectively.

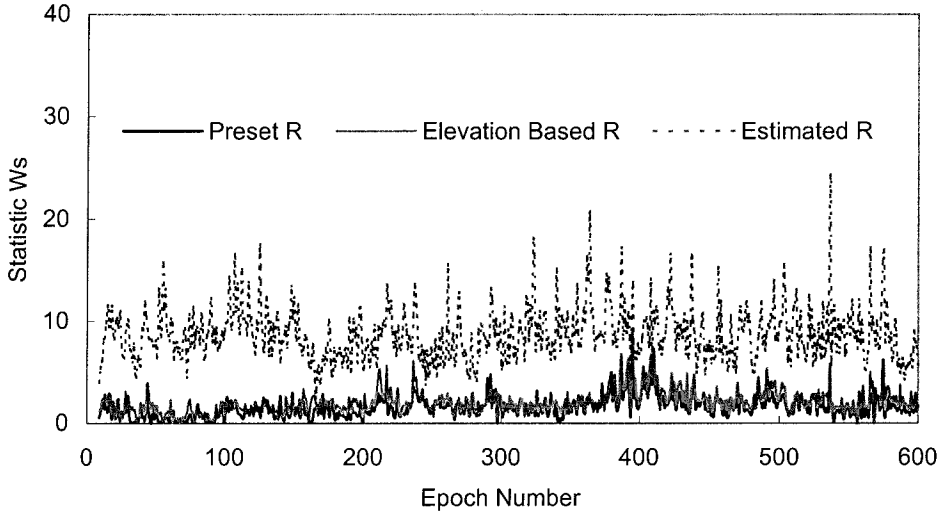

Figure 4.8 Ambiguity discrimination test statistic Ws

for the GPS dual frequency data

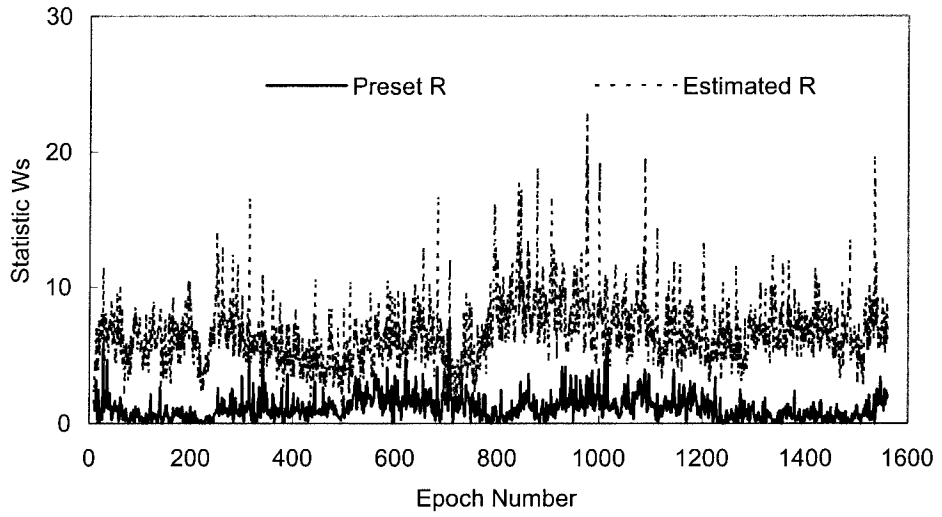

Figure 4.9 Ambiguity discrimination test statistic Ws

for the GPS/GLONASS single frequency data

4.4.4 Impact on Baseline Estimation

A realistic stochastic model can improve the accuracy of the ambiguity fixed solutions. For example, the use of the preset measurement covariance matrix in the GPS/GLONASS data set results in the standard deviations of the baseline components at epoch eight of 0.008m, 0.016m and 0.012m, respectively. At epoch

nine when the filtering process began to utilise the estimated measurement covariance matrix, the standard deviations of the coordinates were reduced to 0.006m, 0.013m and 0.009m, respectively. The differences in the coordinates between the two solutions are around 0.005m.

4.4.5 Optimal Width of the Moving Windows

The estimation of the measurement covariance matrix requires both the preset standard deviations for the one-way measurements and the width of the moving windows. Test results indicate that the small changes in the preset standard deviations (for example, the use of 2.0m instead of setting 1.0m for the GLONASS pseudorange measurements), do not significantly influence the success rate of ambiguity resolution. The reason for this is that the influence of the preset standard deviations will be, to some extent, tuned out in the process of estimating the measurement covariance matrix. The optimal width of the moving window, however, needs to be identified.

Data Set	Width (epochs)	6	7	8	9	10	30	120
GPS	Averaged F-ratio	3.0	16.2	14.3	11.9	11.1	6.0	4.7
	Averaged Ws	2.3	9.3	8.7	8.0	7.8	5.4	4.4
	Success Rate(%)	59.8	100	100	100	100	99.8	97.9
GPS/GLONASS	Averaged F-ratio	3.5	5.2	13.3	12.0	11.1	6.0	4.1
	Averaged Ws	2.4	3.5	6.6	6.3	6.2	4.3	3.3
	Success Rate (%)	62.7	96.9	100	100	100	99.5	94.2

Table 4.1 Impact of the width of moving windows on ambiguity resolution

In order to select an optimal width of the moving windows some numerical tests for various widths have been conducted. The averaged ambiguity validation test statistics and success rate of ambiguity resolution are listed in Table 4.1. This table shows that for the tested GPS and GPS/GLONASS data sets, the optimal values for the width of the moving windows are respectively seven and eight. Initial testing on other data sets indicates that the optimal width varies from seven to 15, and slightly depends on the redundancy of the positioning solutions. In practical implementation, the default width parameter may vary between eight and ten, and then the optimal value for current positioning operation is adaptively determined in real-time.

4.5 Summary

In GPS/GLONASS kinematic positioning, reliable ambiguity resolution and positioning results rely heavily on the correctness of the measurement noise covariance matrix. Common practice assuming that the one-way (code or carrier phase) measurements are statistically independent and have the same accuracy is certainly not realistic. This practice will lead to an unsuitable measurement covariance matrix. Stochastic modelling for code and carrier phase measurements is not trivial for real-time applications. Because the rigorous methods (such as MINQUE) cannot be used due to their requirement of extensive computation, some feasible methods need to be developed and tested for RTK GPS/GLONASS positioning.

Although the satellite elevation-based stochastic model can be easily used in real-time data processing and has a good performance in some situations, it may not significantly improve the success rate of ambiguity resolution. For instance, in the tested GPS dual frequency data set, the success rates of single epoch ambiguity resolution using the preset and elevation based measurement covariance matrices are 49 percent and 68 percent, respectively.

Based on the post-fitted filtering residuals, a new method for the measurement covariance matrix estimation has been proposed. With such a method, the measurement noise covariance matrix can be estimated in real-time data processing, after a short period of time (in the given data sets, 8 epochs) during which a preset covariance matrix is used. By using an estimated covariance matrix, the reliability of ambiguity resolution and the accuracy of kinematic positioning can be significantly improved. For the GPS dual frequency and combined GPS/GLONASS single frequency data sets tested, whilst the preset covariance matrix gives a success rate of the single-epoch ambiguity resolution of 49 percent and 21 percent for each data set, the success rate of the single-epoch ambiguity resolution using the estimated measurement covariance matrix can reach 100 percent.

Chapter 5

AMBIGUITY VALIDATION TEST PROCEDURES

5.1 Introduction

Precise relative GPS and GLONASS positioning requires the reliable determination of the carrier phase integer ambiguity. Over the past few years, many different ambiguity resolution (AR) techniques have been developed for precise GPS positioning. The most commonly used AR techniques are, for instance, the ambiguity function approach (Counselman and Gourevitch, 1981; Remondi, 1991; Mader, 1992; Corbett and Cross, 1995); the least-squares-search approach (Hatch, 1989, 1990; Lachapelle *et al.*, 1992); the fast ambiguity resolution approach (Frei and Beutler, 1990; Landau and Euler, 1992); the least-squares ambiguity decorrelation approach - LAMBDA (Teunissen, 1993); the integer programming method (Wei and Schwarz, 1995), and the *bootstrapping* algorithms for long baseline networks (Blewitt, 1989; Counselman and Abbot, 1989). Reviews and evaluation of existing AR techniques can be found in Hatch and Euler (1994) and, more recently, Han and Rizos (1996b) and de Jonge (1997). Some of the AR techniques developed for precise GPS positioning are also useful in precise GLONASS positioning. In this study, the LAMBDA method is used (see Sections 2.4 and 6.3).

The starting point for most ambiguity resolution techniques is the least-squares estimation of the ambiguity parameters, together with other unknown parameters such as the coordinates of the roving receiver. This float solution of the real-valued ambiguity estimates and their associated statistics is then used to construct a search window which is assumed to contain the correct integer ambiguities. The process of searching all possible integer ambiguity combinations within the search window is then performed using a search criterion based on the minimisation of the quadratic form of the least-squares residuals. During the search process, the compatibility of all the potential integer ambiguity combinations with the associated GPS/GLONASS measurements is statistically tested. If no integer ambiguity combination passes this *acceptance test* (e.g. Tiberius and de Jonge, 1995; Walsh *et al.*, 1995) under the

given confidence level, the correct integer ambiguities cannot be identified with the available data. When one or more integer ambiguity combinations are accepted, the integer ambiguity combination that results in the minimum quadratic form of the least-squares residuals will be considered as the most likely (*best*) solution. The next and most critical step for ambiguity resolution on-the-fly is to apply a so-called *discrimination test* (*ibid.*) to ensure that the most likely integer ambiguity combination is statistically better than the second best combination as defined by the second minimum quadratic form of the least-squares residuals. While the acceptance test procedure can be constructed using classic statistical testing theory, the discrimination test procedure is still under investigation.

A widely used ambiguity discrimination test statistic is the so-called F-ratio of the second minimum quadratic form of the least-squares residuals and the minimum quadratic form of the least-squares residuals. This test statistic was first suggested by S. Gourevitch in 1982 (Counselman and Abbot, 1989). Based on the assumption that both quadratic forms are independent, the F-ratio is considered as having a Fisher-distribution (Frei and Beutler, 1990; Abidin and Subari, 1994; Corbett and Cross, 1995; Han and Rizos, 1996a). Unfortunately, this assumption is not correct (Teunissen, 1996) and the distribution of this test statistic is hard, if not impossible, to be rigorously identified. In the literature, the critical value for the F-ratio is often arbitrarily chosen as 2.0 (e.g. Landau and Euler, 1992; Wei and Schwarz, 1995). As there is no theoretical statistical basis for using a fixed critical value, and, furthermore, redundancy is not taken into account, this type of discrimination test is not rigorous.

Several other different types of ambiguity discrimination statistical test procedures have been proposed, for example, Euler and Schaffrin (1990), Chen (1997) and Han (1997). In these tests, the original null hypothesis is designed to test the best integer ambiguity combination, rather than test the likelihood of the best integer ambiguity combination relative to the second best one. The critical value in these tests actually represents the noncentrality of the distribution with the statistical test having a specified significance level, power and degree of freedom. It must be pointed out that the noncentrality parameters of noncentral distributions should be calculated with the mean of the test statistic under the alternative hypothesis, which depends on

the known variance factor. The variance factor, however, may be unknown in many practical applications.

In this chapter, an ambiguity discrimination test procedure is developed using the likelihood ratio method and the artificial nesting method. In the proposed procedure, the null and alternative hypotheses are assumed to test whether the best ambiguity combination is significantly better than the second best ambiguity combination. The derived test statistic is constructed by the difference between the minimum and second minimum quadratic form of the residuals, and its standard derivation. The stochastic properties of the proposed test statistic have been analysed and, finally, its statistic distribution function has been theoretically identified. The applications of the proposed ambiguity discrimination test procedure will be demonstrated with the data sets collected in the static and kinematic GPS positioning tests.

5.2 Initial Ambiguity Parameter Estimation

In GPS/GLONASS kinematic positioning, double differenced GPS code and carrier phase measurements are favoured because they can, to a large extent, cancel many systematic errors (Section 2.3). Linearised GPS/GLONASS (single- or double-differenced) measurements and the corresponding covariance matrix can be expressed as the following Gauss-Markov models:

$$l = A_c x_c + A_k x_k + v, \tag{5.1}$$

$$D = \sigma^2 Q = \sigma^2 P^{-1}, \tag{5.2}$$

where

- l is the $n \times 1$ vector of the difference between the differenced GPS/GLONASS code and carrier phase measurements and their computed values, simply called the *measurement vector*, and n is the number of the measurements;
- v is the $n \times 1$ vector of the random errors;
- x_k is the $m \times 1$ double differenced ambiguity parameter vector, and m is the number of the ambiguity parameters;

x_c is the $t \times 1$ vector of all other unknown parameters including position and other parameters of interest and t is the number of all other unknowns except ambiguities;

A_k is the design matrix for the ambiguity parameters;

A_c is the design matrix for the other unknown parameters;

D is the covariance matrix;

Q is the cofactor matrix;

P is the weight matrix;

σ^2 is the *a priori* variance factor.

Based on the principle of least squares ($v^{\mathrm{T}}Pv = \text{minimum}$), the estimates of the unknowns $\hat{x}$ in Equation 5.1 can be obtained by:

$$\hat{x} = Q_{\hat{x}} A^{\mathrm{T}} P l, \tag{5.3}$$

with:

$$Q_{\hat{x}} = (A^T P A)^{-1}, \tag{5.4}$$

where $\hat{x} = (\hat{x}_c,\ \hat{x}_k)^T$ and $A = (A_c,\ A_k)$. $Q_{\hat{x}}$ is the cofactor matrix of the estimated vector $\hat{x}$, which can be represented by the following partitioned matrices:

$$Q_{\hat{x}} = \begin{bmatrix} Q_{\hat{x}_c} & Q_{\hat{x}_c \hat{x}_k} \\ Q_{\hat{x}_k \hat{x}_c} & Q_{\hat{x}_k} \end{bmatrix}. \tag{5.5}$$

Furthermore, from Equations 5.1, 5.3 and 5.5, the least-squares residuals are obtained as:

$$\hat{v} = l - A\hat{x} = Q_{\hat{v}} P l, \tag{5.6}$$

where $Q_{\hat{v}} = Q - AQ_{\hat{x}}A^T$ is the cofactor matrix of the residuals. With the estimated residual vector $\hat{v}$ and weight matrix P, the *a posteriori* variance cofactor can be estimated as:

$$\hat{s}_0^2 = \frac{\Omega_0}{f}, \tag{5.7}$$

where:

$$\Omega_0 = \hat{v}^T P\hat{v} = l^T PQ_{\hat{v}}Pl = l^T Pl - l^T PA\hat{x}, \tag{5.8}$$

and $f = n - m - t$ is the degrees of freedom.

The above least-squares estimates are very important statistics for integer ambiguity identification. The reliability of these statistics, however, is highly dependent on the correctness of the functional and stochastic models defined in Equations 5.1 and 5.2. In order to test whether or not the models are correct and complete, a global model test should be performed which compares the *a posteriori* variance factor $\hat{s}_0^2$ with σ^2, the *a priori* variance factor (Caspary, 1988; Teunissen, 1996; Han, 1997, Harvey, 1994). With a given significance level α_0, the following inequality should hold:

$$F(f, \infty; \alpha_0/2) < \frac{\hat{s}_0^2}{\sigma^2} < F(f, \infty; 1-\alpha_0/2), \tag{5.9}$$

where $F(f, \infty; \alpha_0/2)$ and $F(f, \infty; 1-\alpha_0/2)$ are the lower and upper critical values of the F distributed statistic, respectively. Otherwise, if the inequality (5.9) does not hold, the functional and/or stochastic models may be incorrect. Then, specific procedures for outlier and cycle slip detection (Teunissen, 1998) and variance-covariance component estimation of GPS measurements (see Chapters 3 and 4) can be performed.

5.3 Ambiguity Acceptance Test

With the initial float ambiguity estimates $\hat{x}_k$ and their estimated covariance matrix $\hat{s}_0^2 Q_{\hat{x}_k}$, integer ambiguity search windows for individual ambiguity parameters can be determined. Within these search windows, there may be many, say n_a, potential integer ambiguity combinations, described as integer vectors $K_i, i = 1, 2, \ldots\ldots, n_a$. The compatibility of each set of the integer ambiguity combinations with the associated GPS measurements is commonly tested using the following procedure.

When the ambiguity parameter unknowns x_k are assumed to be fixed to K_i, from a statistical point of view, it means that the following constraint equation:

$$Hx = K_i, \tag{5.10}$$

is imposed to the original functional model represented by Equation 5.1. In Equation 5.10, $x = (x_c, x_k)^T$ and:

$$H = [0, E_k], \tag{5.11}$$

where 0 is an $m \times t$ zero matrix and E_k is an $m \times m$ identity matrix.

Under the constraint expressed by Equation 5.10, the least-squares estimates of unknowns in Equation 5.1, denoted as $\hat{x}_i$, and their cofactor matrix read (e.g. Koch, 1988):

$$\hat{x}_i = \hat{x} - Q_{\hat{x}} H^T (H Q_{\hat{x}} H^T)^{-1} (H\hat{x} - K_i), \tag{5.12}$$

$$Q_{\hat{x}_i} = Q_{\hat{x}} - Q_{\hat{x}} H^T (H Q_{\hat{x}} H^T)^{-1} H Q_{\hat{x}}, \tag{5.13}$$

which is also called the *ambiguity-fixed* solution. The corresponding quadratic form of the residuals can be calculated with:

$$\Omega_i = \Omega_0 + R_i, \tag{5.14}$$

where:

$$R_i = (H\hat{x} - K_i)^T (HQ_{\hat{x}}H^T)^{-1}(H\hat{x} - K_i) = (\hat{x}_k - K_i)^T Q_{\hat{x}_k}^{-1}(\hat{x}_k - K_i)\,. \tag{5.15}$$

A statistical test of compatibility of the integer ambiguity combination K_i with the associated measurement vector l can be based on the following null hypothesis:

$$H_0\colon \quad E(Hx) = K_i\,, \tag{5.16}$$

where $E(\circ)$ is a mathematical expectation operator, and the alternative hypothesis:

$$H_a\colon \quad E(Hx) \neq K_i\,. \tag{5.17}$$

Under the assumption that the measurement vector l is normally distributed, this is a standard linear hypothesis testing problem widely discussed in many statistics textbooks (e.g. Koch, 1988). One of the commonly used test statistics reads:

$$T_1 = \frac{n-m-t}{m} \cdot \frac{R_i}{\Omega_0}\,. \tag{5.18}$$

Under the null hypothesis, the test statistic T_1 has an F distribution with the degrees of freedom m and $n-m-t$. Therefore, with a chosen significance level α_1, the rejection criteria for the null hypothesis is:

$$T_1 > F(m, n-m-t; 1-\alpha_1)\,. \tag{5.19}$$

For the above statistical testing problem, an alternative statistic can be formed as

$$T_2 = \frac{\Omega_0}{\Omega_i} = \frac{\Omega_0}{\Omega_0 + R_i}\,. \tag{5.20}$$

According to Beyer (1968, p. 52), under the null hypothesis, the test statistic T_2 has the *Beta* distribution with parameters $(\frac{n-m-t}{2}, \frac{m}{2})$. Since *Beta* tests are lower-tail tests, with a chosen significance level α_2, the rejection criteria for the null hypothesis is:

$$T_2 < Beta(\frac{n-m-t}{2}, \frac{m}{2}; \alpha_2). \tag{5.21}$$

Compared to statistic T_1, statistic T_2 has a smaller value range (0,1). From a statistical point of view, if the measurements are normally distributed, the two statistics will produce the same testing results.

If all potential integer ambiguity combinations are rejected by the criteria represented by Equation 5.19 or 5.21, the attempt to resolve the integer ambiguity parameters is unsuccessful and hence more data are needed to resolve the ambiguity parameters. Once the ambiguity search process has generated one or more integer ambiguity combinations that can pass the compatibility test, the best and second best integer ambiguity combination are identified as K_m and K_s, respectively. Before the best integer ambiguity combination K_m can be accepted as the correct ambiguity value, an ambiguity discrimination test procedure must be conducted (Teunissen, 1996). In the remainder of this chapter, an ambiguity discrimination test procedure based on the likelihood ratio method and the artificial nesting method is discussed.

5.4 Ambiguity Discrimination Test

Ambiguity discrimination testing can be generally considered as the comparison of any two constrained Gauss-Markov models, based on Equations 5.1 and 5.2, with the constrained equations $Hx = c_i$ and $Hx = c_j$, respectively, where elements of the vectors c_i and c_j could be real or integer values. The two compared models are nonnested because neither model is a special case of the other model. Statistical tests for the nonnested models have been extensively discussed in the literature (e.g. Hoel, 1947; Williams and Kloot, 1953; Williams, 1959; Cox, 1962; Atkinson, 1969; Betti *et al.*, 1994). The basic idea behind the tests of Williams and Kloot (1953), Williams (1959) and Atkinson (1969) is to test whether the difference between the

two compared formulae is statistically significant. This is the strategy to be implemented here in the ambiguity discrimination test. There are two methods for constructing the discrimination test statistics, i.e., the likelihood ratio method and the artificial nesting method.

5.4.1 The Likelihood Method

As pointed out by Teunissen (1996), the difference between the two compared ambiguity combinations can be measured by comparing their likelihood. In order to do this, the likelihood function is first introduced. Under the assumption that the measurement vector l is normally distributed in the Gauss-Markov models described by Equations 5.1 and 5.2, the likelihood function can be expressed as (Koch, 1988):

$$L(l; x, \sigma^2) = (2\pi\sigma^2)^{-n/2}\left|Q\right|^{-1/2}.\exp\{-\frac{1}{2\sigma^2}(l - Ax)^T P(l - Ax)\}. \tag{5.22}$$

With a fixed *a priori* σ^2, the above likelihood function is then denoted as $L(l; x)$, called the *conditional* likelihood function. The least-squares estimates of the unknown parameters x in a linear model are identical with the corresponding maximum likelihood estimates obtained by maximising the above (conditional) likelihood function without reference to the variance factor σ^2. The advantage of using the maximum likelihood principle here is that it can directly be applied to evaluate the significance of the difference between any two constrained Gauss-Markov models. With a fixed σ^2, which may be a known value or estimated by other models, the likelihoods of $\hat{x}_{c_i}$ and $\hat{x}_{c_j}$ estimated by the constrained Gauss-Markov models can be represented as:

$$L_{c_i} = Max.L(l; x\left| Hx = c_i\right.) = (2\pi\sigma^2)^{-n/2}\left|Q\right|^{-1/2}\cdot\exp\{-\frac{1}{2\sigma^2}\Omega_{c_i}\}, \tag{5.23a}$$

$$L_{c_j} = Max.L(l; x\left| Hx = c_j\right.) = (2\pi\sigma^2)^{-n/2}\left|Q\right|^{-1/2}\cdot\exp\{-\frac{1}{2\sigma^2}\Omega_{c_j}\}. \tag{5.23b}$$

Based on Equations 5.23a and 5.23b, the ratio of the likelihood L_{c_i} and L_{c_j} of the two constrained solutions $\hat{x}_{c_i}$ and $\hat{x}_{c_j}$ is given by:

$$\psi = \frac{L_{c_i}}{L_{c_j}} = \exp\{\frac{d}{2\sigma^2}\}, \tag{5.24}$$

with:

$$d = \Omega_{c_j} - \Omega_{c_i}, \tag{5.25}$$

where Ω_{c_i} and Ω_{c_j} are the quadratic forms of the residuals of the two compared models, respectively, which can be calculated using Equation 5.14. Previously, Tiberius and Jonge (1995) have used the quantity d, whose critical value was chosen empirically, as the test statistic for ambiguity discrimination testing.

Since σ^2 is a fixed value in the two compared models, the likelihood ratio ψ varies only with d. If $d = 0$, which can be reached, for example, when $(c_i + c_j)/2 = \hat{x}_k$ (see Appendix D), ψ will be exactly equal to one, meaning that the two compared models cannot be distinguished from each other. The larger the (positive or negative) departure of d from zero, the larger is the difference of their likelihoods. A statistical test as to whether or not the random variable d departs significantly from zero requires the construction of the following null and alternative hypotheses:

$$H_0: \quad E(d) = 0, \tag{5.26}$$

$$H_a: \quad E(d) \neq 0. \tag{5.27}$$

To construct an appropriate test statistic for the above hypothesis testing problem, the concrete form of the functional relation between the random variable d and the measurement vector l should be further investigated.

Inserting Equation 5.14 into Equation 5.25 with some algebraic manipulation yields:

$$d = 2(c_i - c_j)^T (H^T Q_{\hat{x}} H)^{-1} H\hat{x} + d_0 = d_1 A^T P l + d_0, \tag{5.28}$$

where $\hat{x}$ is given by equation (5.3), which is estimated with the unconstrained Gauss-Markov models (i.e., float solution) and:

$$d_1 = 2(c_i - c_j)^T (H^T Q_{\hat{x}} H)^{-1} H Q_{\hat{x}}, \tag{5.29}$$

$$d_0 = c_j^T Q_{x_k}^{-1} c_j - c_i^T Q_{x_k}^{-1} c_i. \tag{5.30}$$

d_1 and d_0 are constant terms. From Equation 5.28, it is noted that the random variable d is a linear function of the measurement vector l. If l is assumed as having a normal distribution, d is normally distributed, which is expected because the two compared models are nonnested (e.g. Willams, 1959; Atkinson, 1969; Betti *et al.*, 1994). Therefore, a natural test statistic for testing the above hypotheses can be constructed as:

$$W = \frac{d}{\sqrt{Var(d)}}, \tag{5.31}$$

where $Var(d)$ is the estimated variance of d. By applying the cofactor propagation law to Equation 5.26, the cofactor of d can be derived as:

$$Q_d = 4 \cdot (c_i - c_j)^T (H^T Q_{\hat{x}} H)^{-1} (c_i - c_j) = 4 \cdot (c_i - c_j)^T Q_{\hat{x}_k}^{-1} (c_i - c_j). \tag{5.32}$$

To obtain the estimated variance of d, the *a priori* variance factor σ^2 or the *a posteriori* variance factor $\hat{s}_0^2$ could be employed, depending on the available knowledge about the stochastic model in the Gauss-Markov models. These two cases will be separately discussed as follows.

First, with the known variance factor σ^2, the test statistic W becomes:

$$W_a = \frac{d}{\sigma\sqrt{Q_d}}, \tag{5.33}$$

which has mean zero and standard deviation one under the null hypothesis. Therefore, the test statistic W_a has a standard normal distribution, i.e., N(0, 1).

When we use the test statistic W_a to evaluate the likelihood of the best ambiguity combination K_m relative to the second best combination K_s, the vectors c_i and c_j are replaced by the vectors K_m and K_s, respectively. In this case, the distribution of the test statistic W_a actually is the so-called *truncated normal distribution* (e.g. Cox, 1962, p.419) and the alternative hypothesis should be set up as $E(d) > 0$. Then, with a chosen significance level α, the critical value for the test statistic W_a can be determined as $C_N = N(0, 1; 1-\alpha)$. If the following inequality is true:

$$W_a > N(0, 1; 1-\alpha), \tag{5.34}$$

it will be declared that the likelihood of the integer ambiguity combination K_m is statistically significantly larger than that of the second best combination K_s.

With the estimated test statistic W_a, the confidence level $1-\alpha_N$ can be evaluated using the following formula:

$$1-\alpha_N = P(y < W_a) = \int_{-\infty}^{W_a} N(y)dy, \tag{5.35}$$

where $N(y)$ is the probability density function of a standard normal variable.

Second, with the estimated variance factor $\hat{s}_0^2$ from Equation 5.7, the test statistic W becomes:

$$W_s = \frac{d}{\hat{s}_0\sqrt{Q_d}} = \frac{\frac{d}{\sqrt{\sigma^2 Q_d}}}{\sqrt{\frac{\Omega_0}{\sigma^2 f}}}. \tag{5.36}$$

From the above equation, it is seen that the test statistic W_s is the ratio of the two random variables. The denominator is distributed as the square root of the χ^2-variable with f degrees of freedom (e.g. Koch, 1988), divided by f; the distribution of

the numerator, under the null hypothesis, is the standard normal distribution, ie., N(0, 1). The distribution of such a ratio is Student's t-distribution with f degrees of freedom, if and only if, the denominator and numerator are statistically independent, which can be justified with the independence between the two random variables d and Ω_0 .

According to Koch (1988, p.157), the covariance between d and Ω_0 is described as:

$$Cov(d, \Omega_0) = 2 \cdot Tr(B_1 D B_2 D) + 4 \cdot \tilde{l}^T B_1 D B_2 \tilde{l} , \tag{5.37}$$

where $B_1 = d_1 A^T P$, $B_2 = P Q_{\hat{v}} P$ and $\tilde{l} = E(l)$. Since:

$$\begin{aligned} B_1 D B_2 &= d_1 A^T P \cdot \sigma^2 P^{-1} \cdot P Q_{\hat{v}} P \\ &= \sigma^2 d_1 A^T P Q_{\hat{v}} P \\ &= \sigma^2 d_1 (A^T P - A^T P A Q_{\hat{x}} A^T P) = 0 , \end{aligned} \tag{5.38}$$

one can obtain $Cov(d, \Omega_0) = 0$, which means that the independence between d and Ω_0 will always hold. With this justification, the distribution of the statistic W_s, under the null hypothesis, can be theoretically identified as Student's t distribution.

When the test statistic W_s is used to evaluate the likelihood of the best ambiguity combination K_m relative to the second best combination K_s, the vectors c_i and c_j in the above statistics are replaced by the vectors K_m and K_s, respectively. As in the previous example, the alternative hypothesis becomes $E(d) > 0$. Then, with the chosen significance level α, the critical value for the test statistics W_s, written as $C_t = t(f, 1-\alpha)$, can be determined by:

$$\int_{-\infty}^{C_t} t_f(y) dy = 1 - \alpha , \tag{5.39}$$

where $t_f(y)$ is the central t distributed density function with f degrees of freedom. If the following inequality is true:

$$W_s > t(f, 1-\alpha), \tag{5.40}$$

the likelihood of the integer ambiguity combination K_m is statistically significantly larger than that of the second best one K_s. Conversely, with the estimated test statistic W_s, the confidence level $1-\alpha_t$ can be evaluated using the following formula:

$$1-\alpha_t = P(y < W_s) = \int_{-\infty}^{W_s} t_f(y)dy. \tag{5.41}$$

5.4.2 The Artificial Nesting Method

An alternative method to construct the discrimination test procedure is to artificially nest the two compared models with the so-called *nesting parameter* λ such as :

$$l + v = (1-\lambda)(A_c x_c + A_k c_i) + \lambda(A_c x_c + A_k c_j), \tag{5.42}$$

and, then, test the estimated nesting parameter. This kind of method has its roots in the work of Hoel (1947), Williams (1959) and Atkinson (1969). As commented in Chen (1997), Equation 24 in Han (1997) is equivalent to the above formulation, from which λ is estimated as :

$$\hat{\lambda} = Q_{\hat{\lambda}}(c_j - c_i)Q_{\hat{x}_k}^{-1}(\hat{x}_k - c_i), \tag{5.43}$$

with $Q_{\hat{\lambda}} = [(c_j - c_i)^T Q_{\hat{x}_k}^{-1}(c_j - c_i)]^{-1}$ being the cofactor of $\hat{\lambda}$ (Han, 1997). Furthermore, $\hat{\lambda}$ and $Q_{\hat{\lambda}}$ are derived using d and Q_d as :

$$\hat{\lambda} = \frac{1 - 4dQ_d^{-1}}{2}, \tag{5.44}$$

$$Q_{\hat{\lambda}} = 4Q_d^{-1}. \tag{5.45}$$

It is interesting to note that when λ is equal to $1/2$, the two compared models: $(A_c x_c + A_k c_i)$ and $(A_c x_c + A_k c_j)$ will have the same 'weight' in the above combined model and the associated quadratic forms of the residuals for these two models are the same, i.e. the quantity $d = 0$. In this case, the two compared models cannot be distinguished from each other. Therefore, the null hypothesis could be set up as H_0: $E(\hat{\lambda}) = 1/2$, which indicates that two compared models fit the data equally well. The alternative hypothesis is H_a: $E(\hat{\lambda}) \neq 1/2$.

If l is assumed as having a normal distribution, $\hat{\lambda}$ is normally distributed. Based on the symmetric feature of normal distributions, the corresponding test statistic can be derived as:

$$W_\tau = -\frac{\hat{\lambda} - E(\hat{\lambda})}{\sqrt{Cov(\hat{\lambda})}} = \frac{1 - 2\hat{\lambda}}{2\sqrt{Cov(\hat{\lambda})}}, \tag{5.46}$$

where $Cov(\hat{\lambda})$ is the estimated variance of $\hat{\lambda}$. If $Cov(\hat{\lambda})$ is formulated with the *a priori* variance factor σ^2 as $Cov(\hat{\lambda}) = \sigma^2 Q_{\hat{\lambda}}$, the test statistic W_τ, with Equations 5.44 and 5.45, becomes:

$$W_\tau = \frac{1 - 2\hat{\lambda}}{2\sigma\sqrt{Q_{\hat{\lambda}}}} = \frac{1 - (1 - 4dQ_d^{-1})}{2\sigma\sqrt{4Q_d^{-1}}} = \frac{d}{\sigma\sqrt{Q_d}} = W_a, \tag{5.47}$$

which is identical to Equation 5.33. Similarly, if $Cov(\hat{\lambda})$ is formulated with the *a posteriori* variance factor $\hat{s}_0^2$ as $Cov(\hat{\lambda}) = \hat{s}_0^2 Q_{\hat{\lambda}}$, the test statistic W_τ becomes:

$$W_\tau = \frac{1 - 2\hat{\lambda}}{2\hat{s}_0\sqrt{Q_{\hat{\lambda}}}} = \frac{d}{\hat{s}_0\sqrt{Q_d}} = W_s, \tag{5.48}$$

which is identical to Equation 5.36. It is also possible to obtain an estimator of the variance factor, $\hat{s}_1^2$, from the above nested model as (Han, 1997):

$$\hat{s}_1^2 = \frac{\Omega_{c_i} - \hat{\lambda}^2 Q_{\hat{\lambda}}^{-1}}{n-t-1}, \tag{5.49}$$

with which the test statistic W_τ becomes:

$$W_\lambda = \frac{1-2\hat{\lambda}}{2\hat{s}_1\sqrt{Q_{\hat{\lambda}}}} = \frac{d}{\hat{s}_1\sqrt{Q_d}}. \tag{5.50}$$

Similar to the test statistic W_s, under the null hypothesis, the above test statistic W_λ has a Student's t distribution with degree of freedom $(n-t-1)$.

From the above discussion, it is shown that if the same variance factor is used, the discrimination test statistics derived using both the likelihood ratio method and the artificial nesting method are identical.

An important feature of the above discrimination test procedures is that the null hypothesis is symmetric between the two compared ambiguity combinations. Therefore, the nature of this discrimination test is to evaluate the difference between the two compared ambiguity combinations.

If the vectors c_i and c_j in the above test statistic W_λ are replaced by the two best ambiguity combination vectors K_m and K_s, respectively, the resulting test statistic happens to have a similar form to the discrimination test statistic in (Han, 1997, Equation 32), whose critical value, however, depends on the Type II error, instead of the Type I error (significance level) which is commonly used in statistical testing. Although this statistic can be reached using the procedure discussed here, its derivation (Han, 1997, p.355) is unfortunately not rigorous because the noncentrality parameter is formulated with the estimated variance factor instead of its known value (see Pearson and Hartley, 1972).

5.5 Test Results and Analysis

5.5.1 Static Positioning Data

The static baseline data set was collected on November 16, 1996, in Perth, Australia, using two Leica System 300 dual frequency GPS receivers. The baseline length was about 1.0km and the data sampling rate 15 seconds. During the session of 50 minutes, the curt-off elevation angle was set to 15 degrees and five satellites were tracked. This data set was first processed in static mode to obtain the true ambiguity values which were used to check the correctness of the ambiguity resolved in kinematic mode.

In the kinematic data processing, a total of 200 epochs were divided into 100 batches of two epochs. For each batch, two solutions have been obtained by using one epoch and two epochs of the data respectively. In the data processing, carrier phase and code pseudorange measurements from both L1 and L2 frequencies were used and the double difference measurements were formed. The standard deviations for L1 and L2 carrier phase and code pseudorange, which were estimated from static baseline data processing using the MINQUE method, are 0.0033m, 0.0037m, 0.1050m and 0.1076m, respectively. The covariance between different types of the raw measurements is assumed to be absent in this study (see discussions in Section 4.4.1).

With the ambiguity transformation method developed by Teunissen (1996), the carrier phase measurement equations were reparametrized to contain the wide-lane and L1 double difference carrier phase ambiguity unknowns. By taking the advantage of this transformation, the wide-lane ambiguity was first recovered. With the fixed integer wide-lane ambiguities, the L1 carrier phase integer ambiguity values can be easily identified. Therefore, computation results relating only to the wide-lane ambiguity resolutions will be analysed in detail.

In all the solutions, the best integer ambiguity combinations identified from the search process are identical to the true integer ambiguity values. If the significance level α_1 in the ambiguity acceptance tests is chosen as 0.01 percent, all the best integer ambiguity combinations can pass the acceptance test (Section 5.3).

The graphs in Figures 5.1 and 5.2 show the classic ambiguity discrimination test statistic, which is defined by Landau and Euler (1992) as $F = \Omega_s / \Omega_m$. The new discrimination test statistics W_s and W_λ, formulated with Equations 5.36 and 5.50, are graphed in Figures 5.3 and 5.4, and the corresponding confidence levels $1-\alpha_t$ are shown in Figures 5.5 and 5.6. Note that confidence levels for the F-ratio cannot be shown rigorously because the distribution of this statistic is unknown.

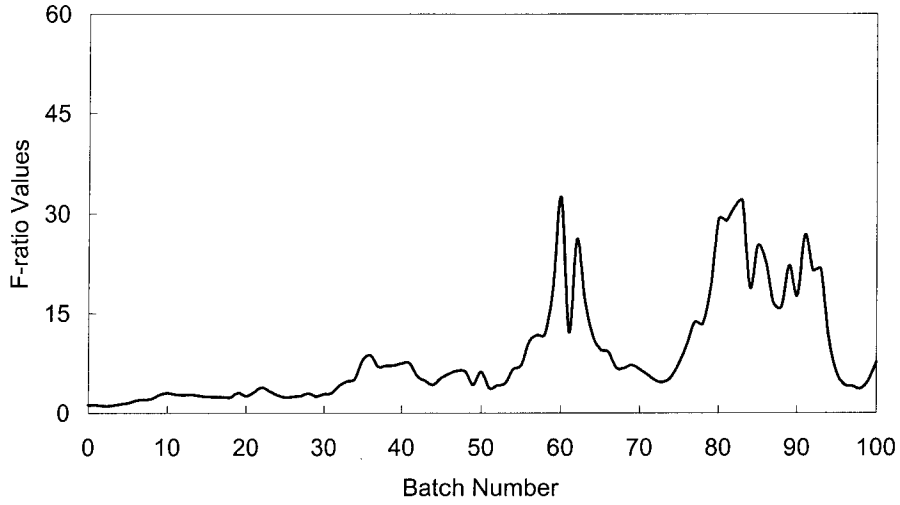

Figure 5.1 F-ratio values for static data (one epoch)

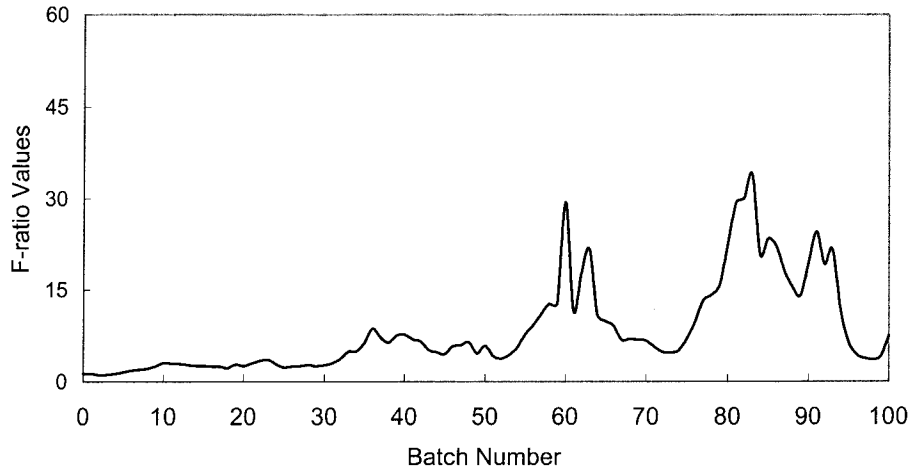

Figure 5.2 *F*-ratio values for static data (two epochs)

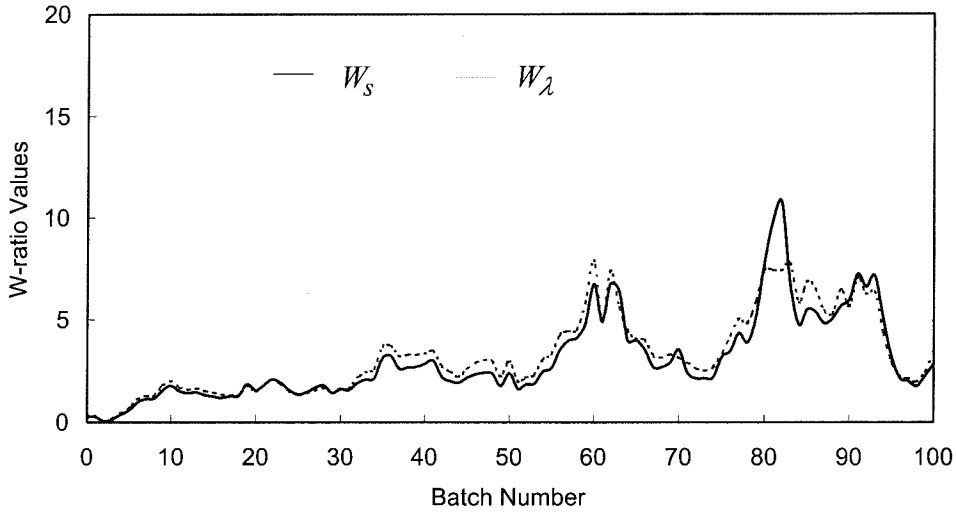

Figure 5.3 *W*-ratio values for static data (one epoch)

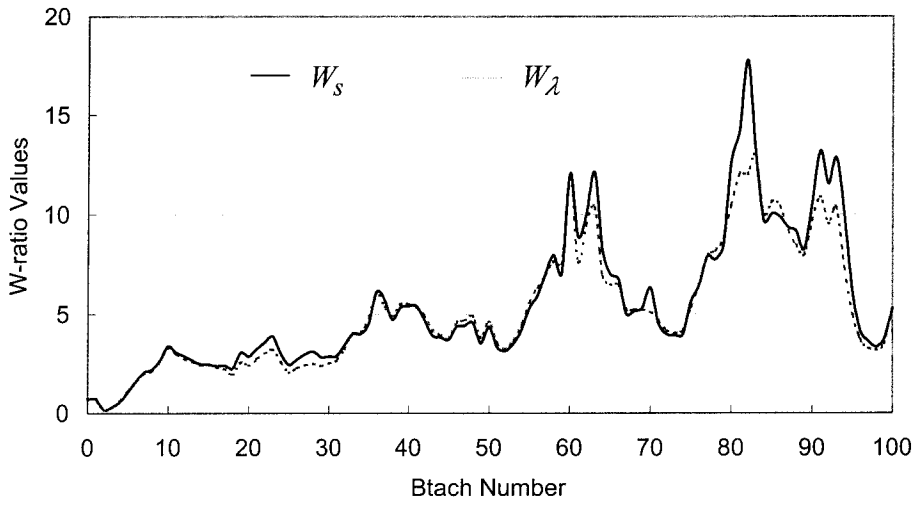

Figure 5.4 *W*-ratio values for static data (two epochs)

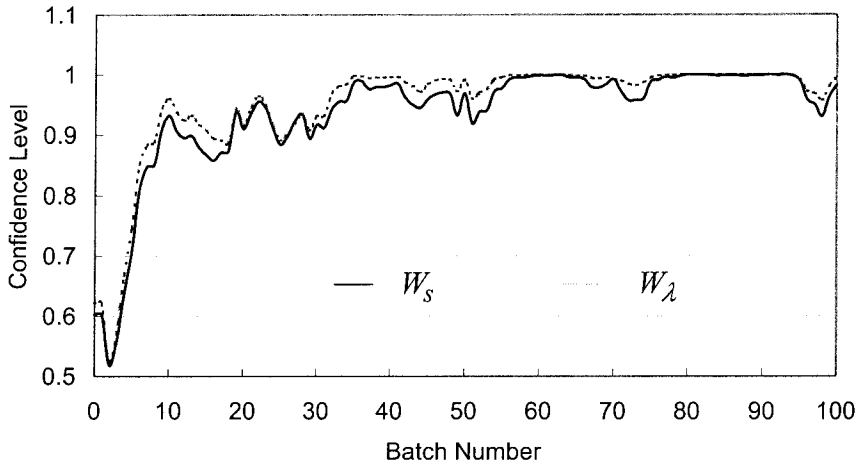

Figure 5.5 Confidence levels for static data (one epoch)

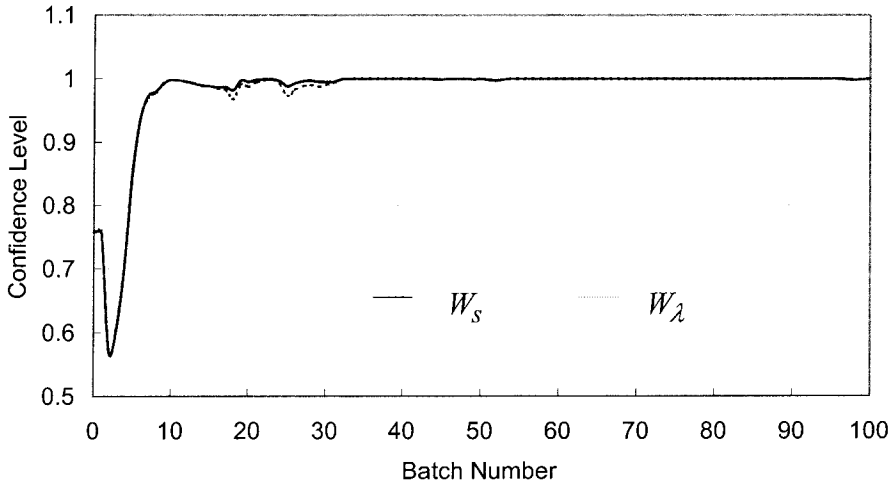

Figure 5.6 Confidence levels for static data (two epochs)

With the ambiguity discrimination test statistics W_s and W_λ, and the corresponding confidence levels, the likelihood of the best integer ambiguity combinations related to the second best combinations can be theoretically evaluated. If the confidence level is chosen as 0.95, the corresponding critical values for the statistic W_s in the cases of one-epoch and two-epoch solutions are 2.01 and 1.73, respectively. The success rates of the ambiguity resolutions for the one-epoch and two-epoch solutions, demonstrated in Figures 5.3 and 5.4, are 62 percent and 94 percent, respectively. With the above chosen significance level, the critical values for the statistic W_λ in the cases of one-epoch and two-epoch solutions are 1.86 and 1.72, respectively. If the test statistic W_λ is used, the success rates of the ambiguity resolutions for the one-epoch and two-epoch solutions, demonstrated also in Figures 5.3 and 5.4, are 71 percent and 94 percent, respectively, which are close to the results for the statistic W_s.

Comparing with the one-epoch solutions, the confidence levels of the discrimination tests with both the statistics W_s and W_λ in the case of the two-epoch solutions are significantly increased. This can be expected because with two-epoch data, the redundancy and geometry of the solutions have been improved.

The above improvement, however, is not as well indicated by the classic ambiguity discrimination test statistics, i.e., *F*-ratios, demonstrated in Figures 5.1 and 5.2. If the critical value of the *F*-ratio is arbitrarily chosen to be 2.0, as is commonly accepted (e.g. Landau and Euler, 1992), the success rate of the ambiguity resolutions for one-epoch solutions is 94 percent, but for two-epoch solutions, the success rate of the ambiguity resolutions is unexpectedly down to 93 percent.

5.5.2 Kinematic Positioning Data

A land kinematic GPS positioning test was carried out on December 18, 1996, also in Perth. Two Trimble 4000SSE dual frequency receivers were employed to collect the kinematic data. The rover receiver antenna was mounted on the roof of a car and driven around the test area (about 2.0km away from the reference station). The trajectory of the roving antenna for this test is shown in Figure 5.7.

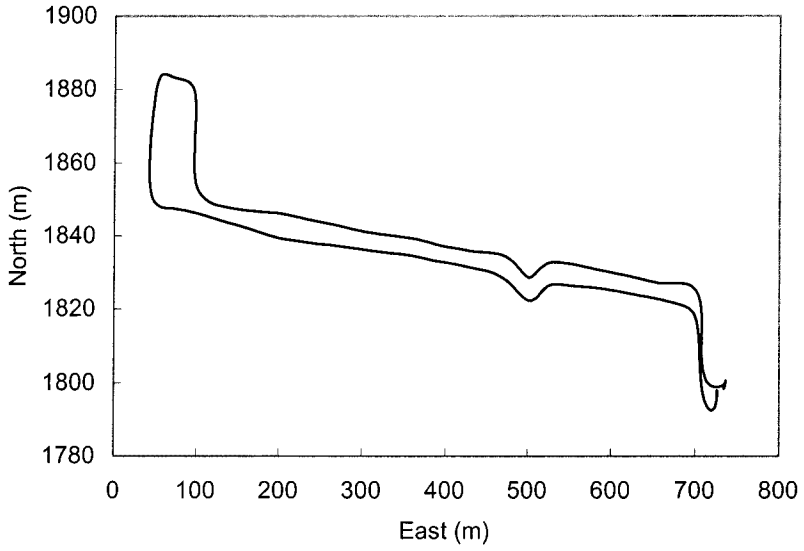

Figure 5.7 Vehicle trajectory for kinematic test

The maximum velocity of the car reached 26 m/sec. During the five minutes of the test, the cut-off elevation angle was set to 15 degrees and seven satellites were tracked and no carrier phase cycle slips occurred. The data sampling rate was one second. Before the beginning of the kinematic test, five minutes static data were collected to obtain the true ambiguity values which were used to check whether or not the kinematic ambiguity solutions are correct.

The kinematic GPS data of total 300 epochs were divided into 100 batches of three epochs. For each batch, two solutions have been obtained by using one epoch and three epochs of the data, respectively.

The data processing procedure using carrier phase and code pseudorange measurements from both L1 and L2 frequencies was identical to that described previously for the static data test. The standard deviations for L1 and L2 carrier phase and code pseudorange are 0.0022m, 0.0034m, 0.3113m and 0.4266m, respectively, which were estimated from the static baseline using the MINQUE method. The covariance between the raw measurements is assumed to be absent. In all the solutions, the best integer ambiguity combinations identified from the search process were identical to the true integer ambiguity values. As in the previous test, with the significance level α_1 in the ambiguity acceptance tests chosen as 0.01 percent, all the best integer ambiguity combinations passed the acceptance test.

Figures 5.8 and 5.9 show, for the kinematic test, the classic ambiguity validation test statistic [$F = \Omega_s / \Omega_m$], while the new discrimination test statistics W_s and W_λ are presented in Figures 5.10 and 5.11, and the corresponding confidence levels are shown in Figures 5.12 and 5.13 .

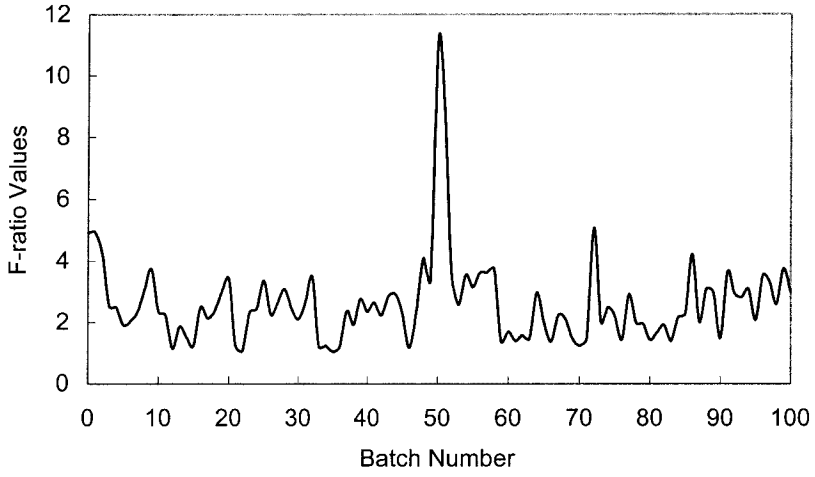

Figure 5.8 *F*-ratio values for kinematic data (one epoch)

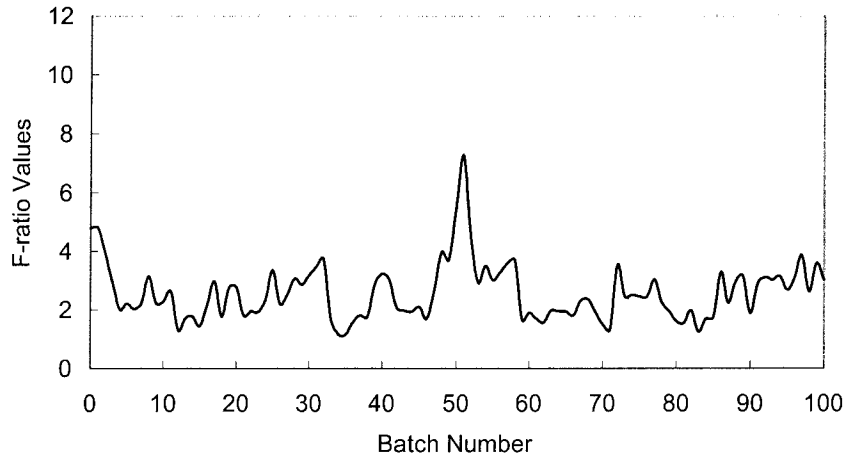

Figure 5.9 *F*-ratio values for kinematic data (three epochs)

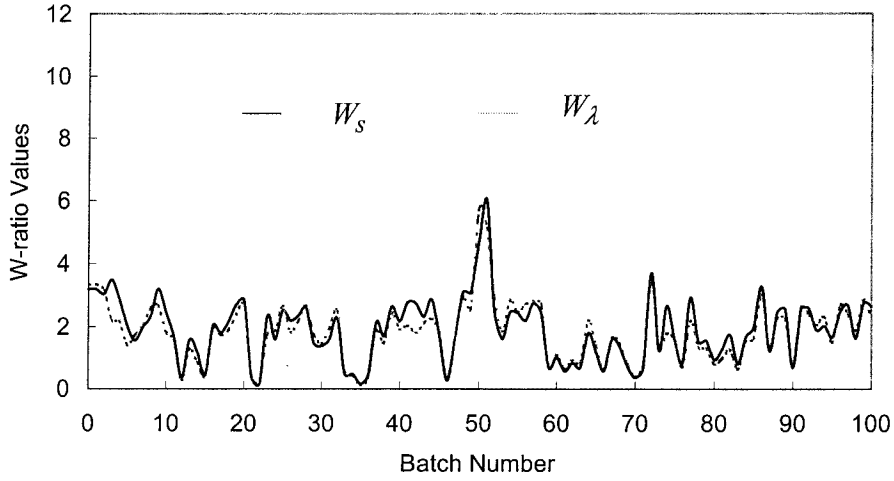

Figure 5.10 W-ratio values for kinematic data (one epoch)

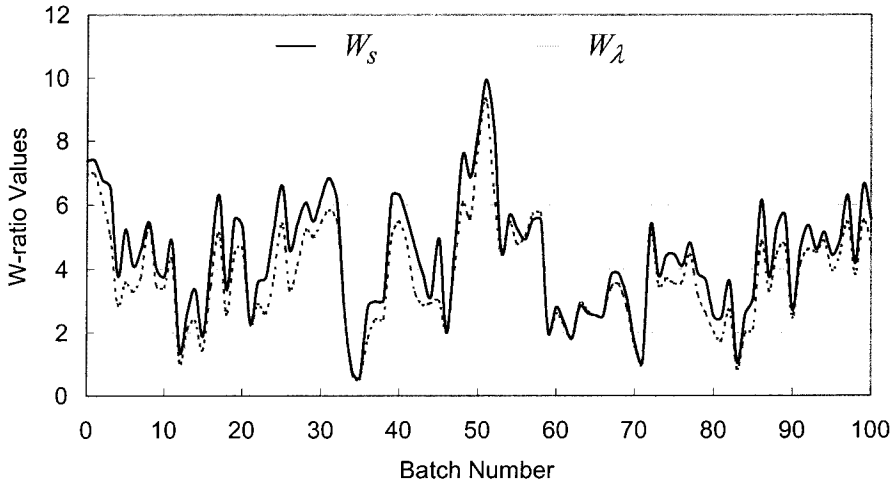

Figure 5.11 W-ratio values for kinematic data (three-epochs)

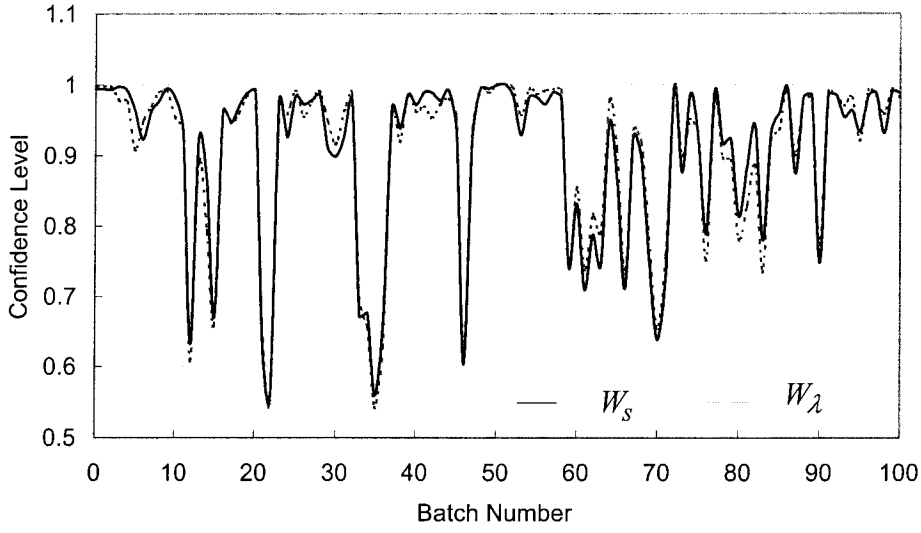

Figure 5.12 Confidence levels for kinematic data (one epoch)

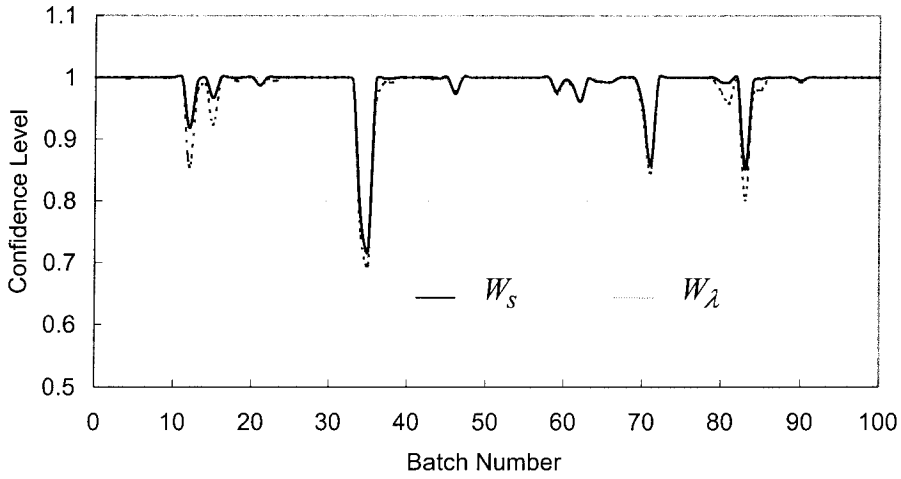

Figure 5.13 Confidence levels for kinematic data (three epochs)

If the confidence level is chosen as 0.95, the corresponding critical values for the statistic W_s in the cases of one-epoch and three-epoch solutions are 1.833 and 1.675, respectively. The success rates of the ambiguity resolutions for the one-epoch and three-epoch solutions, demonstrated in Figures 5.10 and 5.11, are 51 percent and 95 percent, respectively. With the above chosen confidence level, the critical values for the statistic W_λ in the cases of one-epoch and three-epoch solutions are 1.760 and 1.670, respectively. If the test statistic W_λ is used, the success rates of the ambiguity resolutions for the one-epoch and three-epoch solutions, demonstrated also in Figures 5.10 and 5.11, are 54 percent and 93 percent, respectively, which are again fairly close to the results for the statistic W_s.

The above improvement, however, is not as well indicated by the classic ambiguity discrimination test statistics, i.e., *F*-ratios, demonstrated in Figures 5.8 and 5.9. If the critical value of the *F*-ratio is arbitrarily chosen to be 2.0, as is commonly accepted (e.g. Landau and Euler, 1992), the success rate of the ambiguity resolutions for one-epoch solutions is 70 percent, but for three-epoch solutions, the success rate of the ambiguity resolutions is unexpectedly down to 64 percent.

5.5.3 Discussion

In both examples given above, the success rate of ambiguity resolution using the classic ambiguity discrimination test statistics is less for two or three epochs of data

than for a single epoch of data. Clearly, if more epochs of data are available then the improved redundancy and geometry of a solution should lead to an improved success rate. It is therefore evident that a fixed critical value of the *F*-ratio test does not yield particularly statistically relevant results in the above two examples. However, the ambiguity discrimination test, based on the likelihood ratio method or artificial nesting method, exhibits the expected increase in success rate when a greater number of data epochs are added into the solution, demonstrating that these tests do yield statistically relevant results.

5.6 Summary

An ambiguity discrimination test procedure has been derived in detail with both the likelihood ratio method and the nesting method. The distributions of the proposed test statistics have been identified theoretically. With the derived formulae in this chapter, the likelihood of the best integer ambiguity combination relative to the second best can be statistically evaluated.

Although the commonly used *F*-ratio test appears to work satisfactorily in many practical applications (see, Chapters 2, 3, 4 and 6), the distribution of the *F*-ratio statistic is, if not impossible, very difficult to identify. The critical value of the *F*-ratio is usually chosen somewhat arbitrarily and thus the corresponding confidence level is unclear. In contrast, the ambiguity discrimination test procedure based on the likelihood ratio method or artificial nesting method is more robust as the distributions of the test statistics have been identified theoretically and the critical value can be chosen rigorously. Computation results from independent static and kinematic GPS positioning test data observed using different receiver hardware have illustrated the suitability of these statistics to GPS ambiguity quality control.

The proposed ambiguity discrimination test procedure has also been successfully applied in GLONASS and integrated GPS/GLONASS positioning (see Chapters 2, 4 and 6).

Chapter 6

AN APPROACH TO GLONASS AMBIGUITY RESOLUTION

6.1 Introduction

The GLONASS positioning system, like GPS, has a great potential for precise navigation and geodetic applications. It has also been seen that there are many advantages of the integration of the two existing satellite systems. However, due to the fact that the GLONASS satellites transmit their signals at different frequencies, processing the GLONASS carrier phase measurements is much more complicated than processing GPS data only. As discussed in Chapter 2, in processing the GLONASS carrier phases, one of the critical issues is that the standard double-differencing (DD) procedure cannot cancel receiver clock errors and thus results in rank deficiency in the design matrix. As a consequence of this, the normal matrix becomes singular (see Appendix A). To remove this singularity, a number of modelling methods have been investigated in the literature. These modelling methods were reviewed in Section 2.2.

In terms of carrier phase ambiguity resolution, a common feature of many existing models is that all rely on the use of pseudorange measurements, although the pseudoranges are used in a different way for each model (Section 2.2). Unlike GPS, the effects of the inter-channel hardware delays on GLONASS pseudoranges are significant (e.g. Pratt *et al.*, 1997; Wang, 1998a). For reliable ambiguity resolution, specific efforts must be made to accommodate these biases. Therefore, for high-precision geodetic applications of the GLONASS data, it will be also of great importance to develop suitable algorithms to process carrier phase data only. Examples in this direction are Habrich (1998), Povaliaev (1997), Rossbach and Hein (1996).

This chapter emphasises an approach to GLONASS carrier phase ambiguity resolution which is not sensitive to the biases in pseudorange data. Biases in carrier phase data are assumed to be negligible (Section 1.4.3). Mathematical description of

the proposed approach and practical strategies for data processing are presented, and tested using real data sets.

6.2 Modelling GLONAS Phase Measurements

Similar to GPS measurements, so-called *differencing* procedures can eliminate some systematic errors existing in the GLONASS measurements, such as atmospheric delay, satellite orbit and clock errors. The resulting mathematical models are consequently simplified. For short baselines, the mathematical model for single-differenced (SD) carrier phases is usually expressed as (e.g. Leick, 1995; Habrich, 1998; Teunissen and Kleusberg, 1996):

$$\varphi_{km}^{p}(i) = \frac{1}{\lambda_p}\rho_{km}^{p}(i) + \frac{c}{\lambda_p}t_{km}(i) + N_{km}^{p} + \varepsilon_{km}^{p}(i), \tag{6.1}$$

where the superscript p identifies the satellite; the subscripts k and m represent the receivers; the indices i denotes the epoch at which the data are collected; $\varphi_{km}^{p}(i)$ is the SD carrier phase expressed in units of cycles; $\rho_{km}^{p}(i)$ is the SD receiver-satellite range; $t_{km}(i)$ is the relative receiver clock error; c is the speed of light; N_{km}^{p} is the integer carrier-phase ambiguity; $\varepsilon_{km}^{p}(i)$ is the noise of the SD carrier phase; λ_p is the wavelength of the frequency for satellite p. For satellites p and q, the DD carrier phase is further written as:

$$\varphi_{km}^{pq}(i) = \frac{1}{\lambda_p}\rho_{km}^{p}(i) - \frac{1}{\lambda_q}\rho_{km}^{q}(i) + (\frac{c}{\lambda_p} - \frac{c}{\lambda_q})t_{km}(i) + N_{km}^{pq} + \varepsilon_{km}^{pq}(i), \tag{6.2}$$

which shows that unlike GPS, the DD GLONASS carrier phases are sensitive to receiver clock errors (Section 2.2). Consequently, if only DD carrier phase measurements are used in an adjustment, the normal matrix becomes singular. This means that the DD ambiguity parameter cannot be separated from the receiver clock parameter. To cancel the receiver clock errors in DD carrier phases, such strategies as scaling original carrier phases into their linear distances, GLONASS mean frequency or GPS L1 frequency have been proposed in the literature (e.g. Leick *et*

al., 1995; Landau, 1998). It has been shown that the adjustment results using these strategies are identical (see Section 2.2). Scaling the carrier phases into distances and then forming the double differences gives:

$$\phi_{km}^{pq}(i) = \rho_{km}^{pq}(i) + \overline{N}_{km}^{pq} + \overline{\varepsilon}_{km}^{pq}(i), \tag{6.3}$$

with

$$\overline{N}_{km}^{pq} = \lambda_q N_{km}^{pq} + (\lambda_p - \lambda_q) N_{km}^{p}, \tag{6.4}$$

$$\overline{\varepsilon}_{km}^{pq}(i) = \lambda_p \varepsilon_{km}^{p}(i) - \lambda_q \varepsilon_{km}^{q}(i). \tag{6.5}$$

In Equation 6.3, the SD ambiguity parameters are presented. The SD and DD ambiguities are inseparable, however. The lumped parameter $\overline{N}_{km}^{pq}$ is, by definition, not an integer. Obviously, the key issue here is how to determine the integer SD ambiguity value. One possible option to obtain the SD ambiguity value is the use of both SD pseudoranges and SD carrier phases (e.g. Leick *et al.*, 1995; Landau, 1998). For example, at epoch i, the SD ambiguity may be approximated as:

$$N_{km}^{p} = \frac{1}{\lambda_p}[R_{km}^{p}(i) - \lambda_p \varphi_{km}^{p}(i)], \tag{6.6}$$

where $R_{km}^{p}(i)$ is the SD pseudorange. It is easy to see that the correct estimation of SD ambiguities is highly dependent on precise pseudoranges. In many practical situations, however, pseudoranges may be seriously biased by multipath and hardware delays. For example, a 5m error in pseudorange will cause an error of about 26 cycles in the estimated SD ambiguity value. The effect of this wrong SD ambiguity value on the scaled DD carrier phase measurements can reach the level of as high as 0.04m (about 0.2 cycles) and thus make ambiguity resolution unfeasible. Therefore, specific strategies for estimating SD ambiguities need to be further investigated.

6.3 Proposed Approach to Resolve GLONASS Ambiguities

When resolving GPS ambiguities, the principle of the so-called *integer least-squares* is critical (e.g. Teunissen, 1993). Within the search space assumed to contain the correct integer ambiguities, all possible ambiguity combinations are fitted to the GPS measurements. The integer ambiguity combination that results in the minimum quadratic form of the least-squares residuals is considered as the most likely (*best*) solution (Section 5.1). In the case of GLONASS ambiguity resolution, however, not only the DD ambiguities but also the SD ambiguities need to be considered.

To reduce the number of the unknown SD ambiguities in the measurement equations, the satellite p is chosen as a reference satellite in forming all the DD GLONASS carrier phases. Thus N_{km}^{p} is the unique unknown SD ambiguity parameter in the following adjustment. If both SD and DD ambiguities are thought to be integers, the basic principle of fixing the DD ambiguities can also be employed to determine this unknown SD ambiguity. The proposed approach to the SD and DD ambiguity resolution is to be presented in the following.

6.3.1 Estimating Float DD Ambiguities

Based on Equation 6.3, the linearized mathematical model of the DD (scaled) carrier phases reads:

$$Dl_i = DA_i x_c + B_k x_k + f_m x_m + e_i \,, \tag{6.7}$$

where $i = 1, 2, \ldots, s$ denotes the epoch number and

- s is the total number of epochs;
- D is an $(n-1)\times n$ *DD matrix operator* (Teunissen 1997); n is the number of satellites
- l_i is an $n \times 1$ vector of the difference between the SD carrier phase measurements and their calculated values;
- x_c is a 3×1 vector of the unknown increments of baseline components;
- x_k is an $(n-1)\times 1$ vector of the unknown DD ambiguities;
- x_m is an unknown SD ambiguity parameter;

A_i is an $n \times 3$ design matrix capturing the relative satellite-receiver geometry at epoch i;

B_k is an $(n-1) \times (n-1)$ diagonal matrix whose diagonal elements are the wavelengths, say λ_i;

f_m is an $(n-1) \times 1$ vector of the wavelength-difference terms $(\lambda_i - \lambda_p)$;

e_i is an $(n-1) \times 1$ vector of the DD phase noise terms expressed by Equation 6.5.

For the adjustment of all s epochs of data, the mathematical model reads:

$$l = Ax_c + Bx_k + fx_m + e, \tag{6.8}$$

where

$$A = (A_1^T D^T, A_2^T D^T, \ldots, A_s^T D^T)^T;$$
$$B = (B_k, B_k, \ldots, B_k)^T;$$
$$f = (f_m^T, f_m^T, \ldots, f_m^T)^T;$$
$$e = (e_1^T, e_2^T, \ldots, e_s^T)^T.$$

However, it is noted that:

$$(A, B, f)\begin{pmatrix} 0 \\ B_k^{-1} f_m \\ -1 \end{pmatrix} = 0, \tag{6.9}$$

which indicates that a linear dependent combination exists in the column vectors of the design matrices. The resulting normal matrix is therefore singular. This theoretically confirms the above statement that the SD and DD ambiguities are inseparable. To remove the singularity in the normal matrix, the SD ambiguity parameter is assigned an approximate value (m_0) and Equation 6.8 is rewritten as:

$$\bar{l}(m_0) = Ax_c + Bx_k + e, \tag{6.10}$$

with $\bar{l}(m_0) = l - f \cdot m_0$. In Equation 6.10, the unknown SD ambiguity disappears and thus, the unknown DD ambiguity parameters can be estimated together with the baseline components. To do this, a stochastic model (covariance matrix) for the DD carrier phases is also required. By assuming that the unscaled SD carrier phases are statistically independent and have the same variance σ_0^2, the covariance matrix for the DD carrier phases at epoch i is derived as:

$$C_i = \sigma_0^2 \begin{bmatrix} \lambda_1^2 + \lambda_p^2 & \lambda_p^2 & \cdots & \lambda_p^2 \\ \lambda_p^2 & \lambda_2^2 + \lambda_p^2 & \cdots & \lambda_p^2 \\ \cdots & \cdots & \cdots & \cdots \\ \lambda_p^2 & \lambda_p^2 & \cdots & \lambda_n^2 + \lambda_p^2 \end{bmatrix} = \sigma_0^2 P_i^{-1}. \tag{6.11}$$

Actually, the SD carrier phases may not have the same variance (for example, they may be elevation dependent). A realistic estimation of both the variance and covariance can improve the reliability of ambiguity resolution. The covariance matrix for the DD carrier phases can also be estimated using the procedure discussed in Chapter 3. Moreover, with the assumptions that the time correlation between epochs is absent and the covariance matrices for each epoch are identical, the whole covariance matrix in the adjustment is then written as:

$$Cov(e) = C = diag(C_i) = \sigma_0^2 diag(P_i^{-1}) = \sigma_0^2 P^{-1}, \tag{6.12}$$

where P is the weight matrix and P_i are its diagonal block matrices. Based on the mathematical and stochastic models given respectively by Equations 6.10 and 6.12, the least-squares estimators of the unknowns x_c and x_k are derived as

$$\hat{x}_c(m_0) = Q_{\hat{x}_c} A^T P \bar{l}(m_0) + Q_{\hat{x}_c \hat{x}_k} B^T P \bar{l}(m_0), \tag{6.13}$$

$$\hat{x}_k(m_0) = Q_{\hat{x}_k \hat{x}_c} A^T P \bar{l}(m_0) + Q_{\hat{x}_k} B^T P \bar{l}(m_0), \tag{6.14}$$

with the matrices $Q_{\hat{x}_c}$, $Q_{\hat{x}_k}$, $Q_{\hat{x}_c \hat{x}_k}$ and $Q_{\hat{x}_k \hat{x}_c}$ being determined by:

$$\begin{bmatrix} Q_{\hat{x}_c} & Q_{\hat{x}_c\hat{x}_k} \\ Q_{\hat{x}_k\hat{x}_c} & Q_{\hat{x}_k} \end{bmatrix} = \begin{bmatrix} A^T PA & A^T PB \\ B^T PA & B^T PB \end{bmatrix}^{-1}. \tag{6.15}$$

Hence, the least-squares residuals read:

$$\hat{e}(m_0) = \bar{l}(m_0) - A\hat{x}_c(m_0) - B\hat{x}_k(m_0), \tag{6.16}$$

and the estimated variance factor (the variance of SD carrier phases) is:

$$\hat{s}^2(m_0) = \frac{\Omega(m_0)}{r}, \tag{6.17}$$

where $\Omega(m_0) = \hat{e}^T(m_0)P\hat{e}(m_0)$ is the quadratic form of the residuals and $r = (s-1)(n-1)-3$ is the degrees of freedom.

It may be expected that if the SD ambiguity is fixed to its correct integer value, the mathematical model expressed by Equation 6.10 will have a good performance in the following DD ambiguity-float solution. The closer the approximate SD ambiguity m_0 to its correct value, the smaller the resulting quadratic form of residuals. However, the following theorem shows that this is untrue.

Theorem 6.1 *(SD Ambiguity Search)*

Suppose that fixing the SD ambiguity parameter x_m in Equation 6.10 to any two integer values m_i and m_j leads to two sets of statistics for the DD ambiguity-float solutions, namely, $\hat{x}_c(m_i)$, $\hat{x}_k(m_i)$, $\hat{e}(m_i)$, $\Omega(m_i)$, and $\hat{x}_c(m_j)$, $\hat{x}_k(m_j)$, $\hat{e}(m_j)$, $\Omega(m_j)$. It is then concluded that:

(a) $\hat{x}_k(m_i) = \hat{x}_k(m_j) + B_k^{-1} f_m \cdot (m_j - m_i)$; (6.18)

(b) $\hat{x}_c(m_i) = \hat{x}_c(m_j)$; (6.19)

(c) $\hat{e}(m_i) = \hat{e}(m_j)$; (6.20)

(d) $\Omega(m_i) = \Omega(m_j)$. (6.21)

Proof: see Appendix E.

Equation 6.18 shows that, when fixing the SD ambiguity to different values, the DD ambiguity parameters can be easily calculated with no need for reprocessing the whole data set. This result can be used to simplify the process of searching for the best SD ambiguity value. Equations 6.19, 6.20 and 6.21 indicate that the baseline components, the DD phase residuals and the quadratic form of the residuals are independent of the fixed SD ambiguity value in DD ambiguity-float solutions. This means that with the statistics of the DD ambiguity-float solutions, it is impossible to search for the most likely SD ambiguity value. Ambiguity validation criteria need to be further discussed in the subsequent section.

6.3.2 Ambiguity Validation Criteria

Given the SD ambiguity fixed to an approximate value m_i, the real-valued DD ambiguity parameters are estimated, and the so-called ambiguity search process is then performed using a search criterion based on the minimisation of the quadratic form of the least-squares residuals. When one or more integer ambiguity combinations pass the acceptance tests, the integer ambiguity combinations that result in the minimum and second minimum quadratic forms of the least-squares residuals will be considered as the most likely (*best*) and *second best* solutions, respectively. Then, a so-called discrimination test (see Chapter 5) is performed to ensure that the most likely integer ambiguity combination, denoted as K_1, is statistically better than the second best combination, denoted as K_2.

Suppose that fixing the DD ambiguities to K_1 and K_2 produces the quadratic forms of the residuals as $\overline{\Omega}(K_1, m_i)$ and $\overline{\Omega}(K_2, m_i)$, respectively. With the SD ambiguity being fixed to m_i, the acceptance of the best DD ambiguity combination can be evaluated by the following statistic

$$T = \frac{\Omega(m_i)}{\overline{\Omega}(K_1, m_i)}, \tag{6.22}$$

with $\overline{\Omega}(K_1, m_i) = \Omega(m_i) + R(m_i)$ and $R(m_i) = [K_1 - \hat{x}_k(m_i)]^T Q_{\hat{x}_k}^{-1}[K_1 - \hat{x}_k(m_i)]$. If the measurement errors are assumed to be normally distributed, the quadratic forms $\Omega(m_i)$ and $R(m_i)$ are independent and each of them has a Chi-Square distribution (Koch, 1988, p.301). Consequently, the statistic T has a *Beta* distribution (e.g. Beyer 1968, p.52). For the discrimination test, a classic statistic is the so-called *F*-ratio defined by (e.g. Pratt *et al.*, 1997; Walsh *et al.*, 1995)

$$F = \frac{\overline{\Omega}(K_2, m_i)}{\overline{\Omega}(K_1, m_i)}, \tag{6.23}$$

A disadvantage of the *F*-ratio is that its distribution is, if not impossible, very difficult to identify. A more rigorous statistic for ambiguity discrimination testing, called *W-ratio*, can be defined by (see Chapter 5)

$$W = \frac{d}{\hat{s}_1(m_i)\sqrt{Q_d}}, \tag{6.24}$$

with $d = \overline{\Omega}(K_2, m_i) - \overline{\Omega}(K_1, m_i)$, $Q_d = 4 \cdot (K_1 - K_2)^T Q_{\hat{x}_k}^{-1}(K_1 - K_2)$ and

$$\hat{s}_1(m_i) = \sqrt{\frac{\overline{\Omega}(K_1, m_i) - \omega_1}{s \cdot (n-1) - 4}}, \tag{6.25}$$

where $\omega_1 = (Q_d - 4d)^2 / 16Q_d$. The statistic W has a Student's t distribution.

The above acceptance and discrimination test statistics are, as expected, dependent on the fixed SD ambiguity value. The closer the SD ambiguity to its correct value, the larger the statistic T. Similar to the case of the DD ambiguity search, therefore, the SD ambiguity values that result in the maximum and second maximum values of the statistic T are considered as the most likely (*best*) and second best SD ambiguity values, denoted as m_1 and m_2, respectively. When the SD ambiguity is fixed to its most likely value, the correct DD ambiguities should more easily be recovered. It is

noted that in practice, even small error in the SD ambiguity may lead to wrong DD ambiguity resolution (Section 6.4.2)

With the DD ambiguities fixed to their correct values with a high confidence level, the DD ambiguities may be considered as constant parameters in Equation 6.8. Then, one can obtain the following measurement equation:

$$\tilde{l}(K_1) = Ax_c + fx_m + e, \tag{6.26}$$

where $\tilde{l}(K_1) = l - BK_1$ with K_1 being the validated best DD ambiguity combination. Based on the mathematical and stochastic models defined in Equations 6.26 and 6.12, the SD ambiguity-float solution can be obtained, including such statistics as the quadratic form of the residuals $\overline{\Omega}(K_1)$ and the cofactor of the estimated SD ambiguity $Q_{\hat{x}_m}$. Similar to the case of validating DD ambiguities, the most likely SD ambiguity can then be validated. Based on the derivation given in Chapter 5, the acceptance test statistic is defined as:

$$\overline{T} = \frac{\overline{\Omega}(K_1)}{\overline{\Omega}(K_1, m_1)}, \tag{6.27}$$

and the discrimination test statistic of *F-ratio*-type reads

$$\overline{F} = \frac{\overline{\Omega}(K_1, m_2)}{\overline{\Omega}(K_1, m_1)}. \tag{6.28}$$

A *W-ratio* statistic (Section 5.4) can also be derived as:

$$\overline{W} = \frac{\overline{d}}{\hat{s}_2(K_1)\sqrt{Q_{\overline{d}}}}, \tag{6.29}$$

with $\overline{d} = \overline{\Omega}(K_1, m_2) - \overline{\Omega}(K_1, m_1)$, $Q_{\overline{d}} = 4 \cdot (m_1 - m_2)^T Q_{\hat{x}_m}^{-1}(m_1 - m_2)$, and

$$\hat{s}_2(K_1) = \sqrt{\frac{\overline{\Omega}(K_1, m_1) - \omega_2}{s \cdot (n-1) - 4}}, \tag{6.30}$$

where $\omega_2 = (Q_{\bar{d}} - 4\bar{d})^2 / 16Q_{\bar{d}}$.

6.3.3 Practical Procedure for GLONASS Ambiguity Resolution

An important feature in GLONASS ambiguity resolution is that the SD ambiguity value is included. To start the process of ambiguity resolution, an initial SD ambiguity value must be determined. Based on Equation 6.6, an approximate SD ambiguity value m_0 can be estimated from pseudoranges. By assuming that possible biases in SD pseudoranges are less than 20m, a search window for the correct SD ambiguity is then constructed as $(m_0 - 100,\ \ m_0 + 100)$. This is designed to ensure that the correct SD ambiguity is contained in the search window.

On the other hand, it is noted from Equation 6.10 that before the correct SD ambiguity value is identified, systematic model errors caused by the approximate SD ambiguity values will be always present. Denoting ∇m as the integer error in the fixed SD ambiguity value, the systematic error in the DD carrier phase for satellite pair p and q can be derived as:

$$\nabla l^{pq} = (\lambda_p - \lambda_q) \cdot \nabla m, \tag{6.31}$$

which indicates that the size of the systematic error is reference-satellite dependent. However, numerical experiments conducted in this study show that choosing different reference satellites gives almost identical results (to 3 decimal places). The reason for this is that the GLONASS satellite frequencies are very close to each other, with the maximum wavelength difference being 0.0015m. To explain this point clearly, the matrix P_i in Equation 6.11 is approximated as:

$$P_i^{-1} \cong \lambda_0^2 \begin{bmatrix} 2 & 1 & \cdots & 1 \\ 1 & 2 & \cdots & 1 \\ \cdots & \cdots & \cdots & \cdots \\ 1 & 1 & \cdots & 2 \end{bmatrix} = \lambda_0^2 D D^T, \tag{6.32}$$

where λ_0 may be one of the wavelengths $\lambda_1, \lambda_2, ..., \lambda_n$. The errors made in the elements of the above approximate matrix are always less than 0.8 percent, which is not significant. With Equation 6.32, the influence imposed by the SD ambiguity error ∇m on the ambiguity-fixed solution is derived as:

$$\begin{aligned}\nabla\hat{x}_c &= (A^T PA)^{-1} A^T P\bar{f} \cdot \nabla m \\ &= (\sum_{i=1}^{s} A_i^T D^T P_i D A_i)^{-1} \cdot \sum_{i=1}^{s} A_i^T D^T P_i D f_m \cdot \nabla m \\ &= (\sum_{i=1}^{s} A_i^T D^T (DD^T)^{-1} D A_i)^{-1} \cdot \sum_{i=1}^{s} A_i^T D^T (DD^T)^{-1} D f_m \cdot \nabla m\end{aligned} \tag{6.33}$$

in which $D^T(DD^T)^{-1}D = E_n - \frac{1}{n} e_n e_n^T$ is an orthogonal projector matrix (Teunissen, 1997). It is apparent that this matrix is independent of the structure of the double differencing matrix D and thus the choice of reference satellite (Teunissen, 1997). Although using different reference satellites does produce similar results, one may argue that for a good approximation of the SD ambiguity value, it is still better to choose the highest satellite as the reference satellite. Actually, if the search window is large enough to contain the correct SD ambiguity, the ambiguity resolution and position solutions are independent of the approximate SD ambiguity values.

Based on the above analysis, a procedure for GLONASS ambiguity resolution is summarised as the following:

(a) choose a reference satellite;
(b) compute an approximate SD ambiguity for the reference satellite;
(c) set up a search window for the SD ambiguity;
(d) search and identify the most likely SD ambiguity using the statistic T (Equation 6.22);
(e) search and validate the most likely DD ambiguity combination (Equations 6.22-6.24);
(f) validate the most likely SD ambiguity (Equations 6.27-6.29).

It should be noted that although the above discussion focuses on the processing of GLONASS data only, the basic equations and procedure are also valid for use in

combining GLONASS and GPS carrier phases. For the combined GPS and GLONASS data processing, it is proposed that the GPS-GPS and GLONASS-GLONASS DD carrier phases are formulated (see Chapter 2).

6.4 Test Results and Analysis

Three experimental data sets were collected in Perth, Australia, using two Ashtech GG24 GPS/GLONASS receivers. All the data sets are free of cycle slips. The details of these data sets are presented in Table 6.1. The zero baseline and 1.2km baseline data sets are analysed in detail to show the performance of the proposed approach to GLONASS ambiguity resolution, whilst the 0.3km baseline data set (with a longer data span) is processed in a batch mode to discuss the methods dealing with the SD ambiguity in final baseline solutions.

Baseline names	Zero baseline	1.2 km baseline	0.3 km baseline
Baseline length (meters)	0	1216	285
Cut-off angle (degrees)	15	15	15
GLONASS satellites	5	4	4
GPS satellites	0	5	6
Data interval (seconds)	10	10	10
Data span (minutes)	5	5	10
Survey date	July 22, 1997	Feb. 16, 1998	Feb. 9, 1998

Table 6.1 Details of the experimental data sets

6.4.1 Ambiguity Search and Acceptance Tests

Following the above proposed procedure, the SD and DD ambiguity search is performed for both data sets. The DD ambiguity search was conducted using the LAMBDA method (Teunissen, 1993). The resulting statistics for ambiguity validation tests are presented in Figures 6.1-6.6. It is shown in Figure 6.1 that, in the case of the zero baseline, the most likely SD ambiguity is -6, with the maximum value of the statistic T being 0.964. If the confidence level is chosen as 99 percent, the critical value for the statistic T is set to 0.384. Therefore, the best DD ambiguity combination passes the acceptance test. Figure 6.2 indicates that in the case of the 1.2km baseline, the peak value of the statistic T reaches 0.620, with which the most likely SD ambiguity is identified as zero. With the above given confidence level, the critical value for the statistic T is 0.411, and thus, the best DD ambiguity

combination can also statistically be accepted. Both Figures 6.1 and 6.2 show that with the fixed SD ambiguity value approaching its correct value, the value of the statistic T increases, as expected. Some oscillations in Figures 6.1-6.6 may be caused by the noise, residual systematic errors in the measurements and certain geometric structures inherent in statistics T, F and W.

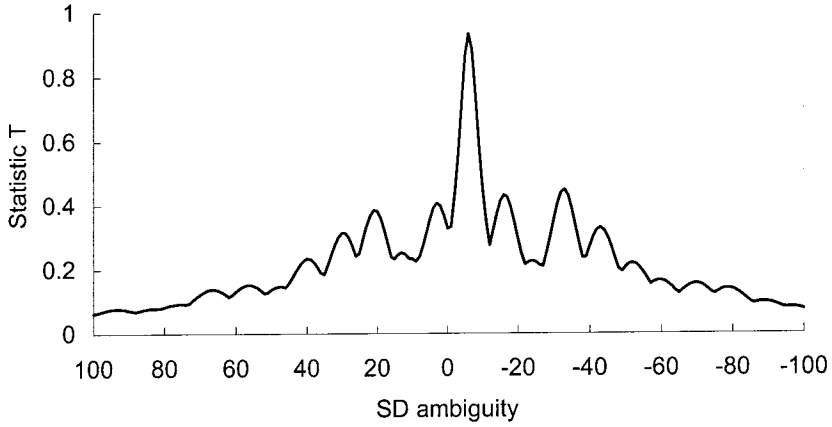

Figure 6.1 Statistic T versus SD ambiguity (zero baseline)

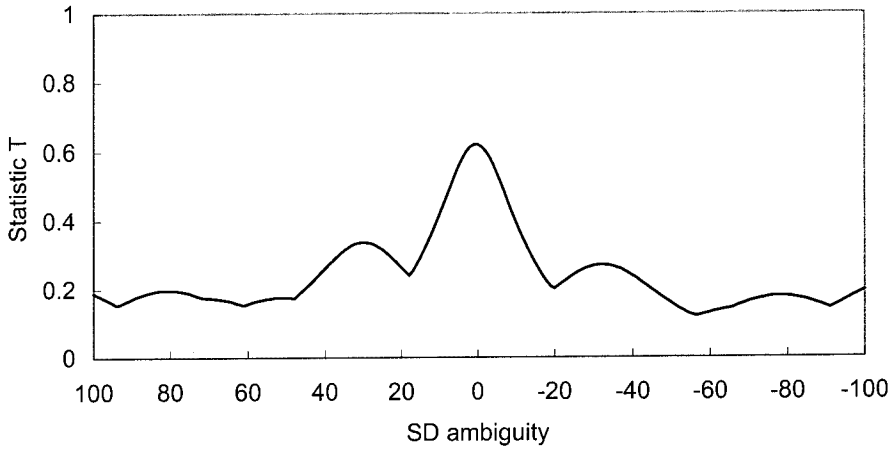

Figure 6.2 Statistic T versus SD ambiguity (1.2km baseline)

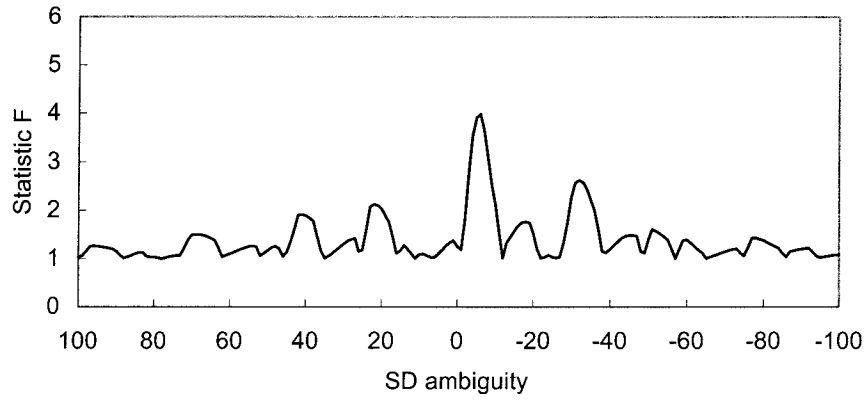

Figure 6.3 Statistic *F* versus SD ambiguity (zero baseline)

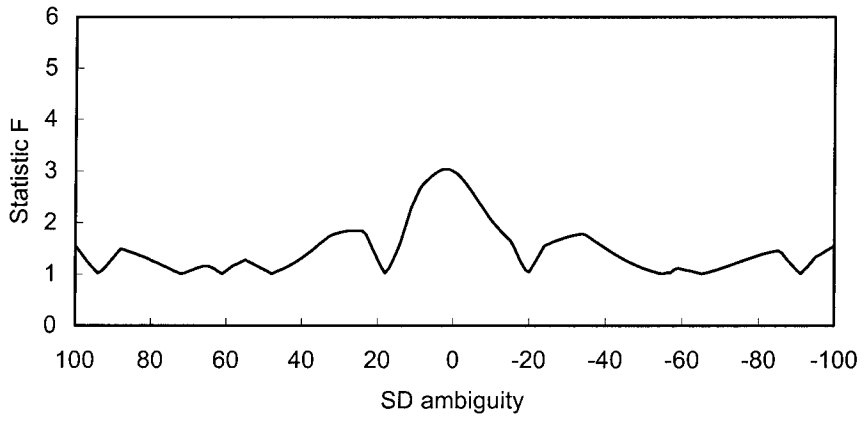

Figure 6.4 Statistic *F* versus SD ambiguity (1.2km baseline)

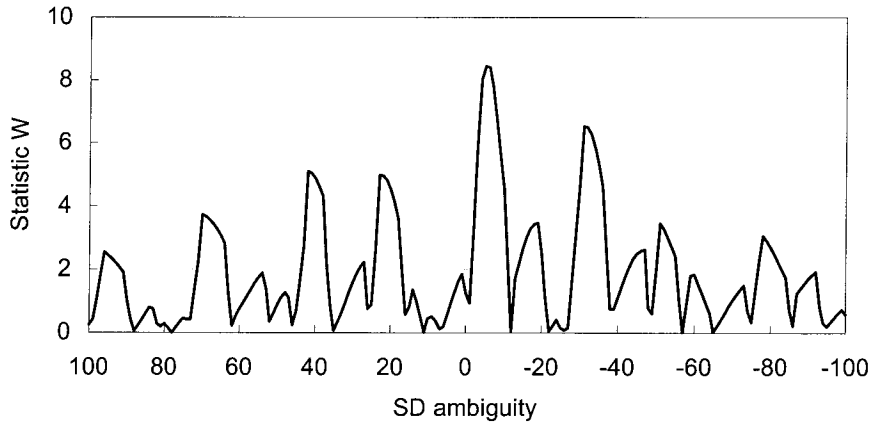

Figure 6.5 Statistic *W* versus SD ambiguity (zero baseline)

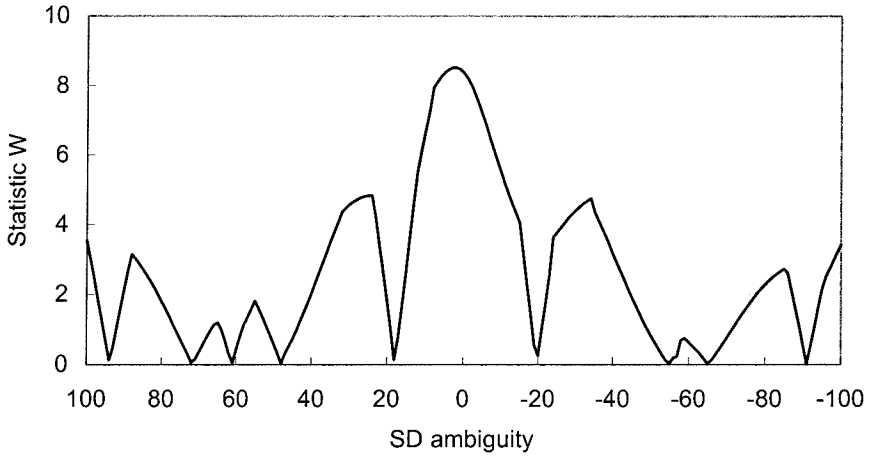

Figure 6.6 Statistic W versus SD ambiguity (1.2km baseline)

6.4.2 DD Ambiguity Discrimination Tests

The DD ambiguity discrimination test statistics F and W are shown in Figures 6.3-6.6, which present a similar trend as in Figures 6.1 and 6.2 for the statistic T. When the SD ambiguity approaches closely to its correct value, the closer the SD ambiguity to the most likely value, the bigger the values of the discrimination test statistics F and W. With the SD ambiguity fixed to its most likely value, the values of both statistics F and W for both data sets are larger than 2.0 (here the value 2.0 is used purely for comparative purposes). This indicates that the two best DD ambiguity combinations can be distinguished very well. With the statistic W, the confidence level of the DD ambiguity discrimination test in each data set is extremely close to 100 percent.

From Figures 6.1 and 6.2, it can be seen that a range of possible values for the SD ambiguity can pass the ambiguity acceptance test. This situation is somewhat similar to that of DD ambiguity resolution. However, the important thing here is that any accepted wrong (or approximate) SD ambiguity value can cause *systematic* model errors and may unfortunately result in wrong DD ambiguity resolution. This did happen in the case of zero baseline. For example, when the SD ambiguity was fixed to the wrong value -33, a wrong DD ambiguity combination was identified as the best one. This wrong ambiguity combination also passed both the acceptance and discrimination tests, in which $T = 0.45$, $F = 2.62$ and $W = 6.26$ (with a

confidence level close to 100 percent). For a reliable DD ambiguity resolution, therefore, it is critical to fix the SD ambiguity to the most likely value.

6.4.3 SD Ambiguity Validation Tests

With the DD ambiguities being fixed to the correct values, the most likely SD ambiguity can be evaluated using the statistics $\overline{T}$, $\overline{F}$ and $\overline{W}$. The validating results of the most likely SD ambiguities in the two data sets are listed in Table 6.2.

Baseline Names	SD ambiguities		Acceptance tests		Discrimination tests		
	M1	M2	$\overline{T}$	Confidence	$\overline{F}$	$\overline{W}$	Confidence ($\overline{W}$)
Zero baseline	-6	-7	0.999	~100%	1.057	1.181	94%
1.2km baseline	0	1	0.999	~100%	1.001	0.083	76%

Table 6.2 Results for SD ambiguity validation tests

The results in Table 6.2 indicate that the statistics of the SD ambiguity acceptance test are very high, with the confidence levels close to 100 percent. This means that the most likely SD ambiguity can fit the data very well. In contrast, however, the statistics for the discrimination test are small, indicating lower confidence levels. One possible reason for this is that the coefficients of the SD ambiguity parameter in Equation 6.26 are much smaller than those of other parameters. This results in a lower precision of the SD parameter. Intuitively, if the SD integer ambiguity cannot be validated, the SD ambiguity should be treated as a real value. For the final baseline solution, two different methods dealing with the SD ambiguity parameter will be further discussed in Section 6.4.5 using a real data set.

6.4.4 Baseline Errors Caused by Wrong SD Ambiguity Values

To evaluate the effects of wrong (or approximate) SD ambiguities on the final baseline solutions, the DD ambiguities were first fixed to their correct values (verified with the known baseline length). Then, with the SD ambiguity being fixed to possible values in the search space, the differences between the solved baseline lengths and the known value were produced for each data set, and are shown in Figures 6.7 and 6.8.

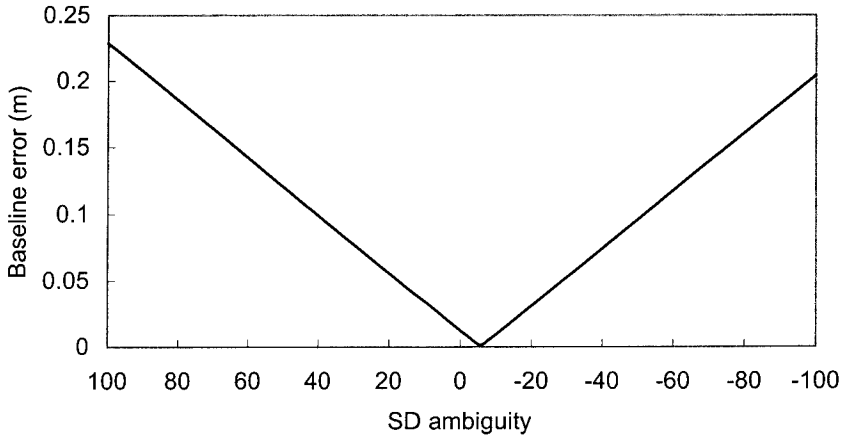

Figure 6.7 Baseline errors versus SD ambiguity (zero baseline)

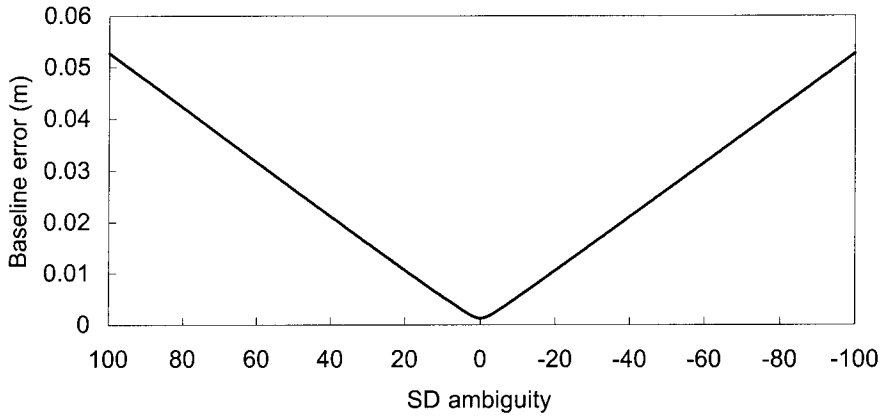

Figure 6.8 Baseline errors versus SD ambiguity (1.2km baseline)

Figures 6.7 and 6.8 demonstrate that, as expected, the best baseline solution is achieved when the SD ambiguity fixed to the most likely value. In the case of the 1.2km baseline (GPS+GLONASS data), as shown in Figure 6.8, an error of five cycles in the SD ambiguity leads to a baseline change of about 1.0mm (the standard deviation of the baseline length is 2.3mm). In some cases, however, small errors in the fixed SD ambiguity values may result in large baseline errors. For example, in the case of the zero baseline (GLONASS data only), as shown in Figure 6.7, an error of five cycles in the SD ambiguity value can bias the baseline length by as much as 10.0mm (the standard deviation of the baseline length is 0.8mm). This indicates

again that the approximate SD ambiguity value computed by pseudoranges may not be accurate enough for precise baseline solutions.

It is noted that the difference in the size of baseline errors between the zero baseline and 1.2km baseline is significant. This is mainly caused by the significant difference in the geometry of this two baseline solutions. While the zero baseline just has 5 GLONASS satellites, the 1.2km baseline has 5 GPS satellites and 4 GLONASS satellites.

6.4.5 Treatment of the SD Ambiguity in Final Baseline Solutions

As mentioned above, even when the DD ambiguities are fixed to their correct values, it is still difficult to validate the SD ambiguity value. There are two methods to deal with the SD ambiguity parameter in the final baseline solutions, namely *Method 1*: fixing the SD ambiguity to its most likely value or *Method 2*: treating the SD ambiguity as a real-valued parameter. To compare these two methods, the 0.3km baseline data set was processed in a batch mode with the segments being two, five and ten minutes, respectively. A total of eight solutions were obtained, and the results are listed in Table 6.3.

Batch Num.	Data Span (min)	Best SD Amb.	DD Ambiguity Resolution Statistics			Final solution: *Method 1*			Final solution: *Method 2*		
			T	*F*	*W*	Correc.* (mm)			Correc.* (mm)		
1	2	-12	0.87	12.9	16.1	5.1	4.2	4.1	5.2	4.2	4.1
2	2	-13	0.86	9.6	13.5	5.1	2.6	1.0	5.0	2.6	1.0
3	2	-14	0.61	8.8	12.8	9.1	7.6	0.1	9.0	7.6	0.1
4	2	-14	0.63	11.5	15.1	6.8	2.3	3.6	6.7	2.4	3.6
5	2	-13	0.43	4.6	8.3	7.1	5.8	2.1	7.1	5.8	2.1
6	5	-12	0.86	10.9	23.4	6.2	4.7	1.5	6.2	4.7	1.5
7	5	-14	0.65	20.9	33.6	7.1	4.3	2.7	7.0	4.4	2.7
8	10	-13	0.81	23.9	51.9	6.5	4.4	2.1	6.5	4.4	2.1

Table 6.3 The results for 0.3km baseline data set
(* estimated corrections to the approximate baseline components.)

It is noted from Table 6.3 that *Methods 1* and *2* produce almost identical baseline components. It is also noted that the standard deviations of the baseline components for *Methods 1* and *2* are also very close (almost identical). One possible reason for this is, as mentioned above, that the coefficients of the SD ambiguity parameter in

Equation 6.26 are much smaller than those of other parameters. This leads to a geometry which is not sensitive to small changes in the SD ambiguity parameter. However, in order to check the SD ambiguity search process, it will be wise to treat the SD ambiguity as a real-valued parameter in the final baseline solution. The integer nearest to this estimated SD ambiguity parameter should be the same as the most likely SD ambiguity value produced by the SD ambiguity research process.

6.5 Summary

Although converting the GLONASS carrier phases to distances before forming the DD measurements can remove the receiver clock terms from the DD measurement equations, both SD and DD ambiguity parameters simultaneously appear in the DD measurement equations. However, this results in a singularity in the normal matrix. In theory, without adding in other information, it is impossible to resolve the SD and DD ambiguities at the same time. This kind of information may be obtained from pseudoranges, which can be used to calculate an approximate SD ambiguity value. With the SD ambiguity being fixed to this approximate value, the DD ambiguity resolution can be performed. However, the SD ambiguity value determined by the pseudoranges may be not accurate enough for reliable DD ambiguity resolution, as pseudoranges may be significantly contaminated by multipath and hardware delays.

In this chapter, the SD ambiguity value is determined using other information, which is mainly based on the two basic facts, namely a) that the possible range or space of the SD ambiguity is sufficiently known, and b) that the closer the SD ambiguity parameter to its correct value, the better the performance of the DD ambiguity resolution, or the smaller the statistic T. By searching through all the possible integer SD ambiguity values, the best (most likely) SD ambiguity value can be identified, which is associated with the maximum value of the statistic T.

When the SD ambiguity value is fixed to its most likely value, the correct DD ambiguities can be more easily recovered. Therefore, the proposed GLONASS ambiguity resolution approach is actually based on a two-level search process, in which all the SD and DD ambiguity combinations are compared using the statistic T. A mathematical relationship between any two DD ambiguity-float solutions based on different SD ambiguity values has been established, which makes the two-level

search process more efficient. The initial experimental results indicate that the proposed approach is feasible for resolving the carrier phase ambiguities in the cases of GLONASS and combined GPS/GLONASS positioning.

Chapter 7

CONCLUSIONS AND RECOMMENDATIONS

7.1 Conclusions

In the case of GPS and GLONASS two fundamental measurements can be decoded from the satellite signals, namely the pseudoranges and the carrier phases. Carrier phase measurements are much more precise than pseudoranges, thus they are the primary measurements for precise positioning. However, the problem is that the carrier phase measurements are "ambiguous", with the "ambiguity" (the integer number of signal wavelengths between satellite and antenna) being an unknown value *a priori*. Hence, the determination of the integer ambiguities, i.e., "ambiguity resolution" (AR), is the most critical data analysis step for either the GPS or the GLONASS satellite positioning operation (Section 1.6).

Ambiguity resolution can be efficiently performed using the integer least squares theory and algorithms initially developed by Teunissen (1993) and refined by others since. However, reliability of ambiguity resolution (hence precise positioning) is very sensitive to the correct definition of both the mathematical and stochastic models for the measurements, and to the application of robust quality control procedures (Section 1.6). Substantial investigations into the most challenging mathematical and stochastic modelling issues and the quality control procedure used in ambiguity resolution have been conducted in this study.

7.1.1 Mathematical Modelling for Integrated GPS and GLONASS Positioning

The mathematical models for precise satellite positioning can be constructed using both single-differenced (SD) and double-differenced (DD) measurements. In the case of SD carrier phase measurements, the SD ambiguities have to be reparametrised as DD ambiguities because the SD ambiguities are too difficult to fix to their expected integer values. In an integrated GPS/GLONASS positioning system, the mathematical models including the receiver clock terms must rely on the use of the SD pseudorange measurements. The number of valid mathematical models has been determined as 18 (Section 2.3). It has been shown that the

performance of these models in ambiguity resolution is different. For the specific data sets, the correct rate of the best ambiguity sets varies from 78.9 percent to 97.5 percent (Section 2.4).

Because control of the receiver clock errors is the key to reliable ambiguity resolution, a specific criterion for model selection, namely the model sensitivity with respect to the receiver clock parameter, has been introduced to identify an optimal mathematical model (Section 2.5). Based on experimental analysis of the model sensitivity for the specific data sets, the optimal model (with the lowest model sensitivity and highest success rate of the best ambiguity sets) has been identified. This model uses the GPS-GPS and GLONASS-GLONASS DD carrier phase measurements, together with the SD GLONASS and DD GPS pesudorange measurements (Section 2.5).

7.1.2 Stochastic Modelling for Static GPS Positioning

It has been demonstrated that the existing stochastic modelling procedures are based on some unrealistic assumptions, thus leading to unreliable stochastic models (Section 3.4.1).

A rigorous stochastic modelling procedure has been developed to estimate the covariance matrix for the measurements (Sections 3.2 and 3.3). This procedure is based on modern statistical theory, i.e., the so-called MINQUE method, ensuring that the estimated stochastic parameters (elements of the covariance matrix) have well defined statistical properties.

With the proposed stochastic modelling procedure, three error models, namely Model A (homoscedastic and uncorrelated error model), Model B (heteroscedastic and uncorrelated error model) and Model C (heteroscedastic and correlated error model), have been tested and analysed using a real data set. Model C is identified as the optimal model because it can more efficiently represent the error features of the measurements (Section 3.4). It has been shown that the proposed stochastic modelling procedure can reduce the volume of the ambiguity search space and improve the reliability of the ambiguity resolution.

7.1.3 Real-time Stochastic Modelling for RTK Positioning

Since the true values of the measurement errors are unknown, stochastic modelling has to be based on the residuals of the measurements which are generated in the process of parameter estimation. A problem here is that the parameter estimation process itself relies on the estimated covariance matrix. To tackle this problem, a feasible method is to perform an *iterative* computation procedure. Although such an iterative procedure has been successfully applied in static positioning, the iterative method is computationally intensive and thus may not be feasible for RTK positioning. Instead, an *adaptive* procedure has been developed.

The basic idea of the adaptive procedure is that the residuals collected from the previous segment (window) of positioning results are used to estimate the covariance matrix of the SD or DD measurements for the current epoch (a preset default covariance matrix is needed to seed the adaptive estimation process). Within a segment (window), the covariance matrix for each epoch is assumed to be the same. Therefore, the formulation of an adaptive stochastic modelling procedure includes two critical steps, namely, a) to derive a suitable formula for use in estimating the covariance matrix, and b) to determine the optimal width of the moving window (or epochs).

Based on the concept of *covariance-matching*, a robust formula for use in calculating the elements of the covariance matrix has been derived (Section 4.3). The advantage of this formula is that it can always produce a positive definite covariance matrix. Initial numerical experiments show that an optimal width for the moving window varies from seven to 15 epochs, depending on the redundancy of the positioning solutions (Section 4.4).

This proposed adaptive stochastic modelling procedure can be easily implemented in a RTK positioning system, significantly reducing the volume of the ambiguity search space and improving the reliability of ambiguity resolution.

7.1.4 A Rigorous Ambiguity Discrimination Testing Procedure

Ambiguity discrimination testing can be generally considered as the comparison of two constrained linear models. These two compared linear models are non-nested,

however (Section 5.4). A statistical testing strategy has been employed to test whether or not the difference between the two compared models is significant. An important feature of this testing strategy is that the null hypothesis is systematic between the two compared models (Section 5.4).

Statistics for ambiguity discrimination testing have been derived using both the likelihood ratio method and the artificial nesting method. The resulting statistics are formulated by the difference (not the ratio as used in current procedures) between the minimum and second minimum quadratic form of the residuals in ambiguity identification, and its standard deviation. The distribution function of the test statistic has been theoretically identified as a standard normal distribution when the known *a priori* variance factor is used, or a Student's t distribution when the estimated variance factor is used (Section 5.4). With this procedure, the ambiguity discrimination test is based on a more rigorous test statistic whose critical value can be calculated with any chosen level of significance.

The rigorous ambiguity discrimination testing procedure has been extensively used in various static and kinematic GPS and GLONASS positioning applications (Chapters 2, 3, 4, 6). Test results indicate that this new testing procedure is reliable for use in ambiguity resolution.

7.1.5 An Approach to GLONASS Ambiguity Resolution

When processing GLONASS carrier phases, the standard double-differencing (DD) procedure cannot cancel receiver clock terms in the DD phase measurement equations due to the multiple frequencies of the carrier phases. Consequently, a receiver clock parameter has to be set up in the measurement equations in addition to baseline components and DD ambiguities. The resulting normal matrix unfortunately becomes singular (Section 2.3.2; Appendix A). It has been noted that converting the GLONASS carrier phases to distances before forming the DD measurements can cancel out the receiver clock terms in the DD measurement equations. However, this modelling method leads to the presence of both the SD and DD ambiguities in the models. A novel approach has been proposed to resolve the GLONASS ambiguities (Section 6.3).

The basic idea behind this new approach is to search for the most likely single-differenced (SD) ambiguity. When the SD ambiguity parameter is fixed to its most likely value, the DD ambiguity resolution will have the best performance which can be measured by the minimum quadratic forms of the least-squares residuals. An efficient procedure searching for the most likely SD ambiguity value has been developed using the mathematical relationship between any two DD ambiguity-float solutions associated with different SD ambiguity values (Section 6.3.2; Appendix E). The initial experimental results demonstrate that the proposed approach is feasible in the cases of GLONASS and combined GPS/GLONASS positioning (Section 6.4).

7.2 Recommendations

Based on both the theoretical and experimental results obtained in this study, the following recommendations are made for further research.

7.2.1 Some Issues in Mathematical Modelling

There are still some critical issues in optimal mathematical modelling for integrated GPS and GLONASS positioning. The identification of the optimal mathematical model is mainly based on the experimental analysis. Theorem 2.1 (Section 2.5.3; Appendix C) has indicated the correctness of the selection of the optimal model in the case of the single epoch solutions. Much theoretical work is needed to compare the model sensitivity in the case of more than one epoch. Further research in this direction should aim to find out whether or not the comparison between the model sensitivity is geometry-dependent. If it is geometry-dependent for different positioning operational modes, the optimal mathematical model would have to be selected using the model sensitivity criterion before positioning is conducted.

Furthermore, other criteria for model selection need to be considered and compared with the criterion used in this study. For example, such a criterion may be the accuracy of the estimated receiver clock terms.

7.2.2 Modelling Temporal Correlations

Temporal correlations between epochs, which have been assumed absent in this study, may exist because the residual systematic errors in the differenced measurements change slowly over time (El-Rabbany, 1994). Actually, in GPS and

GLONASS satellite positioning, the measurements have a heteroscedastic, space- and time-correlated error structure (Wang, 1998b). Any mis-specifications in stochastic models for the measurements will inevitably lead to unreliable statistics in ambiguity resolution and positioning results. Simultaneous estimation of the covariance matrix and the temporal correlations is theoretically possible, and is a topic for further research.

7.2.3 Measuring the Separability between two Ambiguity Combinations

A complete quality control process includes the statistical testing procedure and the specific measures needed to evaluate the performance of the testing procedures. This quality control process can be implemented in data processing and system design to assure the quality of the estimation (such as ambiguity resolution). Based on the ambiguity discrimination testing statistics developed in this study, the performance of the corresponding discrimination testing procedures could be evaluated.

The performance of a statistical testing procedure can be measured by its *power*, which is defined by the probability of correctly rejecting the null hypothesis when it is false. The power of the testing procedure is dependent on the confidence level used in the testing procedure, the noncentrality parameter of the statistic distribution and the model redundancy. Similar to the classic reliability theory developed by Baarda (1968), an inverse problem for the ambiguity discrimination testing can be considered. Given the value of the power, the minimal value of the noncentrality parameter can be derived, which could then be used to measure the separability between any two ambiguity combinations. The separability depends on several factors, such as the covariance matrix of the measurements and the geometry (satellite constellation). The concept of "separability" should be employed to rigorously evaluate and then improve the reliability of integrated RTK GPS-GLONASS positioning systems.

References

Abbidin, H.A. (1993) Computational and Geometrical Aspects of On-the-fly Ambiguity Resolution, *PhD thesis*, Department of Surveying Engineering, Technical Report No.164, University of New Brunswick, Fredericton, Canada, 314 pp.

Abidin, H.Z. and Subari, D.M. (1994) On the Discernibility of the Ambiguity Sets during On-the-fly Ambiguity Resolution, *Australian Journal of Geodesy Photogrammetry and Surveying*, No. 61 (December), pp. 17-40.

Ananga, N., Coleman, R. and Rizos, C. (1994) Variance-covariance Estimation of GPS Networks, *Bulletin Géodésique*, Vol. 68, pp. 77-87.

Ashkenazi, V., Moor, T., Hill, C.J., Ochieng, W.Y. and Chen, W. (1995) Design of a GNSS: Coverage, Accuracy and Integrity, *Proceedings of 8th International Technical Meeting of the Satellite Division of the Institute of Navigation, ION GPS-95*, September 12-15, Palm Springs, CA, pp. 463-472.

Ashjaee, J. and Lorenz, R. (1992) Precision GPS Surveying After Y-Code, *Proceedings of 5th International Technical Meeting of the Satellite Division of the Institute of Navigation, ION GPS-92*, Albuquerque, NM, September 16-18, pp. 657-659.

Atkinson, A.C. (1969) A Test for Discriminating between Models, *Biometrika*, Vol. 56, pp. 337-347.

Baarda, W. (1968) A Testing Procedure for Use in Geodesy Networks, *Netherlands Geodetic Commission Publications on Geodesy, New Series*, Vol. 2, No. 5, Delft, 97 pp.

Barnes, B.J., Ackroyd, N. and Cross, P.A. (1998) Stochastic Modelling for Very High Precision Real-time Kinematic GPS in an Engineering Environment, *Proceedings of FIG XXI International Conference*, July 21-25, Brighton, UK, Commission 6, pp. 61-76.

Bastos, L. and Landau, H. (1988) Fixing Cycle Slips in Dual-Frequency Kinematic GPS Application Using Kalman Filtering, *Manuscripta Geodaetica*, Vol. 13, pp. 249-256.

Bazlov, Y.A., Galazin, V. F., Kaplan, B.L., Maksimov, V.G.and Rogozin, V.P.(1999) GLONASS to GPS: A New Coordinate Transformation, *GPS World*, Vol. 10, No. 1, pp. 54-58.

Beser, J., Balendra, A., Erpelding, E. and Kim, S. (1995) Differential GLONASS, Differential GPS and Integrated Differential GLONASS/GPS - Initial Results, *Proceedings of 8th International Technical Meeting of the Satellite*

Division of the Institute of Navigation, ION GPS-95, Palm Springs, CA, September 12-15, pp. 507-515.

Betti, B., Crespi, M., Sanso, F. and Sguerso, D. (1994) Discriminant Analysis to Test Non-Nested Hypotheses, in: Sanso F (ed.), *Geodetic Theory Today. International Association of Geodesy Symposia,* Vol. 114, Springer Verlag, Berlin, Germany, pp. 259-271.

Beutler, G. (1996) GPS Satellite Orbits, in: Kleusberg, A. and Teunissen, P.J.G. (eds.), *GPS for Geodesy*, Springer Verlag, Berlin, Germany, pp 37-102.

Beyer, W.H. (1968) *Handbook of Tables for Probability and Statistics*, Second edition, The Chemical Rubber Co., OH, 642 pp.

Blewitt, G. (1989) Carrier Phase Ambiguity Resolution for the Global Positioning System Applied to Geodetic Baselines up to 2000km, *Journal of Geophysical Research*, Vol. 94, B8, pp. 10187-10203.

Blewitt, G. (1990) An Automatic Editing Algorithm for GPS Data, *Geophysical Research Letter*, Vol. 17, No. 3, pp. 199-202.

Blewitt, G. (1993) Advances in Global Positioning System Technology for Geodynamics Investigations: 1978-1992, in: Smith, D.E. and Turcotte, D.L. (eds.), *Contributions of Space Geodesy to Geodynamics: Technology.* Geodynamics Series, Vol. 25, AGU, Washington, D.C., pp. 195-213.

Blewitt, G., Lindqwister, U.J. and Hudnut K.W. (1989) Densification of Continuously Operating GPS Arrays Using a Rapid Static Surveying Techniques, *Eos, Transaction of American Geophysics Union*, Vol. 70, No. 43, p. 1054.

Bloomfield, P. and Watson, G.S. (1975) The Inefficiency of Least Squares, *Biometrika*, Vol. 62, pp. 121-128.

Bock, Y., Abbot, R.I., Counselman, C.C., Gourevitch, S.A., and King, R.W. (1986), Interferometric Analysis of GPS Phase Observations, *Manuscripta Geodaetica*, Vol. 11, pp. 282-288.

Bock, Y. (1991) Continuous Monitoring of Crustal Deformation, *GPS World*, Vol. 2, No. 6, pp. 40-47.

Bossler, J.D., Goad, C.C. and Bender, P.L. (1980) Using the Global Positioning System (GPS) for Geodetic Positioning, *Bulletin Géodésique*, Vol. 54, pp. 553-563.

Braasch, M. and van Graas, F. (1992) Mitigation of Multipath in DGPS Ground Reference Stations, *Proceedings of the ION National Technical Meeting*, San Diego, CA, January 12-16, pp. 105-114.

Braff, R. (1997) Description of the FAA's Local Area Augmentation System (LAAS), *Navigation*, Vol. 44, No. 4, pp. 411-423.

Brodin, G. (1996) GNSS Code and Carrier Tracking in the Presence of Multipath, *Proceedings of 9th International Technical Meeting of the Satellite Division of the Institute of Navigation, ION GPS-96*, Kansas City, MO, Sept. 17-19, pp. 1389-1398.

Brown, A. (1989) Extended Differential GPS, *Navigation*, Vol. 36, No. 3, pp. 265-285.

Brown, R.G. (1996) Receiver Autonomous Integrity Monitoring, in: Parkinson, B.W. and Spilker, J.J. (eds.) *Global Positioning System: Theory and Applications* (Vol. II), American Institute of Astronautics, Washington, D.C., pp. 143-165.

Bulletin E-09-98 (1998) Data on Difference between UTC(SU), GLONASS Time, GPS Time and UTC, State Time and Frequency Service of Russia National Time Reference, *http://www.rssi.ru/SFCSIC/bo9.txt.*

CAA-ISN (1998) Error Sources in Combined GPS/GLONASS Positioning, *http://eenisn1.leeds.ac.uk/library/positioning_systems/Errors.htm*

Cannon, M.E. and Lachapelle, G. (1995) Kinematic GPS Trends - Equipment, Methodologies and Applications, in: Beutler, Hein, Melbourne and Seeber (eds.), *GPS Trends in Precise Terrestrial, Airborne, and Spaceborne Applications, IAG Symposium No. 115*, Boulder, CO, July 3-4, 1995, pp. 161-169.

Caspary, W.F. (1988) Concepts of Network and Deformation Analysis, *Monograph 11*, School of Surveying, The University of New South Wales, Sydney, NSW, 183 pp.

Chen, D.S. (1994) Development of a Fast Ambiguity Search Filtering (FASF) Method for GPS Carrier Phase Ambiguity Resolution, *PhD Thesis*, Department of Geomatics Engineering, University of Calgary, Calgary, Canada, 98 pp.

Chen, Y.Q. (1997) An Approach to Validate the Resolved Ambiguities in GPS Rapid Positioning, *Proceedings of KIS'97*, Banff, Canada, June 2-7, pp. 301-309.

Chen, Y.Q., Chrzanowski, A. and Kavouras, M. (1990) Assessment of Observations Using Minimum Norm Quadratic Unbiased Estimation (MINQUE), *CISM Journal of ACSGS*, Ottawa, Canada, Vol. 44, pp. 39-46.

Chin, L. (1979) Advances in Adaptive Filtering, in: Leondes C. T. (ed.), *Advances in Control Systems Theory and Applications*, Academic Press, No.15, pp. 277-356.

Cohen, C.E. (1996) Attitude Determination, in: Parkinson, B.W. and Spilker, J.J. (eds.), *Global Positioning System: Theory and Applications* (Vol. II), American Institute of Astronautics, Washington, D.C., pp. 519-538.

Corbett, S.J. and Cross, P.A. (1995) GPS Single Epoch Ambiguity Resolution, *Survey Review*, Vol. 33, No. 257, pp. 149-160.

Cox, D.R. (1962) Further Results on Tests of Separate Families of Hypotheses, *Journal of the Royal Statistical Society*, Series B, Vol. 24, pp. 406-424.

Counselman, C.C. (1987) Method and System for Determining Position Using Signals from Satellites, *US Patent* 4667203.

Counselman, C.C. and Abbot, R. (1989) Method of Resolving Radio Phase Ambiguity in Satellite Orbit Determination, *Journal of Geophysical Research*, B6, Vol. 94, pp. 7058-7064.

Counselman, C.C. and Gourevitch, S.A. (1981) Miniature Interferometer Terminals for Earth Surveying: Ambiguity and Multipath with Global Positioning System, *IEEE Transactions on Geoscience and Remote Sensing*, Vol. 19, pp. 244-252.

Counselman, C.C., Hinteregger, H.F. and Shapiro, I.I. (1972) Astronomical Applications of Differential Interferometry, *Science*, Vol. 178, pp. 607-608.

Counselman, C.C. and Shapiro, I.I. (1979) Miniature Interferometric Terminals for Earth Surveying, *Bulletin Géodésique*, Vol. 53, pp. 139-163.

Cross, P.A. (1994) Advanced Least Squares Applies to Position Fixing, *Working Paper No. 6*, North East London Polytechnic, London, UK, 205 pp.

Cross, P.A. and Ahmad, N. (1988) Field Validation of GPS Phase Measurements, in: Groten, E. and Strauss, R. (eds.), *GPS Techniques Applied to Geodesy and Surveying*, Springer, Berlin, Germany, pp. 349-360.

Cross, P.A., Hawksbee, D.J. and Nicolai, R. (1994) Quality Measures for Differential GPS Positioning, *The Hydrographic Journal*, No. 72, pp. 17-22.

de Jonge, P.J. (1997) GPS Ambiguity Resolution for Navigation, Rapid Static Surveying and Regional Networks, *Proceedings of IAG Scientific Assembly*, Rio de Janeiro, Brazil, September 3-9, 1997, pp. 223-228.

Delikaraoglou, D., Dragert, H., Kouba, J., Lochhead, K. and Popelar, J. (1990) The Development of Canadian GPS Active Control System, Status of the Current Array, *Proceedings of the Second International Symposium on Precise Positioning with the Global Positioning System*, Ottawa, Canada, September 3-7, pp. 190-202.

Deloach, S.R. (1989) Continuous Deformation Monitoring with GPS, *Journal of Surveying Engineering*, Vol. 115, No. 1, pp. 93-110.

Diggelen, F. (1996) The Ashtech Family of Products, *Proceedings of 9th International Technical Meeting of the Satellite Division of the Institute of Navigation, ION GPS-96*, Kansas City, MO, Sept. 17-19, pp. 131-140.

Dodson, A., Shordlow, P., Hubbard, L., Elgered, G. and Jarlemark, P. (1996) Wet Tropospheric Effects on Precise Relative GPS Height Determination, *Journal of Geodesy*, No. 70, pp. 188-202.

Durnev, V.I. and Silantiev, Y.N. (1996) GLONASS Integrity and Reliability Assessment from Operational Experience of 1995, *Proceedings of 9th International Technical Meeting of the Satellite Division of the Institute of Navigation, ION GPS-96*, Kansas City, MO, September 17-19, pp. 1493-1496.

El-Rabbany A. E. (1994) The Effect of Physical Correlations on the Ambiguity Resolution and Accuracy Estimation in GPS Differential Positioning, *Technical Report,* No. 190, Department of Geodesy and Geomatics Engineering, University of New Brunswick, Canada, 161pp.

Enge, P.K. and Van Dierendonck, A.J. (1996) Wider Area Augmentation System, in: Parkinson, B.W. and Spilker, J.J. (eds.), *Global Positioning System: Theory and Applications* (Vol I), American Institute of Astronautics, Washington, D.C., pp. 117-142.

Euler H. and Goad C.C. (1991) On Optimal Filtering of GPS Dual-Frequency Observations Without Using Orbit Information, *Bulletin Géodésique,* Vol. 65, No. 2, pp. 130-143.

Euler, H.J., Sauermann, K. and Becker, M. (1990) Rapid Ambiguity Fixing in Small Scale Networks, *Proceedings of the Second International Symposium on Precise Positioning with the Global Positioning System*, Ottawa, Canada, September 3-7, pp. 508-523.

Euler, H.J. and Schaffrin, B. (1990) On a Measure of the Discernibility between Different Ambiguity Solutions in the Static-Kinematic GPS-Mode, *Proceedings of the International Symposium on Kinematic Systems in Geodesy, Surveying, and Remote Sensing*, Springer Verlag, Berlin, Germany, September 10-13, pp. 285-295.

Evans, A., Hermann, B., Law, C., Remondi, B., Briggs, T. and Nelson, T. (1995) An Evaluation of Precise Kinematic OTF GPS Positioning with Respect to a Moving Aircraft, *Proceedings of 8th International Technical Meeting of the Satellite Division of the Institute of Navigation, ION GPS-95*, Palm Springs, CA, September 12-15, pp. 1623-1628.

Fenton, P.C., Falkenberg, W.H., Ford, T.J., Ng, K.K. and Van Dierendonck, A.J. (1991) NovAtel's GPS Receiver- the High Performance OEM Sensor of the Future, *Proceedings of 4th International Technical Meeting of the Satellite Division of the Institute of Navigation, ION GPS-91*, Albuquerque, NM, September 11-13, pp. 49-58.

Forward, T. (1998) Integrated GPS and GLONASS Satellite Positioning, *MSc Thesis*, School of Spatial Sciences, Curtin University of Technology, Perth, WA, 160 pp.

Freedman, A.P. (1991) Measuring Earth Orientation with the Global Positioning System, *Bulletin Géodésique*, Vol. 65, pp. 53-65.

Frei, E. and Beutler, G. (1990) Rapid Static Positioning Based on the Fast Ambiguity Resolution Approach FARA: Theory and First Results, *Manuscripta Geodaetica*, Vol. 15, pp. 325-356.

Ganin, A. (1995) Differential GLONASS in Russia: The Ways of Development, *Proceedings of 8th International Technical Meeting of the Satellite Division of the Institute of Navigation, ION GPS-95*, Palm Springs, CA, September 12-15, pp. 1049-1052.

Gao, Y. (1993) Reliability Assurance for GPS Integrity Test, *Proceedings of 6th International Technical Meeting of the Satellite Division of the Institute of Navigation, ION GPS-93,* Salt Lake City, Ut, September 22-24, pp. 567-574.

Gao, Y., McLellan, J.F. and Schleppe, J.B. (1996) An Optimized Fast Ambiguity Search Method for Ambiguity Resolution On-the-fly, *Proceedings of IEEE PLANS*, Atlanta, Ga, pp. 246-253.

Georgiadou, Y. and Doucet, K. (1990) The Issue of Selective Availability, *GPS World*, Vol. 1, No. 5, pp. 53-56.

Georgiadou, Y. and Kleusburg, A. (1989) On Carrier Signal Multipath Effects in Relative GPS Positioning, *Manuscripta Geodaetica*, Vol. 14, pp. 143-148.

Gerdan, G.P. (1995) A Comparison of Four Methods of Weighting Double-Difference Pseudorange Measurements, *Trans Tasman Surveyor*, Canberra, ACT, Vol. 1, pp. 60-66.

Giannou, M. (1995) Quality Analysis of the GPS Observations for Rapid-static and On-the-fly Applications: Problems and Solutions, *Journal for Satellite-based Positioning, Navigation and Communication* (SPN), Wichmann Verlag, Karlsruhe, Germany, Vol. 20, No. 4, pp. 138-146.

Gianniou, M. and Groten, E. (1996) An Advanced Real-Time Algorithm for Code and Phase DGPS, paper presented at DSNS'96 Conference, St. Petersburg, Russia, May 20-24, p. 7.

Goad, C.C. (1985) Precise Relative Position Determination Using Global Positioning System Carrier Phase Measurements in a Non-Difference Mode, *Proceedings of First International Symposium on Precise Positioning with the Global Positioning System*, NOAA, Rockville, MD, April, 15-19, pp. 567-578.

Goad, C.C. (1987) Precise Positioning With the GPS, in: Turner, S. (ed.), *Applied Geodesy, Lecture Notes in Earth Sciences*, Springer Verlag, Berlin, Germany, Vol. 12, pp. 17-30.

Goad, C.C. (1990) Optimal Filtering of Pseudo-ranges and Phases from Single-frequency GPS Receivers, *Navigation*, Vol. 37, No. 3, pp. 249-262.

Goad, C.C. (1996) Short Distance GPS Models, in: Kleusberg, A. and Teunissen, P.J.G. (eds.), *GPS for Geodesy*, Springer Verlag, Berlin, Germany, pp. 239-262.

Goad, C.C. and Remondi, B.W. (1984) Initial Relative Positioning Results Using the Global Positioning System, *Bulletin Géodésique*, Vol. 58, pp. 193-210.

Gourevitch, S.A., Sila-Novitsky, S. and Diggelen, F. (1996) The GG24 Combined GPS+GLONASS Receiver, *Proceedings of 9th International Technical Meeting of the Satellite Division of the Institute of Navigation, ION GPS-96*, Kansas City, MO, September 17-19, pp. 141-145.

Grafarend, E., Kleusberg, A. and Schaffrin, B. (1980) An Introduction to the Variance-covariance Components Estimation of Helmert Type, *Zeitschrift für Vermessungswesen*, Konrad Wittwer GmbH, Stuttgart, Germany, Vol. 105, pp. 129-137.

Habrich, H. (1998) Experiences of the BKG in Processing GLONASS and Combined GLONASS and GPS Observations, http://www.ifa.de/kartogrphie/GF/glo-proc/glo-proc.htm

Hall, T., Burke, B., Pratt, M. and Misra, P. (1997) Comparison of GPS+GLONASS Positioning Performance, *Proceedings of 10th International Technical Meeting of the Satellite Division of the Institute of Navigation, ION GPS-97*, Kansas City, MO, pp. 1543-1549.

Han, S. (1997) Quality Control Issues Relating to Instantaneous Ambiguity Resolution for Real-time GPS Kinematic Positioning, *Journal of Geodesy*, Vol. 71, pp. 351-361.

Han, S. and Rizos, C. (1996a) Validation and Rejection Criteria for Integer Least Squares Estimation, *Survey Review*, Vol. 34, No. 260, pp. 375-382.

Han, S. and Rizos, C. (1996b) "Apples and Oranges": Comparing GPS Ambiguity Resolution Techniques, paper presented at Annual Research Seminar, School of Geomatic Engineering, The University of New South Wales, Sydney, NSW, November.

Han, S. and Rizos, C. (1997) An Instantaneous Ambiguity Resolution Technique for Medium-range GPS Kinematic Positioning, *Proceedings of 10th International Technical Meeting of the Satellite Division of The U.S. Institute of Navigation*, Kansas City, MO, September 16-19, pp. 1789-1800.

Hartinger, H. and Brunner, F.K. (1998) Attainable Accuracy of GPS Measurements in Engineering Surveying, *Proceedings of FIG XXI International Conference*, July 21-25, Brighton, UK, Commission 6, pp. 18-31.

Harvey, B.R. (1994) *Practical Least Squares and Statistics for Surveyors*, Monograph 13, Second Edition, School of Geomatic Engineering, The University of New South Wales, Sydney, NSW, 319 pp.

Hatch, R. (1986) Dynamic Differential GPS at the Centimetre Level, *Proceedings of Fourth International Geodetic Symposium on Satellite Positioning*, Austin, TX, 28 April-2 May, pp. 1287-1298.

Hatch, R. (1989) Ambiguity Resolution in The Fast Lane, *Proceedings of ION GPS-89*, Colorado Springs, CO, September 27-29, pp. 45-50.

Hatch, R. (1990) Instantaneous Ambiguity Resolution, *Proceedings of International Symposium on Kinematic Systems in Geodesy, Surveying, and Remote Sensing*, Springer Verlag, Berlin, Germany, September 10-13, pp. 299-308.

Hatch, R. and Euler, H.J. (1994) Comparison of Several AROF Kinematic Techniques, *Proceedings of 7th International Technical Meeting of the Satellite Division of the Institute of Navigation, ION GPS-94*, Salt Lake City, Ut, September 20-23, pp. 363-370.

Hatch, R.R., Keegan, R. and Stansell, T.A. (1992) Kinematic Receiver Technology from Magnavox, *Proceedings of 6th International Geodetic Symposium on Satellite Positioning*, Columbus, OH, March 17-20, pp. 174-183.

Hatch, R. and Larson, K. (1985) Magnet-4100 GPS Survey Program Processing Techniques and Test Results, *Proceedings of First International Symposium on Precise Positioning with the Global Positioning System*, NOAA, Rockville, MD, April 15-19, pp. 567-578.

Hein, G.W., Rossbach, U. and Eissfeller, B. (1997) Advances in GPS/GLONASS Combined Solutions, *Proceedings of 10th International Technical Meeting of the Satellite Division of the Institute of Navigation, ION GPS-97*, Kansas City, MO, September 16-19, pp. 1533-1541.

Hermann, B., Evans, A., Law, C. and Remondi, B. (1994) Kinematic On-the-fly GPS Positioning Relative a Moving Reference, *Proceedings of 7th International Technical Meeting of the Satellite Division of the Institute of Navigation, ION GPS-94*, Salt Lake City, Ut, September 20-23, pp. 1499-1507.

Hilla, S. (1986) Processing Cycle Slips in Nondifferenced Phase Data from the Macrometer V-1000 Receiver, *Proceedings of Fourth International Geodetic Symposium on Satellite Positioning*, Austin, TX, 28 April — 2 May, pp. 647-661.

Hoel, P.G. (1947) On the Choice of Forecasting Formulas, *Journal of the American Statistical Association*, Vol. 42, pp. 605-611.

Hofmann-Wellenhof, B., Lichtenegger, H. and Collins, J. (1997) *GPS Theory and Practice* (4th Revised Edition), Springer-Verlag, New York, NY, 389 pp.

Hopfield, H.S. (1969) Two-quadratic Tropospheric Refractivity Profile for Correcting Satellite Data, *Journal of Geophysical Research*, Vol. 74, pp. 4487-4499.

Hurn, J. (1989) *GPS: A Guide to the Next Utility*, Trimble Navigation Ltd., 76 pp.

Hurn, J. (1993) *Differential GPS Explained*, Trimble Navigation Ltd., 55 pp.

Hwang, P.Y.C. (1990) Kinematic GPS: Resolving Integer Ambiguities On-the fly, *Proceedings of IEEE Position Location and Navigation Symposium*, Las Vegas, NV, March 20-23, pp. 579-586.

Hwang, P.Y.C. and Brown, R.G. (1990) GPS Navigation: Combining Pseudo-range with Continuous Carrier Phase Using a Kalman Filter, *Navigation*, Vol. 37, No. 2, pp. 181-196.

ICAO, (1995) GLONASS - INTERFACE CONTROL DOCUMENT, *RTCA Paper No. 639-95/SC159-685*, Navtech Seminars and GPS Supply, Alexandria, VA, 43 pp.

Jin, X. (1996) Theory of Carrier Adjusted DGPS Positioning Approach and Some Experimental Results, *PhD Thesis*, Delft University Press, The Netherlands, 165 pp.

JPS (1998) A GPS Tutorial: Basics of High Precision Global Positioning Systems, Javad Positioning Systems, Inc., http://www.javad.com

Kaplan, E.D. (ed.) (1996) *Understanding GPS: Principles and Applications*, Artech House, Norwood, MS, 554 pp.

Kee, C., Parkinson, B.W. and Axelrad, P. (1991) Wide Area Differential GPS, *Navigation*, Vol. 38, No. 2, pp. 123-143.

Kleusberg, A. (1990) Comparing GPS and GLONASS, *GPS World*, Vol. 1, No. 6, pp. 52-54.

Klobuchar J.A. (1987) Ionospheric Time-Delay Algorithm for Single-Frequency GPS Users, *IEEE Transactions on Aerospace and Electronic Systems*, AES-23, pp. 325-331.

Koch, K.R. (1988) *Parameter Estimation and Hypothesis Testing in Linear Models*, Springer Verlag, Berlin, Germany, 378 pp.

Kozlov, D. and Tkachenko, M. (1997) Instant RTK with Low Cost GPS+GLONASS™ C/A Receivers, *Proceedings of 10th International Technical Meeting of the Satellite Division of the Institute of Navigation, ION GPS-97*, Kansas City, MO, September 16-19, pp. 1559-1570.

Krakiwsky, E.J. (1975) *A Synthesis of Recent Advances in the Method of Least Squares*, Department of Surveying Engineering Lecture Notes No. 42, University of Brunswick, Fredericton, Canada, 125 pp.

Kuang, S.L. (1993) Evaluating the Accuracy of GPS Baseline Measurements Using Minimum Norm Quadratic Unbiased Estimation, *Surveying and Land Information Systems*, Vol. 53, No. 2, pp. 103-110.

Lachapelle, G. (1990) GPS Obervables and Error Sources for Kinematic Positioning, *Proceedings of the International Symposium on Kinematic Systems in Geodesy, Surveying, and Remote Sensing*, Springer Verlag, Berlin, Germany, September 10-13, pp 17-26.

Lachapelle, G., Cannon, M.E. and Lu, G. (1992) High Precision GPS Navigation with Emphasis on Carrier Phase Ambiguity Resolution, *Marine Geodesy*, Vol. 15, pp. 253-269.

Lachapelle, G., Sun, H., Cannon, M.E., and Lu, G. (1994) Precise Aircraft-to-Aircraft Positioning Using a Multiple Receiver Configuration, *Proceedings of National Technical Meeting*, The Institute of Navigation, Alexandria, VA, pp. 793-799.

Lamons, W. (1990) A Program Status Report on the Navstar Global Positioning System (GPS), *Proceedings of Second International Symposium on Precise Positioning with the Global Positioning System*, Ottawa, Ontario, September, pp. 3-8.

Landau, H. (1998) Use of GLONASS Data, *TerraSat Report*, Hoehenkirchen, Germany, 32 pp.

Landau, H. and Euler, H.J. (1992) On-the-fly Ambiguity Resolution for Precision Differential Positioning, *Proceedings of 5th International Technical Meeting of the Division of the Institute of Navigation, ION GPS-92*, Albuquerque, NM, September 22-24, pp. 607-613.

Landau, H. and Vollath, U. (1996) Carrier phase Ambiguity Resolution Using GPS and GLONASS signals, *Proceedings of 9th International Technical Meeting of the Division of the Institute of Navigation, ION GPS-96*, Kansas City, MO, September 17-19, pp. 917-923.

Langley, R.B. (1996) GPS Receivers and the Observables, in: Kleusberg, A. and Teunissen, P.J.G. (eds.), *GPS for Geodesy*, Springer Verlag, Berlin, Germany, pp. 141-173.

Langley, R.B. (1997) GLONASS: Rewiew and Update, *GPS World*, Vol. 8, No. 7, pp. 46-51.

Langley, R.B. (1998) RTK GPS, *GPS World*, Vol. 9, No. 9, pp. 70-76.

Leick, A. (1995) *GPS Satellite Surveying* (2nd Edition), John Wiley and Sons, New York, NY, 560 pp.

Leick, A. (1998) GLONASS Satellite Surveying, *Journal of Surveying Engineering*, Vol. 121, pp. 91-99.

Leick, A., Li, J., Beser, J. and Mader G. (1995) Processing GLONASS Carrier Phase Observations: Theory and First Experience, *Proceedings of 8th International Technical Meeting of the Satellite Division of the Institute of Navigation, ION GPS-95*, Palm Springs, CA, September 12-15, pp. 1041-1047.

Lichtenegger, H. and Hofmann-Wellenhof, B. (1989) GPS Data Preprocessing for Cycle Slip Detection, in: Bock, Y. and Leppard, N. (eds.), *Global Positioning System: An Overview*, Springer, New York, NY, pp. 57-68.

Lindlohr, W. and Wells, D. (1985) GPS Design Using Undifferenced Carrier Beat Phase Observations, *Manuscripta Geodaetica*, Vol. 10, pp. 255-295.

Loomis, P. (1989) A Kinematic GPS Double-Differencing Algorithm, *Proceedings of Fifth International Geodetic Symposium on Satellite Positioning*, Las Cruces, NM, March, 13-17, pp. 611-620.

Lu, G. and Lachaplle, G. (1992) Statistical Quality Control for Kinematic GPS Positioning, *Manuscripta Geodaetica*, Vol. 17, pp. 270-281.

MacDoran, P.F. (1979) Satellite Emission Radio Interferometric Earth Surveying Series — GPS Geodetic System, *Bulletin Géodésique,* Vol. 58, pp. 193-210.

Mader, G.L. (1992) Rapid Static and Kinematic Global Positioning System Solutions Using the Ambiguity Function Technique, *Journal of Geophysical Research*, Vol. 97, B3, pp. 3271-3283.

Martin, W. and Ladd, W. (1997) GPS + GLONASS Surveying - Post-Processed and Real-time Results, *Proceedings of 10th International Technical Meeting of the Satellite Division of the Institute of Navigation, ION GPS-97*, Kansas City, MO, September 16-19, pp. 851-856.

Mehra, R.K. (1972) Approaches to Adaptive Filtering, *IEEE Transactions on Automatic Control*, AC-17, October, pp. 693-698.

Miller, K.M. Abbott, V.J. and Capelin, K.(1997) The Reliability of Quality Measures in Differential GPS, *The Hydrographic Journal*, No. 86, pp. 27-31.

Misra, P., Abbot, R.I. and Gaposchkin, E.M. (1996) Integrated use of GPS and GLONASS: Transformation Between WGS 84 AND PZ-90, *Proceedings of 9th International Technical Meeting of the Satellite Division of the Institute of Navigation, ION GPS-96*, Kansas City, MO, September 17-19, pp. 307-314.

Misra, P., Pratt, M. and Burke, B. (1998) Augmentation of GPS/LAAS with GLONASS: Performance Assessment, *Proceedings of 11th International*

Technical Meeting of the Satellite Division of the Institute of Navigation, ION GPS-98, Nashville, TN, September 15-18, pp. 495-501.

Misra, P., Pratt, M., Muchnik, R., Burke, B. and Hall, T. (1996b) GLONASS Performance: Measurement Data Quality and System Upkeep, *Proceedings of 9th International Technical Meeting of the Satellite Division of the Institute of Navigation, ION GPS-96,* Kansas City, MO, September 17-19, pp. 261-269.

Misra, P. and Slater, J.A. (1998) A Report on the Third Meeting of the GLONASS-GPS Interoperability Working Group, *Proceedings of 11th International Technical Meeting of the Satellite Division of the Institute of Navigation, ION GPS-98,* Nashville, TN, September 15-18, pp. 1637-1643.

Neumann, J.B., Van Dierendonck, K.J., Manz A. and Ford T.J. (1997) Real-time Carrier Phase Positioning Using the RTCM Standard Message Types 20/21 and 18/19, *Proceedings of 10th International Technical Meeting of the Satellite Division of the Institute of Navigation, ION GPS-97*, Kansas City, MO, September 16-19, pp. 857-866.

NIMA, (1997) *Department of Defence World Geodetic System 1984: Its Definition and Relationships with Local Geodetic Systems*, NIMA TR8350.2, Third Edition, National Imagery and Mapping Agency, St. Louis, MO, 170 pp.

Paquet, P. and Louis, L. (1988) Recovering Earth Rotation Parameters with GPS, in: Groten, E. and Strauss, R. (eds.), *GPS Techniques Applied to Geodesy and Surveying*, Springer, Berlin, Germany, pp. 442-449.

Parkinson, B.W. (1979) Global Positioning System (NAVSTAR), *Bulletin Géodésique,* Vol. 53, pp. 89-108.

Parkinson, B.W. (1996) GPS Error Analysis, in: Parkinson, B.W. and Spilker, J.J. (eds.), *Global Positioning System: Theory and Applications* (Vol. I), American Institute of Astronautics, Washington, D.C., pp. 469-484.

Pearson, E.S. and Hartley, H.O. (1972) *Biometrika Tables for Statisticians* (Volume II), Cambridge University Press, Cambridge, UK, pp. 53-66.

Pelzer, H. (1985) Statische, Kinematische und Dynamische Punktfelder, in: Pelzer (ed.), Geodätische Netze in Landes- und Ingenieurvermessung II, Stuttgart, Wittwer, 566 pp.

Povaliaev, A. (1997) Using Single Differences for Relative Positioning in GLONASS, *Proceedings of 10th International Technical Meeting of the Satellite Division of the Institute of Navigation, ION GPS-97*, Kansas City, MO, September 16-19, pp. 929-934.

Pratt, M., Burke, B. and Misra, P. (1997) Single Epoch Integer Ambiguity Resolution with GPS-GLONASS L1 Data, *Proceedings of 53th Annual Meeting of the Institute of Navigation,* Albuquerque, NM, June 30-July 2, pp. 691-699.

Preston, R.A., Ergas, R., Hinteregger, H.F., Knight, C.A., Robertson, D.S., Shapiro, I.I., Whitney, A.R., Rogers, A.E.E. and Clark, T.A. (1972) Interferometric Observations of an Artificial Satellite, *Science*, Vol. 178, pp. 407-409.

Qin, X., Gourevitch, S. and Kuhl, M. (1992) Very Precise Differential GPS: Development Status and Results, *Proceedings of ION GPS-92*, Albuquerque, NM, pp. 615-624.

Qiu, W., Lachapelle, G. and Cannon, M.E. (1995) Ionospheric Effect Modelling for Single Frequency GPS Users, *Manuscripta Geodaetica*, Vol. 20, pp. 96-109.

Raby, P. and Daly, P. (1993a) Using the GLONASS System for Geodetic Survey, *Proceedings of 6th International Technical Meeting of the Satellite Division of the Institute of Navigation, ION GPS-93,* Salt Lake City, Ut, September 22-24, pp. 1129-1138.

Raby, P. and Daly, P. (1993b) Integrated GPS/GLONASS Navigation: Algorithm and Results, *Proceedings of 6th International Technical Meeting of the Satellite Division of the Institute of Navigation, ION GPS-93,* Salt Lake City, Ut, September 22-24, pp. 161-170.

Raby, P. and Daly, P. (1994) Surveying with GLONASS: Calibration, Error Sources and Results, *Proceedings of 3rd International Symposium on Differential Satellite Navigation Systems,* Canary Wharf, London, UK, April 18-22.

Rao, C.R. (1970) Estimation of Heterogeneous Variances in Linear Models, *Journal of American Statistical Association*, Vol. 65, pp. 161-172.

Rao, C.R. (1971) Estimation of Variance and Covariance Components — MINQUE, *Journal of Multivariate Analysis*, Vol. 1, pp. 257-275.

Rao, C.R. (1979) MINQUE Theory and Its Relation to ML and MML Estimation of Variance Components, *Sankhya*, Vol. 41, Series B, pp. 138-153.

Rao, C.R. and Kleffe, J. (1988) *Estimation of Variance Components and Applications,* North Holland Press, New York, NY, 370 pp.

Rapoport, L. (1997) General Purpose Kinematic/Static GPS/GLONASS Postprocessing Engine, *Proceedings of 10th International Technical Meeting of the Satellite Division of the Institute of Navigation, ION GPS-97*, Kansas City, MO, September 16-19, pp. 1757-1772.

Remondi, B.W. (1984) Using the Global Positioning System (GPS) Phase Observable for Relative Geodesy: Modeling, Processing, and Results, *PhD Thesis*, University of Texas at Austin, Centre for Space Research, 360 pp.

Remondi, B.W. (1985a) Global Positioning System Carrier Phase Observable: Description and Use, *Bulletin Géodésique,* Vol. 59, pp. 361-377.

Remondi, B.W. (1985b) Performing Centimetre Accuracy Relative Surveys in Seconds Using Carrier Phase, *Proceedings of First International Symposium on Precise Positioning with the Global Positioning System*, Rockville, MD, April 15-19, pp. 789-797.

Remondi, B.W. (1991) Pseudo-Kinematic GPS Results Using the Ambiguity Function Method, *Navigation,* Journal of The Institute of Navigation, Vol. 38, pp. 17-36.

Riley, S., Walsh, D. and Daly, P. (1995) Navigation Results from 20 Channel GPS/GLONASS Receivers, paper presented at 4th International Conference On Differential Satellite Navigation Systems, DSNS-95, April 24-28, Bergen, Norway.

Rizos, C. (1996) Principles and Practice of GPS Surveying, *Monograph* 17, School of Surveying, The University of New South Wales, Sydney, NSW, 560 pp.

Rizos, C., Han, S. and Hirsch, B. (1997) A High Precision Real-time GPS Surveying System Based on the Implementation of a Single-Epoch Ambiguity Resolution Algorithm, *Proceedings of 38th Australian Surveyors Congress*, Newcastle, NSW, April 12-18, pp. 20.1-20.10.

Roberts, W., Rayson, M. and Cross, P. (1997) Verification of the UKOOA Differential GPS Guidelines, *The Hydrographic Journal*, No. 85, pp. 17-21.

Rogers, A.E.E., Knight, C.A., Hinteregger, H.F. and Whitney A.R. (1978) Geodesy by Radio Interferometry: Determination of a 1.24km Base Line Vector with ~5mm Repeatability, *Journal of Geophysical Research*, Vol. 83, No. B1, pp. 325-334.

Romay-Merino, M., Nieto-Recio, J., Cosmen-Shortmann, J. and Martin-Piedelobo, J. (1998) Real Time Ephemeris and Clock Corrections for GPS and GLONASS Satellites, *Proceedings of the IGS Analysis Center Workshop*, February, 9-11, Darmstadt, Germany, pp. 111-125.

Rossbach, U., Habrich, H. and N. Zarraoa, (1996) Transformation Parameters Between PZ-90 and WGS 84, *Proceedings of 9th International Technical Meeting of the Satellite Division of the Institute of Navigation, ION GPS-96*, Kansas City, MO, September 17-19, pp. 279-285.

Rossbach, U. and Hein, G.W. (1996) Treatment of Integer Ambiguities in DGPS/DGLONASS Double Difference Carrier Phase Solutions, *Proceedings of 9th International Technical Meeting of the Satellite Division of the Institute of Navigation, ION GPS-96*, Kansas City, MO, September 17-19, pp. 909-916.

Rothacher, M. (1998) First Precise GLONASS Orbits from CODE, *IGEX Electronic Mail* (No.52), http://lareg.ensg.ign.fr/IGEX/IGEXMAIL/igexmail.mess.0052

Rothacher, M., Beulter, G., Gurtner, W., Schneider, D., Wiget, A., Geiger, A. and Kahle, H.G. (1990) The Role of the Atmosphere in Small GPS Networks, *Proceedings of Second International Symposium on Precise Positioning With the Global Positioning System*, Ottawa, Canada, September 3-7, pp. 581-598.

Saastamoinen, J. (1973) Contributions to the Theory of Atmospheric Refraction, *Bulletin Geodesique*, No. 107, pp. 13-34.

Sahin, M., Cross P.A. and Sellers P.C. (1992) Variance Component Estimation Applied to Satellite Laser Ranging, *Bulletin Geodesique*, Vol. 66, pp. 284-295.

Salzmann, M.A. (1993) Least Squares Filtering and Testing for Geodetic Navigation Applications, *Netherlands Geodetic Commission Publications on Geodesy*, New Series, Vol. 37, Delft, The Netherlands, 209 pp.

Sang, J. and Kubik, K. (1997) A Probabilistic Approach to Derivation of Geometrical Criteria for Evaluating GPS RAIM Detection Availability, *Proceedings of the Institute of Navigation National Technical Meeting*, January 14-16, Santa Monica, CA, pp. 511-517.

Sangsuk-Iam, S. and Bullock, T.E. (1990) Analysis of Discrete-time Kalman Filtering under Incorrect Noise Covariances, *IEEE Transactions on Automatic Control*, Vol. 35, No. 12, pp. 1304-1309.

Schaffrin, B. (1983) Varianz-Kovarianz-Komponenten-Schatzung bei der Ausgleichung heterogener wiederholungsmessungen, *Deutsche Geodätische Kommission*, Reihe C, Munich, Germany, Heft 282.

Schaffrin, B. and Grafarend, E. (1986) Generating Classes of Equivalent Linear Models by Nuisance Parameter Elimination, *Manuscripta Geodaetica*, Vol. 11, pp. 262-271.

Schupler, B.R. and Clark, T.A. (1991) How Different Antennas Affect the GPS Observable, *GPS World*, Vol. 2, No. 10, pp. 32-36.

Seeber, G. (1993) *Satellite Geodesy: Foundations, Methods, and Applications*, Walter de Gruyter, Berlin, Germany, 531 pp.

Seeber, G. and Wübbena, G. (1989) Kinematic Positioning with Carrier Phases and `On the Way' Ambiguity Resolution, *Proceedings of Fifth International Geodetic Symposium on Satellite Positioning*, Las Cruces, NM, March, 13-17, pp. 600-609.

Shardlow, P.J. (1994) Propagation Effects on Precise GPS Heighting, *PhD Thesis*, The University of Nottingham, Nottingham, UK, 221 pp.

Slater, J., Willis, P., Gurtner, W., Beulter, G., Noll, C., Hein, G. and Neilan, R. (1998) The International GLONASS Experiment (IGEX-98), *Proceedings of*

11th ION International Technical Meeting ION GPS-98, Nashville, TN, September 15-18, pp. 1637-1644.

Spilker, J.J. (1978) GPS Signal Structure and Performance Characteristics, *Navigation*, Journal of The (U.S.) Institute of Navigation, Vol. 25, No. 2, pp. 121-146.

Spilker, J.J. (1996) Tropospheric Effects on GPS, in: Parkinson, B.W. and Spilker, J.J. (eds.), *Global Positioning System: Theory and Applications* (Vol. I), American Institute of Astronautics, Washington, D.C., pp. 517-546.

Stewart, M.P. (1998) The Application Of Antenna Phase Centre Models to The West Australian State GPS Network, *Geomatics Research Australasia*, No. 68, pp. 61-78.

Stewart, M. and Tsakiri, M. (1997) The Future of RTK GPS/GLONASS Positioning in the Urban Canyon, *The Australian Surveyor*, Vol. 42, No 4, pp. 13-19.

Talbot, N.C. (1988) Optimal Weighting of GPS Carrier Phase Observations Based on the Signal-to-Noise Ratio, *Proceedings of International Symposium on Global Positioning Systems*, Brisbane, Qld, October, p.4.1-4.17.

Talbot, N.C. (1993) Centimetre in the Field, a User's Perspective of Real-Time Kinematic Positioning in a Production Environment, *Proceedings of 6th International Technical Meeting of Satellite Division of the Institute of Navigation, ION GPS-93*, Salt Lake City, Ut, September 22-24, pp. 1049-1057.

Teunissen, P.J.G. (1993) Least-Squares Estimation of the Integer GPS Ambiguities, *Invited Lecture*, Section IV, Theory and Methodology, IAG General Meeting, Beijing, China, August, 16 pp.

Teunissen, P.J.G. (1996) GPS Carrier Phase Ambiguity Fixing Concepts, in: Kleusberg, A. and Teunissen, P.J.G. (eds.), *Lecture Notes of Earth Sciences, GPS for Geodesy*, Springer, Berlin, Germany, pp. 263-335.

Teunissen, P.J.G. (1997) A Canonical Theory for Short GPS Baselines (Part I-IV), *Journal of Geodesy*, Vol. 71, pp. 320-336, 389-401, 486-501, 513-525.

Teunissen, P.J.G. (1998) Quality Control and GPS, in: Teunissen, P.J.G. and Kleusberg, A. (eds.), *GPS for Geodesy*, Second Edition, Springer Verlag Berlin, Germany, pp. 271-318.

Teunissen, P.J.G., Jonkman, N.F. and Tiberius C.C.J.M. (1998) Weighting GPS Dual Frequency Observations: Bearing the Cross of Cross-Correlation, *GPS Solution*, Vol. 2, No. 2, pp. 28-37.

Teunissen, P.J.G. and Odijk, D. (1997) Ambiguity Dilution of Precision: Definition, Properties and Application, *Proceedings of 10th International Technical*

Meeting of the Satellite Division of the Institute of Navigation, ION GPS-97, September 16-19, Kansas City, MO, pp. 891-900.

Teunissen, P.J.G. and Kleusberg, A. (1996) GPS Observation Equations and Positioning Concepts, in: Kleusberg, A. and Teunissen, P.J.G. (eds.), *GPS for Geodesy*, Springer Verlag, Berlin, Germany, pp. 175-217.

Teunissen, P.J.G. and Salzmann, M.A. (1989) A Recursive Slippage Test for Use in State-Space Filtering, *Manuscripta Geodaetica*, Vol. 14, pp. 383-390.

Tiberius, C.C.J.M. (1998) Quality Control in Positioning, *The Hydrographical Journal*, No. 90, pp. 3-8.

Tiberius, C.C.J.M. and de Jonge, P.J. (1995) Fast Positioning Using the LAMBDA-Method, *Proceedings of 4th International Conference on Differential Satellite Navigation Systems*, Bergen, Norway, 24-28 April, Paper No. 30.

Tralli, D. and Lichten, S. (1990) Stochastic Estimation of Tropospheric Path Delays in Global Positioning System Geodetic Measurements, *Bulletin Geodesique*, Vol. 64, pp. 127-159.

van Graas, F. and Braasch, M.S. (1996) Selective Availability, in: Parkinson, B.W. and Spilker, J.J. (eds.), *Global Positioning System: Theory and Applications* (Vol. I), American Institute of Astronautics, Washington, D.C., pp. 601-322.

van Nee, R. (1993) Spread Spectrum Code and Carrier Synchronization Errors Caused by Multipath and Interference, *IEEE Transactions on Aerospace and Electronic Systems*, Vol. 29, No. 4, pp. 1359-1365.

Walsh, D., Riley, S., Cooper, J. and Daly, P. (1995) Precise Positioning Using GPS/GLONASS Carrier Phase and Code Phase Observables, *Proceedings of 8th International Technical Meeting of the Satellite Division of the Institute of Navigation, ION GPS-95*, Palm Springs, CA, September 12-15, pp. 499-500.

Walsh, D. and Daly, P. (1996) GPS and GLONASS Carrier Phase Ambiguity Resolution, *Proceedings of 9th International Technical Meeting of the Satellite Division of the Institute of Navigation, ION GPS-96*, Kansas City, MO, September 17-19, pp. 899-907.

Walsh, D. and Daly, P. (1997) Combined GPS and GLONASS Carrier Phase Positioning, *Proceedings of International Symposium on Kinematic Systems in Geodesy, Geomatics and Navigation*, Banff, Alberta, June 3-6, pp. 205-212.

Walsh, D. and Daly, P. (1998) Precise Positioning Using GLONASS, *Proceedings of FIG XXI International Conference*, July 21-25, Brighton, UK, paper TS10.3.

Walsh, D., Daly, P. and Rowe, T. (1995) An Analysis of Using Carrier Phase to Fulfil Cat III Required Navigation Performance, *Proceedings of 8th International Technical Meeting of the Satellite Division of the Institute of*

Navigation, ION GPS-95, Palm Springs, CA, September 12-15, pp. 1985-1993.

Walsh, D., Lowe, D., Stefano, C., Daly, P., Richards, G., Wolfe, A., Ingle, G. and Lawson, J. (1997) Design and Evaluation of Combined GPS/GLONASS LAAS Trials, *Proceedings of 10th International Technical Meeting of the Satellite Division of the Institute of Navigation, ION GPS-97*, Kansas City, Missouri, September 16-19, pp. 1631-1639.

Wang, J. (1994a) A Reliability Theory for Singular Linear Models, *Journal of Wuhan Technical University of Surveying and Mapping*, Vol. 21, No. 2, pp. 163-168.

Wang, J. (1994b) GPS Baseline Dilution of Precision and Its Applications, *Geotechnical Investigation and Surveying*, Serial No. 126, pp. 46-49.

Wang, J. (1998a) Mathematical Models for Combined GPS and GLONASS Positioning, *Proceedings of 11th International Technical Meeting of the Satellite Division of the Institute of Navigation, ION GPS-98*, Nashville, TN, September 15-18, pp. 1333-1344.

Wang, J. (1998b) Stochastic Assessment of the GPS Measurements for Precise Positioning, *Proceedings of 11th International Technical Meeting of the Satellite Division of the Institute of Navigation, ION GPS-98*, Nashville, TN, September 15-18, pp. 81-89.

Wang, J. (1998c) Combined GPS and GLONASS Kinematic Positioning: Modelling Aspects, *Proceedings of 39th Australian Surveyors Congress*, Launceston, Tas, November 8-13, pp. 227-235.

Wang, J. (1999) An Approach to GLONASS Ambiguity Resolution, accepted for publication in Journal of Geodesy.

Wang, J. and Chen, Y. (1994a) On the Localizability of Blunders in Correlated Coordinates of Junction Points in Densification Networks, *Australian Journal of Geodesy, Photogrammetry and Surveying*, No. 60, pp. 109-119.

Wang, J. and Chen, Y. (1994b) On the Reliability Measures of Observations, *Acta Geodaetica et Cartographica Sinica* (English Edition), *Journal of Chinese Society of Surveying and Mapping*, pp. 42-51. Also in *Proceedings of FIG XX International Congress*, Melbourne, Vic, March 5-12, 1994, Vol. 6, 654.2/1-12.

Wang, J. and Iz, H.B. (1998) Online Stochastic Modelling for Real-time GPS/GLONASS Satellite Positioning, *Proceedings of International Conference of Spatial Information Science and Technology*, (SIST'98), December 13-16, Wuhan, P.R. China, pp. 17-27.

Wang, J. and Stewart, M. (1996) Stochastic Assessment of the Double Differenced GPS Observations, paper presented at Annual Research Seminar, School of

Geomatic Engineering, The University of New South Wales, Sydney, NSW, November.

Wang, J., Stewart, M. and Tsakiri, M. (1997a) A New Validation Test Procedure for Ambiguity Resolution On-the-fly, *Proceedings of the International Symposium on Kinematic Systems in Geodesy, Geomatics and Navigation KIS'97*, Banff, Canada, June 3-6, pp. 279-287.

Wang, J., Stewart, M. and Tsakiri, M. (1997b) Kinematic GPS Positioning with Adaptive Kalman Filtering Techniques, *Proceedings of the General Meeting of the International Association of Geodesy IAG'97*, Rio de Janeiro, Brazil, September 3-9, Spring Verlag, Berlin, Germany, pp. 389-394.

Wang, J., Stewart, M. and Tsakiri, M. (1997c) On Quality Control in Hydrographic GPS Surveying, *Proceedings of 3rd Australasian Hydrographic Symposium*, Fremantle, WA, November, pp. 136-141.

Wang, J., Stewart, M. and Tsakiri, M. (1998a) A Discrimination Test Procedure for Ambiguity Resolution On-the-fly, *Journal of Geodesy*, Vol. 72, No. 11, pp. 644-653.

Wang, J., Stewart, M. and Tsakiri, M. (1998b) Stochastic Modelling for GPS Static Baseline Data Processing, *Journal of Surveying Engineering*, Vol. 124, No. 4, pp. 171-181.

Wang, J., Stewart, M. and Tsakiri, M. (1998c) Real-time Stochastic Modelling for GPS Kinematic Positioning, *Proceedings of FIG XXI International Conference*, July 21-25, Brighton, UK, Vol. 5, SS2/3.1-9.

Wang, J., Stewart, M. and Tsakiri, M. (1999) Ambiguity Resolution for GLONASS Precise Positioning, *Proceedings of 4th International Symposium on Satellite Navigation Technology and Applications,* Brisbane, Qld, July 20-23, (in press).

Wanninger, L. (1995) Enhancing Differential GPS Using Regional Ionospheric Error Models, *Bulletin Geodesique*, Vol. 69, No. 6, pp. 283-291.

Wei, M. and Schwarz, K.P. (1995) Fast Ambiguity Resolution Using an Integer Nonlinear Programming Method, *Proceedings of ION GPS-95*, Palm Springs, CA, September 12-15, pp. 1101-1110.

Wells, D.E., Beck, N., Delikaraohlou, D., Kleusberg, A., Krakiwsky, E.J., Lachapelle, J., Langley, R.B., Nakiboglu, M., Schwarz, K.P., Tranquilla, J.M. and Vanicek, P. (1987) *Guide to GPS positioning*, 2nd corrected printing, Canadian GPS Associates, Fredericton, New Brunswick, Canada, 503 pp.

Welsch, W.M. (1981) Estimation of Variances and Covariances of Geodetic Observations, *Australian Journal of Geodesy, Photogrammetry and Surveying*, No. 34, pp. 1-14.

Westrop, J., Napier, M.E. and Ashkenazi, V. (1989) Cycle Slips on the Move: Detection and Elimination, *Proceedings of Second International Technical Meeting of the Satellite Division of the Institute of Navigation*, Colorado Springs, CO, September 27-29, pp. 31-34.

Whalley, S. (1990) Precise Orbit Determination for GPS Satellites, *PhD Thesis,* The University of Nottingham, Nottingham, UK, 222 pp.

Williams, E.J. (1959) *Regression Analysis,* Johan and Willey & Sons, Inc., New York, NY, 214 pp.

Williams, E.J. and Kloot, N.H. (1953) Interpolation in a Series of Correlated Observations, *Australian Journal of Applied Science*, Vol. 4, pp. 1-17.

Wooden, W.H. (1985) Navstar Global Positioning System: 1985, *Proceedings of First International Symposium on Precise Positioning with the Global Positioning System*, Rockville, MD, April 15-19, Vol.1, pp. 23-32.

Wübbena, G. Bagge, A., Seeber, G., Böder, V. and Hankemeier P. (1996) Reducing Distance Dependent Errors for Real-time Precise DGPS Applications by Establishing Reference Station Networks, *Proceedings of* 9th *International Technical Meeting of the Satellite Division of the Institute of Navigation, ION GPS-96*, Kansas City, MO, September 17-20, pp. 1845-1852.

Yunck, T.P. (1996) Orbit Determination, in: Parkinson, B.W. and Spilker, J.J. (eds.), *Global Positioning System: Theory and Applications* (Vol. II), American Institute of Astronautics, Washington, D.C., pp. 559-592.

Zumberge, J.F., Watkins M.M. and Webb F.H. (1998) Characteristics and Applications of Precise GPS Clock Solutions Every 30 Seconds, *Navigation*, Vol. 44, No. 4, pp. 449-456.

Appendix A

WHY THE STANDARD DOUBLE DIFFERENCE PROCEDURE DOES NOT WORK FOR GLONASS CARRIER PHASES

The raw GLONASS measurements are contaminated with many error sources, such as satellite clock errors and ionospheric and tropospheric delay errors. Therefore, mathematical representation of these raw observations will involve some undesirable nuisance parameters, which are of no direct interest for positioning. In practical data processing, differenced observations are commonly used, in which many systematic errors are, to a large extent, cancelled for short baselines and the resulting mathematical models exclude some of these nuisance parameters. For short baselines, the DD carrier phase measurements can be written as (e.g. Teunissen and Kleusberg, 1996):

$$\varphi_{km}^{pq} = \frac{1}{\lambda_p}\rho_{km}^{p} - \frac{1}{\lambda_q}\rho_{km}^{q} - (\frac{c}{\lambda_p} - \frac{c}{\lambda_q})dt_{km} + N_{km}^{pq} \qquad (A.1)$$

where the subscripts k and m identify the receivers, and the superscripts p and q denotes the satellites. ρ is the topocentric range to the satellites; λ is the wavelength of the carrier phase frequencies; c is the speed of light; dt is the receiver clock errors. Unlike the situation of processing GPS data, the receiver clock errors cannot be removed from the DD carrier phase measurements in the situation of processing GLONASS data or combined GPS and GLONASS data. The reason for this is that the GLONASS satellites transmit their signals using different frequencies. To have a closer look at the consequence of this fact, the linear(ized) set of DD carrier phase measurements is expressed as

$$DD\varphi = Ax + Bt + Cn \qquad (A.2)$$

where $DD\varphi$ is the vector of the observed minus computed DD carrier phases; and

$$A = \begin{pmatrix} A_1 & & & \\ & A_2 & (0) & \\ & & \cdot & \\ & (0) & & \cdot \\ & & & A_s \end{pmatrix}, \tag{A.3}$$

$$B = \begin{pmatrix} b & & & \\ & b & (0) & \\ & & \cdot & \\ & (0) & & \cdot \\ & & & b \end{pmatrix}, \tag{A.4}$$

and

$$C = \begin{pmatrix} E \\ E \\ \cdot \\ \cdot \\ E \end{pmatrix} \tag{A.5}$$

are the design matrices relating to baseline component unknowns x, receiver clock parameters t and DD ambiguity parameters n, respectively. In equation (A.3), A_i is the $r \times 3$ sub-design-matrix for epoch i; and s is the number of epochs in a solution. In equation (A.4), b is a $r \times 1$ vector of the coefficients of receiver clock parameter for any specific epoch. In equation (A.5), E is an $r \times r$ unit matrix. It can be proved that

$$\begin{pmatrix} A & B & C \end{pmatrix} \begin{pmatrix} 0 \\ e \\ -b \end{pmatrix} = 0, \tag{A.4}$$

with $e = (1, 1, ..., 1)^T$ being an $(s \times r) \times 1$ vector. Equation (A.4) shows that the linear dependent combination exists in the column vectors of the design matrices A, B and C. The resulting normal matrix therefore is singular. This means that the DD ambiguity and receiver clock parameters are theoretically inseparable (e.g. Teunissen and Kleusberg, 1996).

Appendix B

LARGEST POSSIBLE WAVELENGTH IN Rossbach-Hein MODEL

As showed in Chapter 1, the GLONASS satellite frequencies (L1) are dependent on the channel numbers (q, p), i.e.

$$f_q = 1602 + 0.5625 \cdot q(MHZ) = (2848 + q) \cdot \Delta f \tag{B.1}$$

$$f_p = 1602 + 0.5625 \cdot p(MHZ) = (2848 + p) \cdot \Delta f \tag{B.2}$$

where $\Delta f = 0.5625 MHZ$. The above two frequencies refer to the following wavelengths:

$$\lambda_q = \frac{c}{f_q} \tag{B.3}$$

$$\lambda_p = \frac{c}{f_p} \tag{B.4}$$

According to Rossbach and Hein (1996), to retain the integer nature of the DD ambiguity, λ_q and λ_p must satisfy equation (2.2), i.e.

$$\lambda_0 = \frac{c}{k_p \cdot (2848 + p) \cdot \Delta f} = \frac{c}{k_q \cdot (2848 + q) \cdot \Delta f} \tag{B.5}$$

which is the wavelength of the auxiliary frequency used in scaling the carrier phases. In equation (B.5), the channel numbers (q, p) are much smaller than the constant number 2848. Thus, the terms $(2848 + p)$ and $(2848 + q)$ are approximately considered as constant values. Then, it is easy to see that the largest possible wavelength corresponds to the smallest integer factor k_p (or k_q). To this end, the relation between the two factors is further derived as

$$k_p = \frac{2848+q}{2848+p} \cdot k_q = \frac{M^q}{M^p} \cdot k_q \tag{B.6}$$

where $\frac{M^q}{M^p}$ is an irreducible fraction. Therefore, the smallest integer factors are $k_p = M^q$ and $k_q = M^p$, respectively. In equation (B.6),

$$M^q = \frac{2848+q}{n} \tag{B.7}$$

$$M^p = \frac{2848+p}{n} \tag{B.8}$$

where n is the largest common factor for the integers $2848+q$ and $2848+p$. For all the possible frequency channel pairs, the values of n are calculated and listed in Tables B.1 and B.2 for different GLONASS frequency allocations.

From Table B.1, the largest value of n is identified as 19, which corresponds to $p=2$ and $q=21$ (or $p=21$ and $q=2$). The smallest scale factors k_p and k_q are 150 and 151 (or 151 and 150). Although the reduced factors are much smaller than the factors $2848+q$ and $2848+p$ used in Leick (1998), Rossbach and Hein (1996), the largest possible wavelength of the auxiliary frequencies for different GLONASS satellite pairs is 0.00126m.

For the final GLONASS frequency allocation, Table B. 2 shows that the largest value of n is 9, which corresponds to $p=-4$ and $q=5$ (or $p=5$ and $q=-4$). The smallest scale factors k_p and k_q are 316 and 317 (or 317 and 316). Therefore, the largest possible wavelength of the auxiliary frequencies for different GLONASS satellite pairs is 0.000593m.

Table B.1 The largest common factors for the integers 2848 + p and 2848 + q

(p, q =1-14; 21-24, GLONASS frequency plan until 1998)

p/q (1)	1 (2)	2 (3)	3 (4	4 (5)	5 (6)	6 (7)	7 (8)	8 (9)	9 (10)	10 (11)	11 (12)	12 (13)	13 (14)	14 (15)	21 (16)	22 (17)	23 (18)	24 (19)
1		1	1	1	1	1	1	7	1	1	1	11	1	1	1	7	11	1
2			1	2	3	2	5	6	1	2	3	10	1	6	19	10	3	2
3				1	1	1	1	1	1	1	1	1	1	1	1	1	1	1
4					1	2	1	4	1	2	1	4	1	2	1	2	1	4
5						1	1	3	1	1	3	1	1	9	1	1	9	1
6							1	2	1	2	1	2	1	2	1	2	1	2
7								1	1	1	1	5	1	1	1	5	1	1
8									1	2	3	4	1	6	1	14	3	8
9										1	1	1	1	1	1	1	1	1
10											1	2	1	2	1	2	1	2
11												1	1	3	1	1	3	1
12													1	2	1	10	11	4
13														1	1	1	1	1
14															1	2	9	2
21																1	1	1
22																	1	2
23																		1

Table B.2 The largest common factors for the integers 2848 + p and 2848 + q

(p, q = -7 to 6, final GLONASS frequency allocation)

p/q (1)	-7 (2)	-6 (3)	-5 (4	-4 (5)	-3 (6)	-2 (7)	-1 (8)	0 (9)	1 (10)	2 (11)	3 (12)	4 (13)	5 (14)	6 (15)
-7		1	1	3	1	1	3	1	1	3	1	1	3	1
-6			1	2	1	2	1	2	7	2	1	2	1	2
-5				1	1	1	1	1	1	1	1	1	1	1
-4					1	2	3	4	1	6	1	4	9	2
-3						1	1	1	1	5	1	1	1	1
-2							1	2	1	2	1	2	1	2
-1								1	1	3	1	1	3	1
0									1	2	1	4	1	2
1										1	1	1	1	1
2											1	2	3	2
3												1	1	3
4													1	2
5														1

Appendix C

PROOF OF THEOREM 2.1 (MODEL SENSITIVITY)

Theorem (2.1) (Model sensitivity)

For the same pseudo-range formulation,

$$\rho_{t,ck\_M} > \rho_{t,ck\_S} \tag{C.1}$$

Proof:

Equation (C.1) is equivalent to the following equation, ie.

$$d_{\rho^2} = \rho^2_{t,ck\_M} - \rho^2_{t,ck\_S} = c_0 \cdot d_B > 0 \tag{C.2}$$

where

$$c_0 = (\gamma_3 - \gamma_1) / \gamma_2\gamma_3 \tag{C.3}$$

$$d_B = B_\phi^T[\overline{D}_{\phi\_M}^T P_{\phi\_M} \overline{D}_{\phi\_M} - \overline{D}_{\phi\_S}^T P_{\phi\_S} \overline{D}_{\phi\_S}]B_\phi \tag{C.4}$$

It can be easily proved that $c_0 > 0$. Therefore, $d_{\rho^2} > 0$ is equivalent to $d_B > 0$, which is independent of the geometry and the pseudo-range measurement formulations. For a $(n-1)\times n$ DD operator matrix D, one can obtain (Teunissen, 1997)

$$D^T(DD^T)^{-1}D = E_n - \frac{1}{n} l_n l_n^T \tag{C.5}$$

where $l_n = (1,1,\ldots..,1)^T$ is an $n \times 1$ vector with all the elements are equal to 1. Using equation (C.11), d_B can be further derived as

$$d_B = \frac{1}{\alpha} m\omega_0^2 f(y) \tag{C.6}$$

where

$$f(y) = f_1 y^2 - 2y + f_0 \tag{C.7}$$

with $f_0 = \frac{m}{m_2} - 1$; $f_1 = \frac{m}{m_1} - 1$; $y = \frac{\omega_1}{\omega_0}$; $\omega_0 = \sum_{i=1+m_1}^{m} \lambda_i^{-1}$; $\omega_1 = \sum_{i=1}^{m_1} \lambda_i^{-1}$.

To find the absolute extreme of function $f(y)$, its first and second derivatives are formulated as

$$\frac{d}{dy} f(y) = 2f_1 y - 2, \tag{C.8}$$

$$\frac{d^2}{dy^2} f(y) = 2f_1 > 0, \tag{C.9}$$

which indicate that function $f(y)$ has minimum at

$$y_0 = \frac{1}{f_1} = \frac{m_1}{m_2} \tag{C.10}$$

The minimum is

$$f(y_0) = f_1 y_0^2 - 2y_0 + f_0 = 0. \tag{C.11}$$

Due to the multiple frequencies of the GLONASS signals, $y \neq y_0$, and thus

$$f(y) > 0. \tag{C.12}$$

Substitution of equation (C.12) into (C.6) proves $d_B > 0$ and $d_{\rho 2} > 0$. *End of proof.*

Appendix D

AN INSEPARABLE CONDITION FOR TWO AMBIGUITY COMBINATIONS

Since

$$
\begin{aligned}
d &= \Omega_{c_j} - \Omega_{c_i} \\
&= (\hat{x}_k - c_j)^T Q_{\hat{x}_k}^{-1}(\hat{x}_k - c_j) - (\hat{x}_k - c_i)^T Q_{\hat{x}_k}^{-1}(\hat{x}_k - c_i) \\
&= (\hat{x}_k - c_i + c_i - c_j)^T Q_{\hat{x}_k}^{-1}(\hat{x}_k - c_i + c_i - c_j) - (\hat{x}_k - c_i)^T Q_{\hat{x}_k}^{-1}(\hat{x}_k - c_i) \\
&= (\hat{x}_k - c_i)^T Q_{\hat{x}_k}^{-1}(\hat{x}_k - c_i) + 2(c_i - c_j)^T Q_{\hat{x}_k}^{-1}(\hat{x}_k - c_i) \\
&\qquad + (c_i - c_j)^T Q_{\hat{x}_k}^{-1}(c_i - c_j) - (\hat{x}_k - c_i)^T Q_{\hat{x}_k}^{-1}(\hat{x}_k - c_i) \\
&= 2(c_i - c_j)^T Q_{\hat{x}_k}^{-1}(\hat{x}_k - c_i) + (c_i - c_j)^T Q_{\hat{x}_k}^{-1}(c_i - c_j) \\
&= (c_i - c_j)^T Q_{\hat{x}_k}^{-1}(2\hat{x}_k - 2c_i + c_i - c_j) \\
&= (c_i - c_j)^T Q_{\hat{x}_k}^{-1}(2\hat{x}_k - c_i - c_j)
\end{aligned}
$$

if $\hat{x}_k = \dfrac{c_i + c_j}{2}$, $d = 0$. This means that the two associated linear models or ambiguity combinations are completely inseparable.

Appendix E

PROOF OF THEOREM 6.1 (SD Ambiguity Search)

From equation (6.15), one can obtain

$$Q_{\hat{x}_c} = G^{-1} + G^{-1}A^T PBQ_{\hat{x}_k} B^T PAG^{-1}, \tag{E.1}$$

$$Q_{\hat{x}_c\hat{x}_k} = Q^T_{\hat{x}_c\hat{x}_k} = -G^{-1}A^T PBQ_{\hat{x}_k}, \tag{E.2}$$

$$\begin{aligned} Q_{\hat{x}_k} &= [B^T PB - B^T PAG^{-1}A^T PB]^{-1} \\ &= [s \cdot B_k P_i B_k - B_k P_i HG^{-1}H^T P_i B_k]^{-1} \\ &= [B_k P_i \Lambda P_i B_k]^{-1}, \end{aligned} \tag{E.3}$$

where

$$G = A^T PA, \tag{E.4}$$

$$H = \sum_{i=1}^{s} DA_i, \tag{E.5}$$

$$\Lambda = s \cdot P_i^{-1} - HG^{-1}H^T \tag{E.6}$$

Case a) :

$$\begin{aligned} \hat{x}_k(m_i) - \hat{x}_k(m_j) &= Q_{\hat{x}_k\hat{x}_c} A^T P[\bar{l}(m_i) - \bar{l}(m_j)] + Q_{\hat{x}_k} B^T P[\bar{l}(m_i) - \bar{l}(m_j)] \\ &= Q_{\hat{x}_k}[B^T P - B^T PAG^{-1}A^T P] f \cdot (m_j - m_i) \\ &= Q_{\hat{x}_k}[B_k P_i \Lambda P_i] f_m \cdot (m_j - m_i) \\ &= B_k^{-1} P_i^{-1} \Lambda^{-1} P_i^{-1} B_k^{-1} B_k P_i \Lambda P_i f_m \cdot (m_j - m_i) \\ &= B_k^{-1} f_m \cdot (m_j - m_i) \end{aligned} \tag{E.7}$$

Case b) :

$$\begin{aligned}
\hat{x}_c(m_i) - \hat{x}_c(m_j) &= Q_{\hat{x}_c} A^T P[\bar{l}(m_i) - \bar{l}(m_j)] + Q_{\hat{x}_c \hat{x}_k} B^T P[\bar{l}(m_i) - \bar{l}(m_j)] \\
&= G^{-1} A^T P f \cdot (m_j - m_i) - \\
&\quad G^{-1} A^T P B Q_{\hat{x}_k} [B^T P - B^T P A G^{-1} A^T P] f \cdot (m_j - m_i) \\
&= G^{-1} H^T P_i f_m \cdot (m_j - m_i) - G^{-1} H^T P_i B_k Q_{\hat{x}_k} [B_k P_i \Lambda P_i] f_m \cdot (m_j - m_i) \\
&= G^{-1} H^T P_i f_m \cdot (m_j - m_i) - G^{-1} H^T P_i f_m \cdot (m_j - m_i) \\
&= 0
\end{aligned} \tag{E.8}$$

Case c):

$$\begin{aligned}
\hat{e}(m_i) - \hat{e}(m_j) &= \bar{l}(m_i) - A\hat{x}_c(m_i) - B\hat{x}_k(m_i) - [\bar{l}(m_j) - A\hat{x}_c(m_j) - B\hat{x}_k(m_j)] \\
&= f \cdot (m_j - m_i) - B[\hat{x}_k(m_i) - \hat{x}_k(m_j)] \\
&= f \cdot (m_j - m_i) - B \cdot B_k^{-1} f_m \cdot (m_j - m_i) \\
&= f \cdot (m_j - m_i) - f \cdot (m_j - m_i) \\
&= 0
\end{aligned} \tag{E.9}$$

Based on the result of c), case d) is apparently true. *End of proof.*

Publications from the

SCHOOL OF GEOMATIC ENGINEERING

THE UNIVERSITY OF NEW SOUTH WALES
ABN 57 195 873 179

To order, write to:
Publications Officer, School of Geomatic Engineering
The University of New South Wales, UNSW SYDNEY NSW 2052, AUSTRALIA

NOTE: ALL ORDERS MUST BE PREPAID. CREDIT CARDS ARE ACCEPTED.
SEE BACKPAGE FOR OUR CREDIT CARD ORDER FORM.

MONOGRAPHS

Australian prices include postage by surface mail and GST.
Overseas prices include delivery by UNSW's air-lifted mail service (~2-4 weeks to Europe and North America).
Rates for air mail through Australia Post on application.

(Prices effective February 2001)

		Price Australia (incl. GST)	**Price** Overseas
M1.	R. S. Mather, "The Theory and Geodetic Use of some Common Projections", (2nd edition), 125 pp, 1978.	$ 16.50	$ 15.00
M2.	R. S. Mather, "The Analysis of the Earth's Gravity Field", 172 pp, 1971.	$ 8.80	$ 8.00
M3.	G. G. Bennett, "Tables for Prediction of Daylight Stars", 24 pp, 1974.	$ 5.50	$ 5.00
M4.	G. G. Bennett, J. G. Freislich & M. Maughan, "Star Prediction Tables for the Fixing of Position", 200 pp, 1974.	$ 8.80	$ 8.00
M8.	A. H. W. Kearsley, "Geodetic Surveying", 96 pp, 1988.	$ 13.20	$ 12.00
M11.	W. F. Caspary, "Concepts of Network and Deformation Analysis", 183 pp, 2000.	$ 27.50	$ 25.00
M12.	F. K. Brunner, "Atmospheric Effects on Geodetic Space Measurements", 110 pp, 1988.	$ 17.60	$ 16.00
M13.	B. R. Harvey, "Practical Least Squares and Statistics for Surveyors", (2nd edition, reprinted with corrections), 319 pp, 1998.	$ 33.00	$ 30.00
M14.	E. G. Masters and J. R. Pollard (Eds.), "Land Information Management", 269 pp, 1991. (Proceedings LIM Conference, July 1991).	$ 22.00	$ 20.00
M15/1	E. G. Masters and J. R. Pollard (Eds.), "Land Information Management - Geographic Information Systems - Advance Remote Sensing Vol. 1", 295 pp, 1993 (Proceedings of LIM & GIS Conference, July 1993).	$ 33.00	$ 30.00
M15/2	E. G. Masters and J. R. Pollard (Eds.), "Land Information Management - Geographic Information Systems - Advance Remote Sensing Vol. 2", 376 pp, 1993 (Proceedings of Advanced Remote Sensing Conference, July 1993).	$ 33.00	$ 30.00
M16.	A. Stolz, "An Introduction to Geodesy", 2nd extended edition, 148 pp, 2000.	$ 24.20	$ 22.00
M17.	C. Rizos, "Principles and Practice of GPS Surveying", 565 pp, 1997.	$ 46.20	$ 42.00

UNISURV REPORTS - S SERIES

(Prices effective February 2001)

Australian Prices *:	S8 - S20		$11.00
	S29 onwards	Individuals	$27.50
		Institutions	$33.00
Overseas Prices **:	S8 - S20		$10.00
	S29 onwards	Individuals	$25.00
		Institutions	$30.00

* Australian prices include postage by surface mail and GST.
** Overseas prices include delivery by UNSW's air-lifted mail service (~2-4 weeks to Europe and North America). Rates for air mail through Australia Post on application.

S8. A. Stolz, "Three-D Cartesian Co-ordinates of Part of the Australian Geodetic Network by the Use of Local Astronomic Vector Systems", Unisurv Rep. S8, 182 pp, 1972.

S14. E. G. Anderson, "The Effect of Topography on Solutions of Stokes` Problem", Unisurv Rep. S14, 252 pp, 1976.

S16. K. Bretreger, "Earth Tide Effects on Geodetic Observations", Unisurv S16, 173 pp, 1978.

S17. C. Rizos, "The Role of the Gravity Field in Sea Surface Topography Studies", Unisurv S17, 299 pp, 1980.

S18. B. C. Forster, "Some Measures of Urban Residential Quality from LANDSAT Multi-Spectral Data", Unisurv S18, 223 pp, 1981.

S19. R. Coleman, "A Geodetic Basis for Recovering Ocean Dynamic Information from Satellite Altimetry", Unisurv S19, 332 pp, 1981.

S29. G. S. Chisholm, "Integration of GPS into Hydrographic Survey Operations", Unisurv S29, 190 pp, 1987.

S30. G. A. Jeffress, "An Investigation of Doppler Satellite Positioning Multi-Station Software", Unisurv S30, 118 pp, 1987.

S31. J. Soetandi, "A Model for a Cadastral Land Information System for Indonesia", Unisurv S31, 168 pp, 1988.

S33. R. D. Holloway, "The Integration of GPS Heights into the Australian Height Datum", Unisurv S33, 151 pp, 1988.

S34. R. C. Mullin, "Data Update in a Land Information Network", Unisurv S34, 168 pp, 1988.

S35. B. Merminod, "The Use of Kalman Filters in GPS Navigation", Unisurv S35, 203 pp, 1989.

S36. A. R. Marshall, "Network Design and Optimisation in Close Range Photogrammetry", Unisurv S36, 249 pp, 1989.

S37. W. Jaroondhampinij, "A Model of Computerised Parcel-Based Land Information System for the Department of Lands, Thailand", Unisurv S37, 281 pp, 1989.

S38. C. Rizos (Ed.), D. B. Grant, A. Stolz, B. Merminod, C. C. Mazur, "Contributions to GPS Studies", Unisurv S38, 204 pp, 1990.

S39. C. Bosloper, "Multipath and GPS Short Periodic Components of the Time Variation of the Differential Dispersive Delay", Unisurv S39, 214 pp, 1990.

S40. J. M. Nolan, "Development of a Navigational System Utilizing the Global Positioning System in a Real Time, Differential Mode", Unisurv S40, 163 pp, 1990.

S41. R. T. Macleod, "The Resolution of Mean Sea Level Anomalies along the NSW Coastline Using the Global Positioning System", Unisurv S41, 278 pp, 1990.

S42. D. A. Kinlyside, "Densification Surveys in New South Wales - Coping with Distortions", Unisurv S42, 209 pp, 1992.

S43. A. H. W. Kearsley (ed.), Z. Ahmad, B. R. Harvey and A. Kasenda, "Contributions to Geoid Evaluations and GPS Heighting", Unisurv S43, 209 pp, 1993.

S44. P. Tregoning, "GPS Measurements in the Australian and Indonesian Regions (1989-1993)", Unisurv S44, 134 + xiii pp, 1996.

S45. W.-X. Fu, "A Study of GPS and Other Navigation Systems for High Precision Navigation and Attitude Determinations", Unisurv S45, 332 pp, 1996.

S46. P. Morgan et al, "A Zero Order GPS Network for the Australia Region", Unisurv S46, 187 + xii pp, 1996.

S47. Y. Huang, "A Digital Photogrammetry System for Industrial Monitoring", Unisurv S47, 145 + xiv pp, 1997.

S48. K. Mobbs, "Tectonic Interpretation of the Papua New Guinea Region from Repeat Satellite Measurements", Unisurv S48, 256 + xc pp, 1997.

S49. S. Han, "Carrier Phase-Based Long-Range GPS Kinematic Positioning", Unisurv S49, 185 + xi pp, 1997.

S50. M. D. Subari, "Low-cost GPS Systems for Intermediate Surveying and Mapping Accuracy Applications", Unisurv S50, 179 + xiii pp, 1997.

S51. L.-S. Lin, "Real-Time Estimation of Ionospheric Delay Using GPS Measurements", Unisurv S51, 199 + xix pp, 1997.

S53. D. B. Lemon, "The Nature and Management of Positional Relationships within a Local Government Geographic Information System", Unisurv S53, 273 + xvi pp, 1997.

S54. C. Ticehurst, "Development of Models for Monitoring the Urban Environment Using Radar Remote Sensing", Unisurv S54, 282 + xix pp, 1998.

S55. S. S. Boey, "A Model for Establishing the Legal Traceability of GPS Measurements for Cadastral Surveying in Australia", Unisurv S55, 186 + xi pp, 1999.

S56. P. Morgan and M. Pearse, "A First-Order Network for New Zealand", Unisurv S56, 134 + x pp, 1999.

S57. P. N. Tiangco, "A Multi-Parameter Radar Approach to Stand Structure and Forest Biomass Estimation", Unisurv S57, 319 + xxii pp, 2000.

S58. M. A. Syafi'i, "Object–Relational Database Management Systems (ORDBMS) for Managing Marine Spatial Data: ADCP Data Case Study", Unisurv S58, 123 + ix pp, 2000.

S59. X.-Q. Lu, "Strategies for Improving the Determination of Displacements of Sea Surface Temperature Patterns Using Consecutive AVHRR Thermal Images", Unisurv S59, 209 + xiii pp, 2000.

S60. G. Dickson, "GPS-Controlled Photography: The Design, Development and Evaluation of an Operational System Utilising Long-Range Kinematic GPS", Unisurv S60, 417 + x pp, 2000.

S61. J. Wang, "Modelling and Quality Control for Precise GPS and GLONASS Satellite Positioning", Unisurv S61, 171 + x pp, 2001.

Credit Card Orders / Payment

from / to

School of Geomatic Engineering

The University of New South Wales

Name and postal address of ordering person/organisation:

_____

_____

_____

_____

_____

Date : _____

Day time phone number : _____

Credit Card debit for:

_____ $ _____

_____ $ _____

_____ $ _____

_____ $ _____

Total $ _____

Please debit my credit card: ☐ Mastercard ☐ Visa ☐ Bankcard

Card Name: _____ Signature: _____

Card No: | | | | | | | | | | | | | | | | Expiry Date : _____

Note: UNSW requires that you attach a photocopy of your credit card to this order.